DOI: 10.47093/2218-7332.2025.16.4

ISSN 2218-7332 (Print)
ISSN 2658-3348 (Online)

СЕЧЕНОВСКИЙ УНИВЕРСИТЕТ
НАУК О ЖИЗНИ

Первый Московский государственный медицинский университет имени И.М. Сеченова
(Сеченовский Университет)

Сеченовский вестник

SECHENOV MEDICAL JOURNAL

Том/Volume 16
№ 4, 2025

НАУЧНО-ПРАКТИЧЕСКИЙ МЕДИЦИНСКИЙ ЖУРНАЛ

ORIGINAL STUDY:
AI-assisted 3D liver surgery planning

ORIGINAL STUDY:
Compression load test setup for multilayer bandages

CLINICAL CASE:
Alport syndrome with diffuse leiomyomatosis

Sechenov Medical Journal

ISSN 2218-7332 (Print)
ISSN 2658-3348 (Online)

SECHENOV UNIVERSITY
LIFE SCIENCES

Volume 16 | Issue 4 | 2025 | DOI: 10.47093/2218-7332.2025.16.4

Focus and Scope: The Sechenov Medical Journal publishes peer-reviewed original research articles, clinical and translational studies, reviews, and brief reports in biomedical, fundamental, and clinical medicine. It serves as a venue for sharing clinically relevant, methodologically robust research that can inform and improve medical practice. The information contained in Sechenov Medical Journal is intended for healthcare professionals only.

Founded: the journal has been published since 2010
Frequency: 4 times per year
DOI Prefix: 10.47093
Mass Media Registration Certificate: PI No FS77-78884 as of 28 August 2020 issued by the Federal Service for Supervision of Communications, Information Technology and Mass Media (Roskomnadzor)
Distribution: content is distributed under Creative Commons Attribution 4.0 License
Founder, Publisher, Editorial Office: Federal State Autonomous Educational Institution of Higher Education I.M. Sechenov First Moscow State Medical University of the Ministry of Health of the Russian Federation (Sechenov University)
Address: 8/2, Trubetskaya str., Moscow, 119048
Editorial office phone number: +7 (495) 6091400, ext. 1012
Website: https://www.sechenovmedj.com/jour

E-mail: sechenovmedj@staff.sechenov.ru
Published: 30.12.2025

Indexation: the Journal is included in the «White list»; in the index of periodical publications recommended by the State Commission for Academic Degrees and Titles, and in the Russian Science Citation Index database
Subscription index in the "Pressa Rossii" agency catalogue: 29124
Price: flexible
Technical Editor: Kseniya A. Gulyaeva
Editors-proofreaders: Irina S. Pigulevskaya, Lev A. Zelexon
Page layout: Olga A. Yunina
Printed by: LLC BEAN
Address: 1, Barrikad str., Nizhny Novgorod, 603003
Format 60×90 1/8. Off set print. Print run 200 copies

Сеченовский вестник

ISSN 2218-7332 (Print)
ISSN 2658-3348 (Online)

Том 16 | № 4 | 2025 | DOI: 10.47093/2218-7332.2025.16.4

Цели и задачи: журнал Sechenov Medical Journal публикует рецензируемые оригинальные исследования, клинические и трансляционные работы, обзоры и краткие сообщения по биомедицине, фундаментальной и клинической медицине. Это площадка, где врачи и исследователи делятся клинически значимыми и методологически обоснованными результатами, которые помогают развивать медицинскую практику и улучшать помощь пациентам. Издание предназначено для профессионалов в области здравоохранения.

История издания журнала: издается с 2010 г.
Периодичность: выходит 4 раза в год
Префикс DOI: 10.47093
Свидетельство о регистрации средства массовой информации: ПИ № ФС77-78884 от 28 августа 2020 года выдано Федеральной службой по надзору в сфере связи, информационных технологий и массовых коммуникаций (Роскомнадзор)
Условия распространения материалов: контент доступен под лицензией Creative Commons Attribution 4.0 License
Учредитель, издатель, редакция: федеральное государственное автономное образовательное учреждение высшего образования «Первый Московский государственный медицинский университет имени И.М. Сеченова» Министерства здравоохранения Российской Федерации (Сеченовский университет)
Адрес: 119048, г. Москва, ул. Трубецкая, д. 8, стр. 2
Телефон редакции: +7 (495) 6091400, доб. 1012

Сайт: https://www.sechenovmedj.com/jour
E-mail: sechenovmedj@staff.sechenov.ru
Выход в свет: 30.12.2025

Индексирование: журнал входит в «Белый список», в перечень изданий, рекомендованных ВАК, и библиографическую базу данных РИНЦ
Подписной индекс: в каталоге агентства «Пресса России» – 29124
Цена: свободная
Технический редактор: К.А. Гуляева
Редакторы-корректоры: И.С. Пигулевская, Л.А. Зелексон
Верстка: О.А. Юнина
Отпечатано: ООО «БЕАН»
Адрес: 603003, г. Нижний Новгород, ул. Баррикад, д. 1
Формат 60×90 1/8. Печать офсетная. Тираж 200 экз.

CONTENT

СОДЕРЖАНИЕ

SURGERY

Artificial intelligence – assisted three-dimensional preoperative planning in liver tumor surgery: a comparative real-world study
Alexey V. Shabunin, Mikhail M. Tavobilov, Alexey A. Karpov, Mark N. Aladin, Aysa V. Lantsynova, Kirill A. Abramov, Evgeny B. Kudryash

Validation of a test setup for measuring compression load under elements of multilayer bandages: an *in vitro* study
Sergey K. Zazulin, Svetlana M. Titkova, Mikhail V. Anurov, Gregory G. Gabuzov, Ekaterina Yu. Chizh, Alexey E. Brovkin

Development and validation of an environmental protocol to enhance sleep and pain outcomes in intensive care unit patients
Barkah Waladani, Endah Setianingsih, Muhammad N.W. Hidayah

Management of a massive retrosternal goiter after prior thyroid surgery: a clinical case
Didiek D.T. Setyo, Iwan Sidharta

INTERNAL DISEASES

Familial co-occurrence of diffuse leiomyomatosis and Alport syndrome: a clinical case report
Muqaddas Boltaboeva, Abdulhamid Haydarov, Marifat Ganieva, Davron Kholmatov, Oksana Efimenko, Lola Rakhmanova

EDITORIAL

Acknowledgements for peer review and assistance in preparing manuscripts for publication

ХИРУРГИЯ

4 Искусственный интеллект в сочетании с трехмерным предоперационным планированием в хирургии опухолей печени: сравнительное исследование в реальной клинической практике
А.В. Шабунин, М.М. Тавобилов, А.А. Карпов, М.Н. Аладин, А.В. Ланцынова, К.А. Абрамов, Е.Б. Кудряш

20 Валидация испытательного стенда для измерения компрессионной нагрузки под элементами многослойных повязок: исследование *in vitro*
С.К. Зазулин, С.М. Титкова, М.В. Ануров, Г.Г. Габузов, Е.Ю. Чиж, А.Е. Бровкин

31 Разработка и валидация протокола модификации окружающей среды, влияющей на качество сна и интенсивность боли у пациентов отделения интенсивной терапии
Б. Валадани, Э. Сетианингсих, М.Н.В. Хидая

41 Стратегия лечения массивного ретростернального зоба после ранее перенесенной операции на щитовидной железе: клинический случай
Д.Д.Т. Сетьо, И. Сидхарта

ВНУТРЕННИЕ БОЛЕЗНИ

49 Семейное сочетание диффузного лейомиоматоза и синдрома Альпорта: клинический случай
М. Болтабоева, А. Хайдаров, М. Ганиева, Д. Холматов, О. Ефименко, Л. Рахманова

ОТ РЕДАКЦИИ

58 Благодарность за рецензирование и помощь в подготовке рукописей к публикации

Original article / Оригинальная статья
https://doi.org/10.47093/2218-7332.2025.16.4.4-19

Artificial intelligence – assisted three-dimensional preoperative planning in liver tumor surgery: a comparative real-world study

Alexey V. Shabunin[1,2], Mikhail M. Tavobilov[1,2], Alexey A. Karpov[1,2], Mark N. Aladin[1,✉], Aysa V. Lantsynova[1], Kirill A. Abramov[1], Evgeny B. Kudryash[1,2]

[1] *Botkin Hospital*
5, 2nd Botkinsky proezd, Moscow, 125284, Russia
[2] *Russian Medical Academy of Continuous Professional Education*
2/1, bld. 1, Barrikadnaya str., Moscow, 125993, Russia

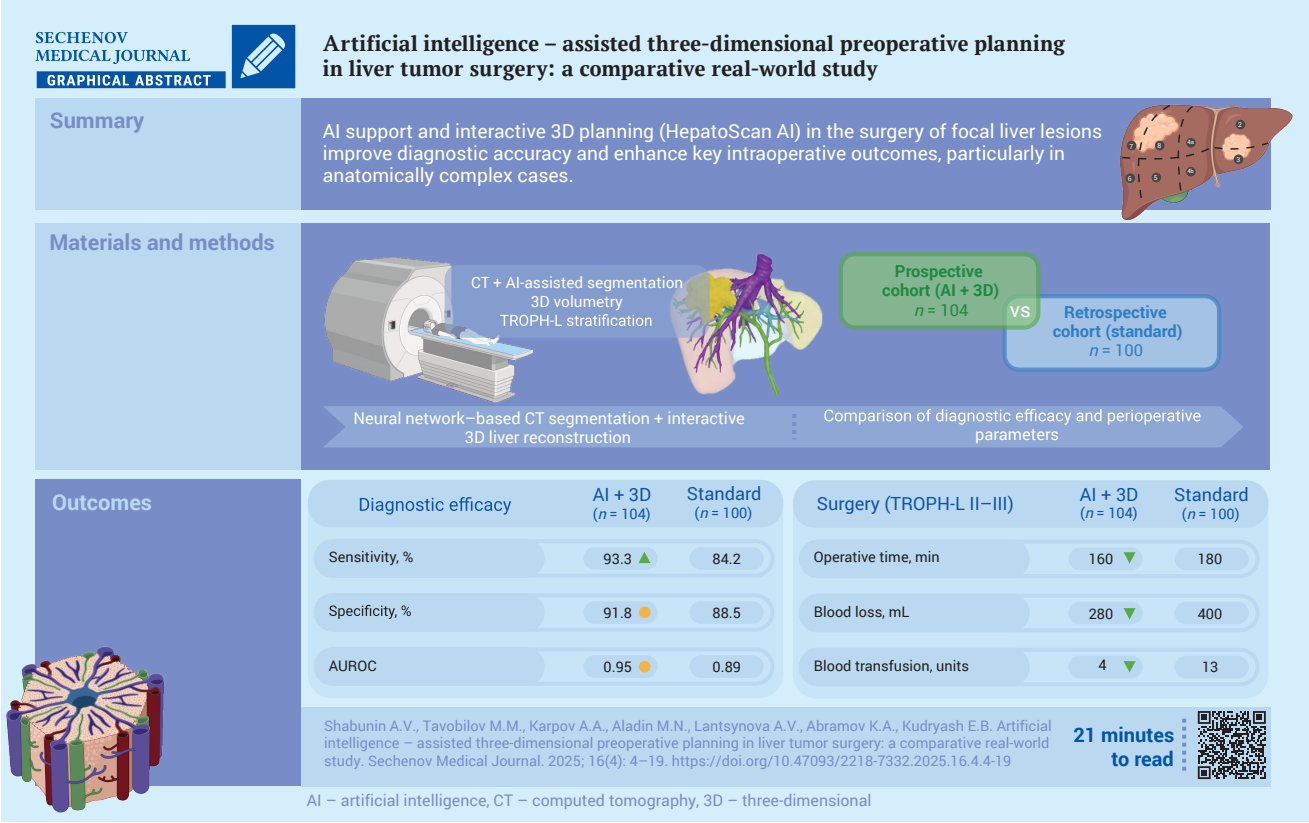

Abstract

Aim. Evaluation of the diagnostic and clinical effectiveness of the HepatoScan AI system, integrating neural network–based computed tomography (CT) analysis and interactive three-dimensional (3D) preoperative modeling in real-world clinical practice.

Materials and methods. A single-center comparative study was conducted, including a prospective cohort with artificial intelligence-assisted (AI) preoperative planning (*n* = 104) and a purposefully matched retrospective cohort undergoing standard preoperative planning (*n* = 100). In the AI-assisted group, automated liver and lesion segmentation, 3D volumetry, and stratification of anatomical complexity using the TROPH-L (Tumor – Regional capsule – Outflow veins – Portal vein – Hepatic bile – Localization) classification were applied. Diagnostic performance was assessed at the patient level using sensitivity, specificity, and AUROC (area under the receiver operating characteristic curve), with histopathological confirmation for malignant tumors and expert interpretation of multiphasic CT for benign lesions. Clinical effectiveness was analyzed in patients classified as TROPH-L II–III.

Results. The compared groups were well balanced in terms of demographic and clinical characteristics, lesion parameters, and distribution of TROPH-L categories. In the overall cohort, the use of HepatoScan AI was associated with a higher sensitivity of preoperative diagnosis compared with the standard approach (93.3% vs. 84.2%; $p = 0.008$), while maintaining high specificity. The AUROC was higher in the AI group (0.954 vs. 0.892), although the difference was not statistically significant; a similar trend was observed across nosological subgroups.
Among patients classified as TROPH-L II–III ($n = 54$ in the AI group and $n = 55$ in the standard planning group), AI-assisted planning was associated with a shorter operative time (160 vs. 180 minutes; $p = 0.01$) and reduced intraoperative blood loss (280 vs. 400 mL; $p = 0.004$). In addition, a higher rate of R0 resections (100% vs. 91.3%) and lower rates of postoperative complications and in-hospital mortality were observed in the AI group, although these differences were not statistically significant.
Conclusion. Integration of the HepatoScan AI system with interactive 3D preoperative planning is associated with improved diagnostic performance and favorable intraoperative metrics in patients with liver tumors, particularly in anatomically complex cases (TROPH-L II–III). These findings highlight the strong potential of the proposed digital technologies to optimize preoperative planning and warrant further prospective multicenter validation.

Keywords: computed tomography; medical image segmentation; surgical outcomes; diagnostic accuracy; volumetric analysis; clinical decision support systems; TROPH-L classification
MeSH terms:
LIVER NEOPLASMS – DIAGNOSTIC IMAGING
LIVER NEOPLASMS – SURGERY
LIVER – DIAGNOSTIC IMAGING
LIVER – PATHOLOGY
LIVER – SURGERY
IMAGING, THREE-DIMENSIONAL
ARTIFICIAL INTELLIGENCE
OPERATIONS SCHEDULING
For citation: Shabunin A.V., Tavobilov M.M., Karpov A.A., Aladin M.N., Lantsynova A.V., Abramov K.A., Kudryash E.B. Artificial intelligence – assisted three-dimensional preoperative planning in liver tumor surgery: a comparative real-world study. Sechenov Medical Journal. 2025; 16(4): 4–19. https://doi.org/10.47093/2218-7332.2025.16.4.4-19

CONTACT INFORMATION:
Mark N. Aladin, Junior Researcher, Surgeon, Department of Hepatopancreatobiliary Surgery, Botkin Hospital.
Address: 5, 2nd Botkinsky proezd, Moscow, 125284, Russia
E-mail: aladinmark97@gmail.com

Ethics statements. The study was approved by the Local Ethics Committee (Protocol No. 15 dated 11 October 2022) of the Russian Medical Academy of Continuous Professional Education, Ministry of Health of the Russian Federation.
Data availability. The data confirming the findings of this study are available from the authors upon reasonable request. Data and statistical methods used in the article were examined by a professional biostatistician on the Sechenov Medical Journal editorial staff.
Conflict of interest. The authors declare that there is no conflict of interests.
Financing. This study was supported by a government-funded Research and Development project aimed at reducing postoperative complications and mortality and improving survival outcomes in patients with benign and malignant liver diseases through the use of neural network technologies and preoperative three-dimensional modeling (EGISU No. 123042600026-2). The project was approved by the Moscow City Health Department under Order No. 1196 dated December 21, 2022, covering the period 2023–2025.
Acknowledgements. The authors express their deep gratitude to the Head of the Department of Radiology of Botkin Hospital Maxim P. Onishchenko for his assistance in organizing radiological examinations, as well as to the staff of the Research and Practical Clinical Center for Diagnostics and Telemedicine Technologies: Chief Physician Yuri A. Vasiliev, Head of the Directorate for Scientific Division Management Olga V. Omelyanskaya, Head of the Department of Medical Informatics, Radiomics, and Radiogenomics Kirill M. Arzamasov, Deputy Head of the Department of Medical Informatics, Radiomics and Radiogenomics Lev D. Pestrenin, and Junior Researcher of the Department of Radiomics and Radiogenomics Ekaterina F. Savkina, for their contribution to the development of the HepatoScan AI system and to the processing and analysis of radiological examinations.

Received: 16.10.2025
Accepted: 04.12.2025
Date of publication: 30.12.2025

УДК 616.36-006.6-089.163

Искусственный интеллект в сочетании с трехмерным предоперационным планированием в хирургии опухолей печени: сравнительное исследование в реальной клинической практике

А.В. Шабунин[1,2], М.М. Тавобилов[1,2], А.А. Карпов[1,2], М.Н. Аладин[1,✉], А.В. Ланцынова[1], К.А. Абрамов[1], Е.Б. Кудряш[1,2]

[1] ГБУЗ «Московский многопрофильный научно-клинический центр имени С.П. Боткина» Департамента здравоохранения города Москвы
пр-д 2-й Боткинский, д. 5, г. Москва, 125284, Россия
[2] ФГБОУ ДПО «Российская медицинская академия непрерывного профессионального образования» Министерства здравоохранения Российской Федерации
ул. Баррикадная, д. 2/1, стр. 1, г. Москва, 125993, Россия

Аннотация

Цель. Оценка диагностической и клинической эффективности системы HepatoScan AI, объединяющей нейросетевой анализ компьютерных томограмм (КТ) и интерактивное трехмерное (3D, three-dimensional) предоперационное моделирование в реальной клинической практике.

Материалы и методы. Выполнено одноцентровое сравнительное исследование с проспективной когортой пациентов, у которых предоперационное планирование выполнялось с поддержкой искусственного интеллекта (ИИ, *n* = 104) и целенаправленно подобранной ретроспективной когортой стандартного планирования (*n* = 100). В группе ИИ применялись автоматическая сегментация печени и очагов, 3D-волюметрия и стратификация анатомической сложности по шкале TROPH-L (Tumor – Regional capsule – Outflow veins – Portal vein – Hepatic bile – Localization, опухоль – отношение к капсуле печени – печеночные вены – воротная вена – желчные протоки – локализация). Диагностическую эффективность оценивали на уровне пациента с использованием показателей чувствительности, специфичности и площади под ROC-кривой (AUROC, area under the receiver operating characteristic curve) с использованием морфологической верификации для злокачественных опухолей и экспертного заключения по мультифазной КТ для доброкачественных образований. Клиническую эффективность анализировали у пациентов категорий TROPH-L II–III.

Результаты. Сравниваемые группы были сопоставимы по демографическим и клиническим характеристикам, параметрам очагов и распределению категорий TROPH-L. В общей выборке применение HepatoScan AI сопровождалось увеличением чувствительности предоперационной диагностики до 93,3% по сравнению со стандартным подходом (84,2%; *p* = 0,008) при сохранении высокой специфичности. AUROC была выше в группе ИИ (0,954 против 0,892), однако различия не достигли значимости; в нозологических подгруппах отмечалась сходная тенденция. Среди пациентов с TROPH-L II–III (*n* = 54 – группа ИИ, *n* = 55 – стандартное планирование) применение ИИ ассоциировалось с сокращением длительности операции (160 против 180 мин; *p* = 0,01) и объема интраоперационной кровопотери (280 против 400 мл; *p* = 0,004), более высокой частотой R0-резекций (100% против 91,3%) и меньшей частотой послеоперационных осложнений и внутригоспитальной летальности, без достижения статистической значимости.

Заключение. Интеграция системы HepatoScan AI и интерактивного 3D-предоперационного планирования ассоциируется с повышением диагностической эффективности и улучшением отдельных интраоперационных показателей у пациентов с опухолями печени, особенно при анатомически сложных случаях (TROPH-L II–III). Полученные результаты подтверждают высокий потенциал предложенных цифровых технологий для оптимизации предоперационного планирования и требуют дальнейшей проспективной многоцентровой валидации.

Ключевые слова: компьютерная томография; сегментация медицинских изображений; хирургические исходы; диагностическая точность; волюметрический анализ; системы поддержки принятия клинических решений; классификация TROPH-L

Рубрики MeSH:
ПЕЧЕНИ НОВООБРАЗОВАНИЯ – ДИАГНОСТИЧЕСКОЕ ИЗОБРАЖЕНИЕ
ПЕЧЕНИ НОВООБРАЗОВАНИЯ – ХИРУРГИЯ
ПЕЧЕНЬ – ДИАГНОСТИЧЕСКОЕ ИЗОБРАЖЕНИЕ
ПЕЧЕНЬ – ПАТОЛОГИЯ
ПЕЧЕНЬ – ХИРУРГИЯ
ТРЕХМЕРНОГО ИЗОБРАЖЕНИЯ ПОСТРОЕНИЕ
ИСКУССТВЕННЫЙ ИНТЕЛЛЕКТ
ОПЕРАЦИИ ПЛАНИРОВАНИЕ
Для цитирования: Шабунин А.В., Тавобилов М.М., Карпов А.А., Аладин М.Н., Ланцынова А.В., Абрамов К.А., Кудряш Е.Б. Искусственный интеллект в сочетании с трехмерным предоперационным планированием в хирургии опухолей печени: сравнительное исследование в реальной клинической практике. Сеченовский вестник. 2025; 16(4): 4–19. https://doi.org/10.47093/2218-7332.2025.16.4.4-19

КОНТАКТНАЯ ИНФОРМАЦИЯ:
Аладин Марк Николаевич, младший научный сотрудник, врач-хирург отделения хирургии печени и поджелудочной железы ГБУЗ «ММНКЦ им. С.П. Боткина ДЗМ».
Адрес: пр-д 2-й Боткинский, д. 5, г. Москва, 125284, Россия
E-mail: aladinmark97@gmail.com

Соответствие принципам этики. Исследование одобрено на заседании Локального этического комитета (протокол № 15 от 11.10.2022) ФГБОУ ДПО РМАНПО Минздрава России.
Доступ к данным исследования. Данные, подтверждающие выводы этого исследования, можно получить у авторов по обоснованному запросу. Данные и статистические методы, представленные в статье, прошли статистическое рецензирование редактором журнала – сертифицированным специалистом по биостатистике.
Конфликт интересов. Авторы заявляют об отсутствии конфликта интересов.
Финансирование. Статья подготовлена в рамках НИОКТР «Программа снижения послеоперационных осложнений, летальности и улучшения показателей выживаемости у больных с доброкачественными и онкологическими заболеваниями печени посредством технологии нейронных сетей и предоперационного трехмерного моделирования» (№ ЕГИСУ: 123042600026-2) в соответствии с Приказом Департамента здравоохранения г. Москвы от 21.12.2022 № 1196 «Об утверждении государственных заданий, финансовое обеспечение которых осуществляется за счет средств бюджета города Москвы, государственным бюджетным (автономным) учреждениям, подведомственным Департаменту здравоохранения города Москвы, на 2023 год и плановый период 2024 и 2025 годов».
Благодарность. Авторы выражают благодарность заведующему отделением лучевой диагностики ГБУЗ «ММНКЦ им. С.П. Боткина ДЗМ» Онищенко Максиму Павловичу за содействие в организации лучевых исследований, а также сотрудникам ГБУЗ «НПКЦ ДиТ ДЗМ»: главному врачу Васильеву Юрию Александровичу, руководителю по управлению подразделениями Дирекции Наука Омелянской Ольге Васильевне, руководителю отдела медицинской информатики, радиомики и радиогеномики Арзамасову Кириллу Михайловичу, заместителю руководителя отдела медицинской информатики, радиомики и радиогеномики Пестренину Льву Дмитриевичу и младшему научному сотруднику отдела радиомики и радиогеномики Савкиной Екатерине Феликсовне за вклад в разработку системы HepatoScan AI, обработку и анализ лучевых исследований.

Поступила: 16.10.2025
Принята: 04.12.2025
Дата печати: 30.12.2025

Abbreviations:

AI – artificial intelligence
CT – computed tomography
FNH – focal nodular hyperplasia
TROPH-L – Tumor – Regional capsule – Outflow veins – Portal vein – Hepatic bile – Localization
3D – three-dimensional

HIGHLIGHTS

HepatoScan AI enables objective preoperative assessment by providing automated segmentation and quantitative evaluation of the liver's anatomical and volumetric parameters.

Integration of HepatoScan AI into the diagnostic workflow for liver tumors increases the sensitivity of preoperative detection of focal liver lesions while maintaining high specificity.

The TROPH-L classification standardizes the assessment of the anatomical complexity of focal liver lesions and improves the reproducibility of surgical planning.

The use of artificial intelligence-assisted support and three-dimensional planning in patients with TROPH-L II–III lesions is associated with improved intraoperative metrics and more accurate delineation of organ-preserving R0 resection.

Liver tumors represent a major global healthcare challenge and remain one of the leading causes of cancer-related mortality worldwide [1]. In routine clinical practice, modern tertiary care centers are increasingly required to make rapid, accurate, and evidence-based diagnostic and therapeutic decisions when managing patients with focal liver lesions [2]. This group of diseases remains particularly complex: radical treatment is often associated with a high risk of intraoperative and postoperative complications, while long-term outcomes are frequently suboptimal [3].

Importantly, comprehensive diagnostic assessment and surgical planning are required not only for malignant tumors but also for benign focal liver lesions. Large hemangiomas, adenomas, focal nodular hyperplasia (FNH), and complex cystic lesions may, in selected cases, cause significant pain, carry a risk of rupture, or lead to compression of vascular and biliary structures. As a result, these conditions can become clinically relevant and necessitate detailed preoperative evaluation [4].

In this context, there has been a growing interest in the integration of artificial intelligence (AI) technologies and three-dimensional (3D) modeling into clinical hepatobiliary surgery [5]. The combined use of AI-based tools and 3D visualization fundamentally transforms clinical decision-making by shifting it from subjective image interpretation toward objective, quantitative data analysis [6]. Contemporary deep learning algorithms have already demonstrated the ability to automatically segment hepatic structures on contrast-enhanced computed tomography (CT) images with an accuracy of up to 92–94%, improving diagnostic reproducibility while significantly reducing interpretation time [7].

The synergistic application of AI services and 3D modeling enables the creation of highly accurate, patient-specific virtual reconstructions of the liver, allowing detailed visualization of focal lesions and their anatomical relationships with vascular structures and the biliary tree [8]. This approach contributes to a more efficient diagnostic workflow, reducing the need for certain invasive procedures and decreasing the overall burden on the patient [9]. Clinical studies have shown that the use of 3D navigation and reconstruction techniques is associated with a significant reduction in operative time and a lower incidence of R1 resections, thereby directly improving the safety and oncological quality of surgical interventions [4, 10]. Consequently, digital technologies not only streamline the diagnostic and planning stages but also enhance the overall quality of surgical care for patients with liver tumors [11].

Objective of the study: to evaluate the diagnostic and clinical effectiveness of the HepatoScan AI clinical decision support system which integrates neural network–based medical image analysis with interactive 3D visualization, in real-world clinical practice.

MATERIALS AND METHODS

Development of the neural network algorithm

The development and validation of the clinical decision support system HepatoScan AI for focal liver lesions was carried out in collaboration between Botkin Hospital and the Research and Practical Clinical Center for Diagnostics and Telemedicine Technologies. The system is officially registered in the Russian Federation as computer software [12].

A detailed description of the training process and the performance metrics for the classification of benign and malignant liver lesions has been published previously [13].

Development of the TROPH-L clinical and instrumental classification

To standardize the description of morphological and anatomical characteristics of focal liver lesions and to unify preoperative planning, we developed the TROPH-L classification (Tumor – Regional capsule – Outflow veins – Portal vein – Hepatic bile – Localization). This classification is designed for the systematic analysis of spatial relationships between the tumor and the major hepatic structures, based on data derived from 3D modeling and neural network–based segmentation.

The TROPH-L classification integrates morphological and topographic–anatomical features obtained from patient-specific virtual 3D models with clinically relevant resectability parameters. The classification criteria include:

- T (Tumor size and growth type) – lesion size and growth pattern.
- R (Relation to capsule) – relationship of the lesion to the hepatic capsule.

- O (Outflow veins involvement) – involvement of the hepatic veins.
- P (Portal vein involvement) – degree of involvement of portal vein branches.
- H (Hepatic bile involvement) – anatomical relationship with the biliary tree.
- L (Localization) – anatomical localization according to the Couinaud segmental system, specifying the lobe and segment.

Algorithm for three-dimensional preoperative modeling

For preoperative planning, a dedicated 3D modeling workflow was used, including the calculation of volumetric liver parameters and subsequent patient stratification according to the TROPH-L classification. Contrast-enhanced preoperative CT scans were imported into the 3D Slicer software environment in NIfTI format. At this stage, anatomical reconstruction of the liver was performed with semi-automatic segmentation of vascular and biliary structures [14].

In the second stage, the Slicer-Liver extension was applied to automatically delineate Couinaud liver segments and to calculate centerlines of the vascular trees. This was followed by virtual liver resection planning. Using the Resections module, the proposed resection plane was defined, with automatic calculation of hepatic parenchymal volumes, including total liver volume (TLV), resection volume (RV), remnant liver volume (RLV), and tumor volume (TuV).

The relative future liver remnant volume (aFLR, adjusted future liver remnant) was calculated automatically, reflecting the proportion of functionally preserved parenchyma and serving as a key safety criterion for the planned intervention (optimal threshold ⩾ 30%). The finalized 3D models were exported in STL format, underwent post-processing in Blender software (Blender Online Community, version 4.0.2) with color labeling of anatomical structures, and were subsequently converted into glTF (.glb) format for use in 3D visualization and augmented reality systems[1].

The entire 3D modeling workflow was performed by surgeons from the specialized hepatopancreatobiliary surgery department with experience in 3D modeling, in close collaboration with a radiologist from Botkin Hospital. The initial automatic CT segmentation generated by the HepatoScan AI system was reviewed and, when necessary, manually corrected by the head of the radiology department (Maxim P. Onishchenko).

Final construction of the virtual liver models and determination of the planned RV were conducted through close interdisciplinary collaboration between the operating surgeons (Mikhail M. Tavobilov, Alexey A. Karpov, Aysa V. Lantsynova, Mark N. Aladin, Kirill A. Abramov, Evgeny B. Kudryash) and the 3D modeling specialist (Mark N. Aladin). The average time required to generate an individualized 3D liver model was approximately one hour (Fig. 1).

Patient stratification according to the TROPH-L classification

The proposed TROPH-L classification enables structured characterization of the morphologic and anatomical features of focal liver lesions and allows stratification of patients into three categories of surgical complexity, which is of critical importance for determining the extent of resection and selecting the optimal treatment strategy (Table 1).

This stratification makes it possible to anticipate the scope and technical complexity of surgery, the potential need for extended or combined resections, and the expected risk of postoperative complications. Integration of the TROPH-L classification with the HepatoScan AI system and 3D modeling algorithms provides a comprehensive preoperative planning framework

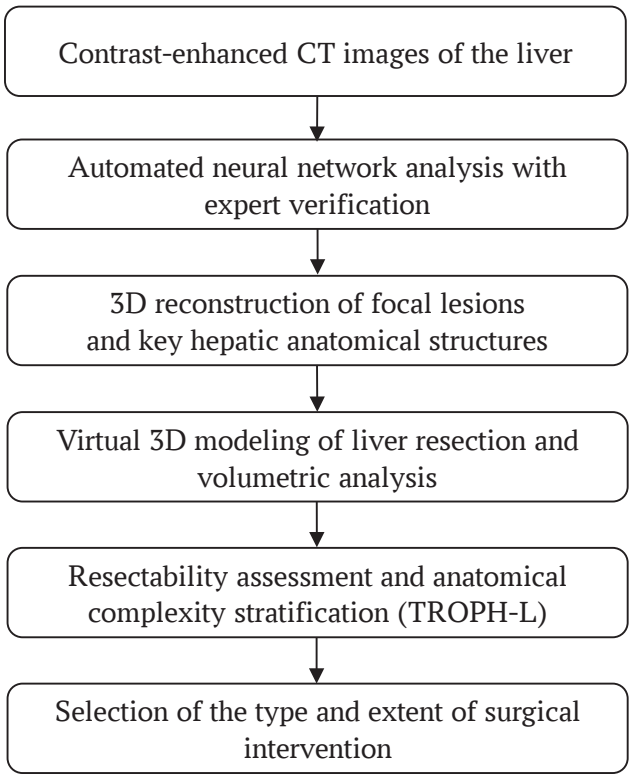

FIG. 1. Workflow of three-dimensional preoperative modeling in the surgical management of focal liver lesions.

Note: CT – computed tomography; TROPH-L – Tumor – Regional capsule – Outflow veins – Portal vein – Hepatic bile – Localization; 3D – three-dimensional.

[1] Blender Foundation. Blender — free and open-source 3D creation suite. Amsterdam: Blender Foundation; 2025. https://www.blender.org (access date: 24.10.2025).

based on objective anatomical and functional data. This approach ensures greater accuracy and consistency of surgical decision-making compared with traditional, largely subjective assessment methods.

Study design

A single-center comparative real-world study including a prospective AI-assisted cohort and a purposively matched retrospective cohort treated with conventional preoperative planning.

Sample size calculation

The required sample size was calculated based on the primary endpoint–differences in diagnostic performance, specifically sensitivity for detection and differential diagnosis of focal liver lesions. According to published data, the implementation of AI algorithms in radiological diagnostics is associated with an 8–12% increase in diagnostic sensitivity. Assuming an expected sensitivity improvement of at least 8%, a two-sided significance level of $\alpha = 0.05$, and a study power of 80%, the minimum required sample size was estimated to be no fewer than 90 patients per group.

Patient enrollment

All patients who underwent surgical treatment in the specialized Hepatopancreatobiliary Surgery Department of Botkin Hospital between January 21, 2021, and June 27, 2025, were screened for eligibility.

Inclusion criteria:

- age ⩾ 18 years;
- written informed consent for study participation;
- presence of a focal liver lesion requiring surgical treatment;
- availability of preoperative multiphasic contrast-enhanced abdominal CT;
- availability of intraoperative assessment data and/or histological verification.

Exclusion criteria:

- parasitic liver cysts;
- metastatic liver tumors and primary hepatic sarcomas;
- diagnostically non-informative CT images;
- incomplete clinical or radiological data.

The prospective AI-assisted cohort included patients treated between February 1, 2023, and June 27, 2025, in which the HepatoScan AI clinical decision support system integrated with 3D modeling

Table 1. **Surgical complexity categories according to the TROPH-L classification**

Characteristic	I (low risk)	II (moderate risk)	III (high risk)
Lesion size and growth pattern	<5 cm, peripheral location	5–10 cm	centrally located or multifocal tumor
Relationship of the lesion to the hepatic capsule	subcapsular	subcapsular or intraparenchymal	subcapsular or intraparenchymal
Hepatic vein involvement	none	invasion of segmental veins	invasion of major hepatic vein branches
Portal vein branch involvement	none	invasion of segmental branches	invasion of major portal vein branches
Biliary hypertension	none	segmental or sectoral hypertension	lobal hypertension
Surgical planning	technically safe RV	use of 3D modeling to define the resection plane	detailed 3D reconstruction and assessment of the aFLR
Volumetric assessment	not required	calculation recommended: TLV, RV, RLV, TuV, aFLR	mandatory calculation: TLV, RV, RLV, TuV, aFLR
Segmentation example	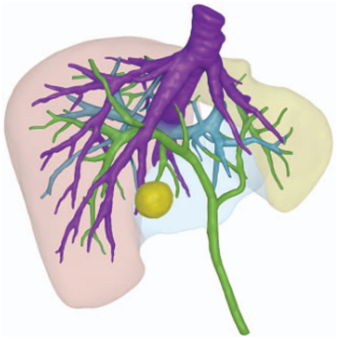	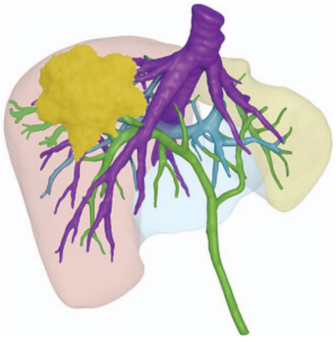	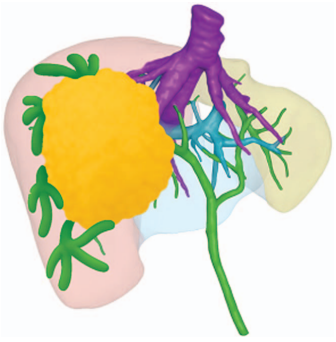
Coding example	Tc1R1O0P0H0 – L4b	Ti4R0O1P2H1 – L7	Ti3R1O3P3H3R – L4–L7

Notes: green indicates the biliary ducts, purple represents the hepatic venous system, blue corresponds to the portal venous system, and yellow denotes the focal lesion.
aFLR – adjusted future liver remnant; RLV – remnant liver volume; RV – resection volume; TLV – total liver volume; TuV – tumor volume; 3D – three-dimensional.

was used during preoperative planning. Initially, 148 patients were assessed for inclusion; 44 patients met the exclusion criteria. A total of 104 patients were included in the final analysis (Fig. 2). The distribution by pathology was as follows: liver carcinomas (n = 30), including cholangiocarcinoma (CCA, n = 11) and hepatocellular carcinoma (HCC, n = 19), liver hemangiomas (n = 22), simple liver cysts (n = 30), and FNH (n = 22).

To minimize the impact of differences in pathological composition on diagnostic and surgical outcomes, a purposefully matched retrospective cohort was formed in accordance with established methodology for comparative surgical studies. Matching was performed at the subgroup level according to lesion type, with consideration of lesion size and key demographic characteristics.

For inclusion in the standard preoperative planning group (retrospective cohort), 174 patients with focal liver lesions who underwent surgical treatment between January 21, 2021, and January 25, 2023, were evaluated. Seventy-four patients were excluded based on the exclusion criteria. The final retrospective cohort consisted of 100 patients with the following diagnoses: liver carcinomas (n = 27), including CCA (n = 7) and HCC (n = 20), liver hemangiomas (n = 23), simple liver cysts (n = 30), and FNH (n = 20). Patient inclusion and allocation are illustrated in Figure 2.

Analysis of diagnostic effectiveness

All patients from both cohorts were included in the analysis of diagnostic effectiveness. For each patient, a unified preoperative diagnostic conclusion regarding the nature of the focal liver lesion was established and used to calculate diagnostic performance metrics. In patients with multiple lesions, analysis was performed at the level of the clinically dominant lesion that determined the surgical strategy.

Comparison of HepatoScan AI–assisted results with the reference standard was performed by expert assessment at the level of the final clinical diagnostic conclusion.

The reference standard varied depending on lesion type. For suspected malignant tumors, diagnostic accuracy was assessed by comparing the preoperative HepatoScan AI conclusion with results of preoperative morphological verification (biopsy), followed by confirmation of the final diagnosis based on histopathological examination of the resected specimen. For benign focal liver lesions, the reference standard was the conclusion of an experienced radiologist based on multiphasic contrast-enhanced CT, corroborated by intraoperative findings and the clinical course of the disease.

Analysis of clinical effectiveness

The analysis of clinical effectiveness of the HepatoScan AI clinical decision support system included patients from both cohorts with anatomically complex focal liver lesions corresponding to TROPH-L categories II–III.

Patients with TROPH-L category I lesions were excluded from this analysis: 50 patients from the prospective cohort and 45 patients from the retrospective cohort. All patients with simple liver cysts in both cohorts were excluded; all of them underwent cyst fenestration.

The final clinical effectiveness analysis included 54 patients from the prospective cohort and 55 patients from the retrospective cohort with liver carcinomas, hemangiomas, and FNH. The compared groups were evaluated with respect to operative time, intraoperative blood loss, and the rate of blood transfusions. In addition, oncological radicality in patients with liver carcinomas (rate of R0 resections), postoperative complication rates – including severe complications graded III–V according to the Clavien–Dindo classification – length of hospital stay, and in-hospital mortality were analyzed.

Surgical technique

All surgical procedures were performed using standard surgical techniques. The choice of surgical approach (open or laparoscopic) was determined on an individual basis, taking into account lesion localization, size, relationships with vascular and biliary structures, and the planned extent of resection. Liver parenchymal transection was carried out using an ultrasonic dissector and bipolar coagulation; in selected cases, an ultrasonic aspirator–destructor was employed with stepwise identification and control of vascular and biliary structures. The Pringle maneuver was applied selectively and only when indicated, in cases with an anticipated risk of significant intraoperative blood loss.

Statistical analysis

Statistical analysis was performed using IBM SPSS Statistics software version 30.0 (SPSS: An IBM Company, USA) and the R programming language (version 4.4.1), with the use of specialized packages *pROC* (version 1.18.0) and *stats* (base R package).

Quantitative variables were initially assessed for normality using the Shapiro–Wilk test. Depending on the distribution, data are presented as mean with standard deviation ($M \pm SD$) or median with interquartile range (Me ($Q1$; $Q3$)). Between-group comparisons of continuous variables were performed using Student's t-test for normally distributed data or the Mann–Whitney U test for non-normally distributed data.

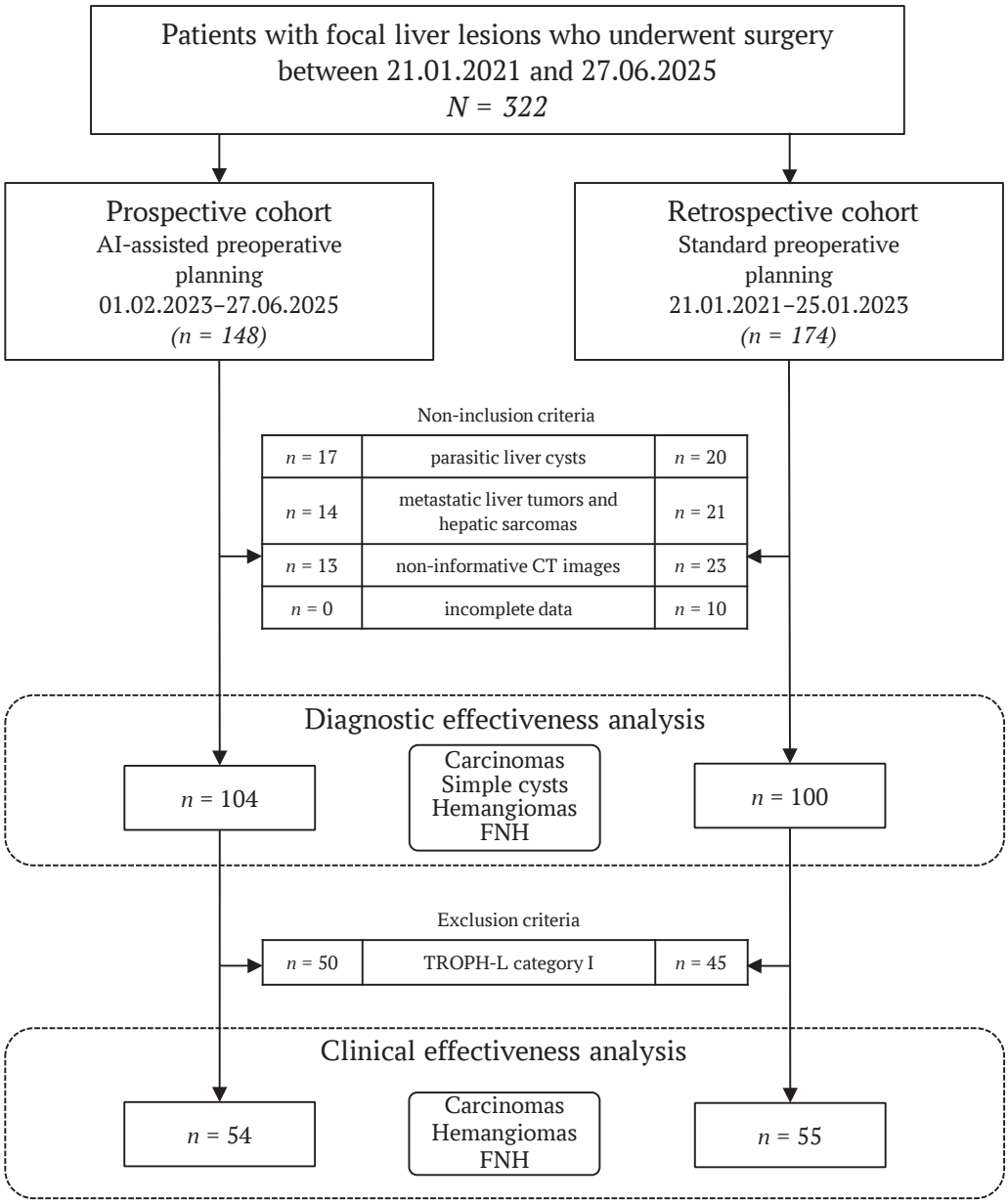

FIG. 2. Flow diagram of patient inclusion in the study.

Note: AI – artificial intelligence; CT – computed tomography; TROPH-L – Tumor – Regional capsule – Outflow veins – Portal vein – Hepatic bile – Localization; FNH – focal nodular hyperplasia.

Categorical variables are presented as absolute and relative frequencies and were compared using Pearson's χ^2 test or Fisher's exact test when expected cell counts were below five. Comparisons of blood transfusion rates between groups were performed using aggregated data and a Poisson regression model to calculate incidence rate ratios (IRR).

Diagnostic performance of the HepatoScan AI system was evaluated on a per-patient basis and included calculation of sensitivity, specificity, and the area under the ROC curve (AUROC), with corresponding 95% confidence intervals (CI).

For malignant focal liver lesions, the reference standard was based on preoperative morphological verification (biopsy) followed by confirmation of the final diagnosis through histopathological examination of the resected specimen. For benign focal liver lesions, the reference standard consisted of the radiologist's conclusion based on multiphasic contrast-enhanced CT, corroborated by intraoperative findings and the clinical course of the disease. Comparisons of AUROC values between groups were performed using the nonparametric DeLong test.

Differences were considered statistically significant at $p < 0.05$.

RESULTS

Diagnostic performance of the HepatoScan AI system

The study groups did not differ significantly with respect to key demographic characteristics, including age, sex, and the presence of comorbid or background diseases. No statistically significant differences were observed between groups in terms of lesion size, number, multiplicity, or anatomical localization. Retrospective assessment of case complexity in the standard preoperative planning group using the TROPH-L classification demonstrated a distribution of risk categories comparable to that of the prospective AI-assisted preoperative planning group (Table 2).

When individual nosological subgroups were analyzed, no statistically significant differences in sensitivity, specificity, or AUROC of the ROC curve were observed between the groups. Across all subgroups, a consistent trend toward higher diagnostic performance metrics was noted in the AI-assisted preoperative planning group; however, due to the limited size of the subgroups, these differences did not reach statistical significance. When diagnostic metrics were compared across all types of focal liver lesions, integration of the HepatoScan AI system was associated with improved diagnostic sensitivity for focal liver lesions compared with the standard diagnostic approach (Table 3).

Clinical effectiveness of the HepatoScan AI system and three-dimensional preoperative modeling

The use of 3D modeling was most clinically justified in patients classified as TROPH-L categories II and III. This subgroup included 54 patients from the prospective cohort and 55 patients from the retrospective cohort. The compared groups did not differ significantly in terms of key clinical and demographic characteristics, prevalence of comorbidities, lesion size, anatomical localization, lesion multiplicity, or – among patients with carcinomas – tumor stage and histological grade (Table 4).

At the surgical stage, integration of the neural network–based clinical decision support system HepatoScan AI in combination with 3D preoperative modeling had a meaningful impact on the choice of surgical strategy in patients classified as TROPH-L categories II–III. In the AI-assisted preoperative planning group, a trend toward a more parenchyma-sparing approach was observed: extended anatomical liver resections were performed less frequently (27.8% vs 38.2% in the standard preoperative planning group), while the proportion of non-anatomical (atypical) resections was higher (55.6% vs 45.5%). The frequency of segmentectomies did not differ significantly between groups (Table 5).

In the subgroup of patients with carcinomas, R0 resection was achieved in all patients in the AI-assisted preoperative planning group (100%) compared with 91.3% in the standard preoperative planning group; however, this difference did not reach statistical significance ($p = 0.18$).

The use of AI technologies and 3D modeling was associated with improved intraoperative parameters. In the AI-assisted preoperative planning group, the mean operative time was reduced by approximately 20 minutes. A more pronounced effect was observed for intraoperative blood loss: mean blood loss in the AI-assisted group was 120 mL lower than in the standard preoperative planning group. In the AI-assisted preoperative planning group, a total of 4 units of packed red blood cells were transfused in 54 patients, corresponding to 0.07 units per patient, whereas in the standard preoperative planning group 13 units were transfused in 55 patients (0.24 units per patient). Accordingly, the rate of blood transfusion use was approximately 3.2 times higher in the standard preoperative planning group (incidence rate ratio 3.19; 95% CI 1.04–9.76).

The reduction in intraoperative surgical trauma was reflected in postoperative outcomes. In the AI-assisted preoperative planning group, a trend toward a lower overall rate of postoperative complications (28% vs 40%) as well as severe complications (Clavien–Dindo grades III–V: 9% vs 18%) was observed compared with the standard preoperative planning group; however, given the sample size, these differences did not reach statistical significance ($p = 0.17$).

In the AI-assisted preoperative planning group, severe complications were recorded in five patients and included postoperative bleeding ($n = 3$), pulmonary embolism ($n = 1$), and a biliary fistula Grade B according to the International Study Group of Liver Surgery (ISGLS) classification ($n = 1$) requiring percutaneous drainage under ultrasound guidance. No cases of acute postoperative liver failure were observed in this group. In the standard preoperative planning group, severe postoperative complications ($n = 10$) included acute postoperative liver failure ($n = 3$), clinically significant postoperative bleeding ($n = 4$), pulmonary embolism ($n = 1$), and biliary complications in the form of ISGLS Grade B biliary fistulas ($n = 2$), which required percutaneous drainage under ultrasound guidance.

In-hospital mortality was observed only in the standard preoperative planning group ($n = 2$); in both cases, death was attributable to progression of acute postoperative liver failure following extensive liver resections.

DISCUSSION

The results of the present study demonstrate that integration of AI technologies into the diagnostic

Table 2. **Baseline characteristics of patients in the study groups**

Parameter	AI-assisted group (*n* = 104)	Conventional planning group (*n* = 100)	*p* value
Age, years	59.7 ± 11.1	60.3 ± 10.5	0.62
Male / female	56 / 44 (54% / 46%)	53 / 47 (53% / 47%)	0.67
BMI, kg/m²	27.1 (24.4; 29.8)	26.8 (24.0; 29.6)	0.51
Arterial hypertension	52 (50%)	49 (49%)	0.89
Type 2 diabetes mellitus	21 (20.2%)	19 (19%)	0.83
Chronic liver disease	10 (9.6%)	13 (13%)	0.45
Cardiovascular diseases	30 (28.8%)	28 (28%)	0.89
ASA physical status, class			
I–II	64 (61.5%)	58 (58%)	0.61
III	40 (38.5%)	42 (42%)	
Lesion diameter, mm	65 (45; 85)	60 (43; 77)	0.61
Multiple lesions (≥ 2)	26 (25%)	20 (20%)	0.39
Lesion localization			
right lobe	62 (60%)	65 (65%)	0.71
left lobe	31 (30%)	25 (25%)	
both lobes	11 (10%)	10 (10%)	
TROPH-L categories			
I	50 (48%)	45 (45%)	0.90
II	40 (38.5%)	40 (40%)	
III	14 (13.5%)	15 (15%)	
Carcinomas, stage	*n* = 30	*n* = 27	
I	12 (40%)	10 (37%)	0.97
II	13 (43%)	12 (44%)	
III	5 (17%)	5 (19%)	
Carcinomas, histological grade	*n* = 30	*n* = 27	
high	9 (30%)	8 (30%)	0.98
medium	15 (50%)	13 (48%)	
low	6 (20%)	6 (22%)	

Notes: quantitative variables are presented as mean with standard deviation (*M ± SD*) or median with interquartile range (Me (Q1; Q3)), categorical variables are presented as the absolute number of patients with the characteristic and the proportion within the group, expressed as a percentage (in parentheses).

AI – artificial intelligence; ASA – American Society of Anesthesiologists; BMI – body mass index; TROPH-L – Tumor – Regional capsule – Outflow veins – Portal vein – Hepatic bile – Localization.

workflow for liver tumors is associated with improved detection of focal liver lesions. Compared with the standard diagnostic approach, use of the HepatoScan AI system resulted in a statistically significant increase in the sensitivity of preoperative diagnosis for all focal liver lesions by 9.1% (from 84.2% to 93.3%), while maintaining a high level of specificity (91.8%).

The observed improvement in diagnostic accuracy with AI assistance is consistent with current literature. Several studies have shown that deep learning models are capable of detecting hepatic tumor lesions with accuracy comparable to expert radiologist assessment and, in some cases, identifying additional lesions not recognized during conventional visual analysis [6, 9]. Moreover, it has been reported that the combined use of expert interpretation and AI algorithms increases the sensitivity of focal liver lesion detection from approximately 80% to 88% [15].

Visualization of the liver as an interactive 3D model enables "virtual navigation" within the organ, precise calculation of RV, and prediction of the risk of postoperative liver failure – features that are particularly important in cases of complex tumor localization. The TROPH-L classification developed and first introduced in this study integrates AI-based segmentation with 3D reconstruction and illustrates the feasibility of using objective morphological and topographic–anatomical parameters for standardized stratification of surgical risk. Overall, this approach aligns with the global trend toward personalized surgical treatment based on large-scale data analysis and the application of AI [16].

In the present study, automated 3D reconstruction of liver anatomy demonstrated clear clinical benefits in patients with moderate and high surgical risk, corresponding to TROPH-L categories II–III. Compared

Table 3. **Diagnostic performance of the HepatoScan AI system in determining the nature of focal liver lesions**

	AI-assisted group (*n* = 104)	Conventional planning group (*n* = 100)	*p* value
Carcinoma	*n* = 30	*n* = 27	
sensitivity	92.9 (78.7–98.2)	81.5 (63.3–91.8)	n.s.
specificity	93 (85.1–97.1)	90 (81.5–95.3)	n.s.
AUROC	0.95 (0.89–1.00)	0.88 (0.79–0.97)	n.s.
Focal nodular hyperplasia	*n* = 22	*n* = 20	
sensitivity	88.2 (66.7–95.3)	78.6 (58.4–91.9)	n.s.
specificity	90.5 (81.9–95.0)	88 (78.5–93.1)	n.s.
AUROC	0.93 (0.85–1.00)	0.87 (0.77–0.97)	n.s.
Hemangioma	*n* = 22	*n* = 23	
sensitivity	96.3 (78.2–99.2)	85 (67.9–95.5)	n.s.
specificity	94.2	89.5 (80.8–94.6)	n.s.
AUROC	0.97 (0.92–1.00)	0.90 (0.81–0.99)	n.s.
Simple liver cyst	*n* = 30	*n* = 30	
sensitivity	98.1 (83.3–99.4)	92 (78.7–98.2)	n.s.
specificity	95.3 (86.9–97.9)	90.8 (82.5–96.0)	n.s.
AUROC	0.98 (0.94–1.00)	0.93 (0.86–1.00)	n.s.
All types of focal liver lesions			
sensitivity	93.3 (88.2–97.1)	84.2 (77.1–90.3)	0.008
specificity	91.8 (86.7–96.4)	88.5 (82.4–93.7)	n.s.
AUROC	0.95 (0.90–1.00)	0.89 (0.81–0.98)	n.s.

Notes: sensitivity and specificity data are presented as percentages with 95% CI (in parentheses), and AUROC as a value with a 95% CI (in parentheses).
AI – artificial intelligence; AUROC – area under the receiver operating characteristic curve; CI – confidence interval; n.s. – not significant.

with standard preoperative planning, the AI-assisted group showed more favorable intraoperative and postoperative outcomes: operative time was reduced by an average of 11%, intraoperative blood loss was approximately 30% lower, and the need for blood transfusions was reduced by about 3.2-fold. These findings reflect improved selection of surgical approach and extent of resection based on detailed preoperative 3D anatomical analysis.

Our results are consistent with data from multicenter studies demonstrating that the use of 3D visualization in liver resection planning leads to statistically significant reductions in operative time and blood loss, lower rates of postoperative liver failure and other complications, and shorter hospital stays [10, 11]. In particular, a recent prospective study showed that preoperative assessment using 3D reconstruction is associated with reduced surgical trauma and faster postoperative recovery compared with standard two-dimensional navigation [11].

The impact of 3D planning on oncological outcomes should also be emphasized. According to published data, the use of 3D navigation facilitates more accurate definition of resection margins and increases the rate of R0 resections [17]. In the present study, no cases of positive surgical margins (R1 resections) were observed in the group undergoing 3D reconstruction, whereas such cases occurred, albeit infrequently, in the standard preoperative planning group (2 of 23 patients, 8.7%). These findings are in agreement with meta-analyses demonstrating that 3D-assisted liver resections are associated with wider resection margins and lower recurrence rates [11, 16, 17].

Furthermore, more accurate calculation of the aFLR and detailed 3D visualization of tumor relationships with vascular and biliary structures may have contributed to a higher rate of parenchyma-sparing yet oncologically radical resections, avoiding unjustifiably extensive liver resections. This approach was associated with a trend toward a lower incidence of severe postoperative complications (Clavien–Dindo grade ⩾ III) and the absence of perioperative mortality, reflecting improved surgical safety [17, 18].

Taken together, these findings suggest that integration of neural network–based algorithms and 3D modeling can serve as an effective decision-support tool for personalized surgical planning. Such an approach has the potential to enhance the quality of preoperative diagnosis and improve short-term surgical outcomes in patients with focal liver lesions, making operative planning more objective and reproducible and surgical interventions safer and more effective.

Table 4. **Baseline characteristics of patients in the study groups with TROPH-L complexity categories II–III**

Parameter	AI-assisted group (*n* = 54)	Conventional planning group (*n* = 55)	*p* value
Age, years	60.5 ± 10.2	61.2 ± 9.8	n.s.
Male / female	29 / 25 (54% / 46%)	29 / 26 (53% / 47%)	n.s.
BMI, kg/m²	27.4 (24.5; 31.2)	27.0 (24.0; 30.8)	n.s.
Arterial hypertension	27 (50%)	27 (49%)	n.s.
Type 2 diabetes mellitus	11 (20%)	10 (18%)	n.s.
Chronic liver disease	5 (9%)	7 (13%)	n.s.
Cardiovascular diseases	16 (30%)	15 (27%)	n.s.
ASA physical status, class			
I–II	33 (61%)	32 (58%)	n.s.
III	21 (39%)	23 (42%)	
Lesion diameter, mm	75 (55; 95)	70 (50; 90)	n.s.
Multiple lesions (≥ 2)	17 (32%)	14 (25.5%)	n.s.
Lesion localization			
right lobe	32 (59%)	36 (65.5%)	n.s.
left lobe	16 (30%)	14 (25.5%)	
both lobes	6 (11%)	5 (9%)	
TROPH-L categories			
II	40 (74%)	40 (73%)	n.s.
III	14 (26%)	15 (27%)	
Carcinomas, stage	*n* = 26	*n* = 23	
I	8 (31%)	6 (26%)	n.s.
II	13 (50%)	12 (52%)	
III	5 (19%)	5 (22%)	
Carcinomas, histological grade	*n* = 26	*n* = 23	
high	8 (31%)	7 (30%)	n.s.
medium	13 (50%)	11 (48%)	
low	5 (19%)	5 (22%)	

Notes: quantitative variables are presented as mean with standard deviation (*M* ± *SD*) or median with interquartile range (Me (*Q*1; *Q*3)), categorical variables are presented as the absolute number of patients with the characteristic and the proportion within the group, expressed as a percentage (in parentheses).
AI – artificial intelligence; ASA – American Society of Anesthesiologists; BMI – body mass index; n.s. – not significant; TROPH-L – Tumor – Regional capsule – Outflow veins – Portal vein – Hepatic bile – Localization.

At the same time, widespread implementation of these systems requires further investigation and resolution of several organizational and technical challenges. It should be acknowledged that most studies on AI-based liver imaging are based on retrospective data from relatively small cohorts [19], which limits the strength of conclusions. Nevertheless, the rapid advancement of machine learning technologies and the accumulation of prospective clinical data provide grounds to anticipate an increasingly prominent role for such tools in routine clinical practice.

Limitations

When interpreting the results of this study, several limitations should be considered. First, the comparison between a retrospective cohort (2021–2023) and a prospective cohort (2023–2025) may reflect not only the impact of digital technology implementation but also temporal changes in surgical techniques and perioperative patient management. Second, the relatively small sample size – particularly after stratification by nosological subgroups and TROPH-L complexity categories – limits the statistical power of the analysis and the ability to detect differences in certain clinical outcomes. In addition, different reference standards were applied for different types of focal liver lesions, and comparisons involving the HepatoScan AI system were performed at the level of the final clinical diagnostic conclusion, which does not fully exclude the influence of expert interpretation. Finally, the single-center design of the study and the use of the proprietary TROPH-L classification may limit the generalizability of the findings and their direct comparability with results from other studies.

Table 5. **Clinical effectiveness of the HepatoScan AI system and three-dimensional preoperative modeling**

Characteristic	AI-assisted group (*n* = 54)	Conventional planning group (*n* = 55)	*p* value
Type of surgical procedure			
extended anatomical liver resection	15 (28%)	21 (38%)	
non-anatomical (atypical) resection	30 (56%)	25 (46%)	n.s.
segmentectomy	9 (17%)	9 (16%)	
Operative time, min	160 (135; 190)	180 (150; 210)	0.01
Intraoperative blood loss, mL	280 (200; 400)	400 (300; 600)	0.004
Blood transfusions, number of packed red blood cell units, *n*	4	13	0.04
R0 resection for liver carcinomas, number of patients	26 out of 26 (100%)	21 out of 23 (91%)	n.s.
All postoperative complications, number of patients	15 (28%)	22 (40%)	n.s.
Severe complications (Clavien–Dindo grades III–V), number of patients	5 (9%)	10 (18%)	n.s.
Length of hospital stay, days	11 (9; 13)	12 (10; 15)	n.s.
In-hospital mortality, number of patients	0	2 (3.6%)	n.s.

Notes: quantitative variables are presented as median with interquartile range (Me (*Q*1; *Q*3)), categorical variables are presented as the absolute number of patients with the characteristic and the proportion within the group, expressed as a percentage (in parentheses).
AI – artificial intelligence; n.s. – not significant.

CONCLUSION

In this single-center comparative study, integration of neural network–based CT analysis with interactive 3D preoperative modeling (HepatoScan AI) was associated with increased sensitivity for detection and classification of focal liver lesions compared with the standard approach. Automated segmentation, quantitative 3D volumetry, and the TROPH-L classification enabled standardized assessment of anatomical complexity and resectability, which was particularly relevant for patients classified as TROPH-L categories II–III. In this subgroup, AI assistance and 3D planning were associated with improvements in selected intraoperative parameters and a trend toward a lower incidence of severe postoperative complications, while maintaining oncological radicality. Further prospective multicenter studies are warranted to standardize methodologies for evaluating digital tools in liver surgery and to validate these findings across broader clinical settings.

AUTHORS CONTRIBUTIONS

Alexey V. Shabunin and Mikhail M. Tavobilov conceptualized and designed the study and contributed to the surgical procedures. Mark N. Aladin curated the clinical data, contributed to the surgical procedures, performed 3D image segmentation and post-processing, conducted data analysis, and contributed to the development and validation of artificial intelligence algorithms and 3D modeling. Alexey A. Karpov contributed to the surgical procedures and provided organizational and methodological oversight of the surgical component of the study. Aysa V. Lantsynova and Kirill A. Abramov contributed to the surgical procedures, conducted the literature review, and supported clinical data analysis. Evgeny B. Kudryash contributed to the surgical procedures and performed statistical analysis and interpretation of the results. Alexey V. Shabunin, Mikhail M. Tavobilov, and Mark N. Aladin contributed to manuscript drafting and critical revision. All authors reviewed and approved the final manuscript.

ВКЛАД АВТОРОВ

А.В. Шабунин и М.М. Тавобилов разработали концепцию и дизайн исследования, принимали участие в выполнении хирургических вмешательств. М.Н. Аладин осуществлял сбор клинического материала, принимал участие в хирургических вмешательствах, выполнял сегментацию и постобработку 3D-изображений, анализ данных, а также участвовал в разработке и валидации алгоритмов ИИ и 3D-моделирования. А.А. Карпов принимал участие в выполнении хирургических вмешательств и обеспечивал организационно-методическое сопровождение хирургического этапа исследования. А.В. Ланцынова и К.А. Абрамов принимали участие в хирургических вмешательствах, выполняли научный поиск литературы и участвовали в клиническом анализе данных. Е.Б. Кудряш принимал участие в хирургических вмешательствах, статистическом анализе и интерпретации результатов. А.В. Шабунин, М.М. Тавобилов и М.Н. Аладин участвовали в написании и научной редактуре текста статьи. Все авторы утвердили окончательную версию публикации.

REFERENCES / ЛИТЕРАТУРА

1. *Rumgay H., Arnold M., Ferlay J., et al.* Global burden of primary liver cancer in 2020 and predictions to 2040. J Hepatol. 2022 Dec; 77(6): 1598–1606. https://doi.org/10.1016/j.jhep.2022.08.021. Epub 2022 Oct 5. PMID: 36208844
2. *Ding Z.B., Shi Y.H., Chen J.F., et al.* Recent advances in surgical management strategies for hepatocellular carcinoma. hLife. 2024; 2(9): 439–453. https://doi.org/10.1016/j.hlife.2024.06.007
3. *Yang S., Ni H., Zhang A., et al.* Impact of postoperative morbidity on the prognosis of patients with hepatocellular carcinoma after laparoscopic liver resection: a multicenter observational study. Sci Rep. 2025 Jan; 15(1): 1724. https://doi.org/10.1038/s41598-024-85020-9. PMID: 39799160
4. *Rahman H., Bukht T.F.N., Imran A., et al.* A Deep Learning Approach for Liver and Tumor Segmentation in CT Images

Using ResUNet. Bioengineering (Basel). 2022 Aug; 9(8): 368. https://doi.org/10.3390/bioengineering9080368. PMID: 36004893
5. *Chatzikomnitsa P., Gkaitatzi A.D., Papakonstantinou M., et al*. The role of artificial intelligence and 3D printing in minimally invasive liver surgery. Mini-invasive Surg. 2025; 9: 8. https://doi.org/10.20517/2574-1225.2024.78
6. *Efstathiou A., Charitaki E., Triantopoulou C., Delis S.* Artificial Intelligence and Digital Tools Across the Hepato-Pancreato-Biliary Surgical Pathway: A Systematic Review. J Clin Med. 2025 Sep; 14(18): 6501. https://doi.org/10.3390/jcm14186501. PMID: 41010705
7. *Manjunath R.V., Kwadiki K.* Modified U-NET on CT images for automatic segmentation of liver and its tumor. Biomedical Engineering Advances. 2022; 4: 100043. https://doi.org/10.1016/j.bea.2022.100043
8. *Banchini F., Capelli P., Hasnaoui A., et al.* 3-D reconstruction in liver surgery: a systematic review. HPB (Oxford). 2024 Oct; 26(10): 1205–1215. https://doi.org/10.1016/j.hpb.2024.06.006. Epub 2024 Jun 18. PMID: 38960762
9. *Yin C., Zhang H., Du J., et al*. Artificial intelligence in imaging for liver disease diagnosis. Front Med (Lausanne). 2025 Apr; 12: 1591523. https://doi.org/10.3389/fmed.2025.1591523. PMID: 40351457
10. *Zeng X., Tao H., Dong Y., et al*. Impact of three-dimensional reconstruction visualization technology on short-term and long-term outcomes after hepatectomy in patients with hepatocellular carcinoma: a propensity-score-matched and inverse probability of treatment-weighted multicenter study. Int J Surg. 2024 Mar; 110(3): 1663–1676. https://doi.org/10.1097/JS9.0000000000001047. PMID: 38241321
11. *Agrawal H., Tanwar H., Gupta N.* Revolutionizing hepatobiliary surgery: Impact of three-dimensional imaging and virtual surgical planning on precision, complications, and patient outcomes. Artif Intell Gastroenterol. 2025; 6(1): 106746. https://doi.org/10.35712/aig.v6.i1.106746
12. *Васильев Ю.А., Владзимирский А.В., Омелянская О.В. и др.* MOSMEDSOFT: CT HepatoScan AI. Свидетельство о государственной регистрации программы для ЭВМ RU 2025683642. Российская Федерация; заявка № 2025682549; дата регистрации 28.08.2025; дата публикации 05.09.2025. / *Vasilyev Yu.A., Vladzimirskiy A.V., Omelyanskaya O.V., et al.* MOSMEDSOFT: ST HepatoScan AI. Certificate of state registration of computer software No. RU 2025683642. Russian Federation; 2025 (In Russian).
13. *Шабунин А.В., Васильев Ю.А., Тавобилов М.М.* и др. Разработка системы помощи принятия врачебных решений в диагностике объемных новообразований печени на основе методов искусственного интеллекта. Анналы хирургической гепатологии. 2025; 30(2): 23–32. https://doi.org/10.16931/1995-5464.2025-2-23-32. EDN: NKWRDR / *Shabunin A.V., Vasilyev Y.A., Tavobilov M.M., et al.* Development of a clinical decision support system for the diagnosis of space-occupying liver lesions using artificial intelligence methods. Annaly khirurgicheskoy gepatologii = Annals of HPB surgery. 2025; 30(2): 23–32 (In Russian). https://doi.org/10.16931/1995-5464.2025-2-23-32. EDN: NKWRDR
14. *Fedorov A., Beichel R., Kalpathy-Cramer J., et al*. 3D Slicer as an image computing platform for the Quantitative Imaging Network. Magn Reson Imaging. 2012 Nov; 30(9): 1323–1341. https://doi.org/10.1016/j.mri.2012.05.001. PMID: 22770690
15. *Dai H., Xiao Y., Fu C., et al*. Deep Learning-Based Approach for Identifying and Measuring Focal Liver Lesions on Contrast-Enhanced MRI. J Magn Reson Imaging. 2025 Jan; 61(1): 111–120. https://doi.org/10.1002/jmri.29404. Epub 2024 Jun 3. PMID: 38826142
16. *Mei G., Yu J.* Research on CT image segmentation and classification of liver tumors based on attention mechanism and improved U-Net model. Technol Health Care. 2025 Sep; 33(5): 2468–2483. https://doi.org/10.1177/09287329251329294. Epub 2025 Apr 30. PMID: 40302502
17. *Montalti R., Rompianesi G., Cassese G., et al*. Role of preoperative 3D rendering for minimally invasive parenchyma sparing liver resections. HPB. 2023; 25(8): 915–923. https://doi.org/10.1016/j.hpb.2023.04.008
18. *Hori M., Suzuki Y., Sofue K., et al*. Artificial intelligence in imaging diagnosis of liver tumors: current status and future prospects. Abdom Radiol (NY). 2025 Jun. https://doi.org/10.1007/s00261-025-05059-8. Epub ahead of print. PMID: 40536541
19. *Li L., Cheng S., Li J., et al*. Randomized comparison of AI enhanced 3D printing and traditional simulations in hepatobiliary surgery. NPJ Digit Med. 2025 Jun; 8(1): 293. https://doi.org/10.1038/s41746-025-01571-9. PMID: 40457016

INFORMATION ABOUT THE AUTHORS / ИНФОРМАЦИЯ ОБ АВТОРАХ

Alexey V. Shabunin, Dr. of Sci. (Medicine), Professor, Academician of the RAS, Head of Department of Surgery, Transplantology and Applied Oncology, Russian Medical Academy of Continuing Professional Education; Director, Botkin Hospital.
ORCID: https://orcid.org/0000-0002-4230-8033

Шабунин Алексей Васильевич, д-р мед. наук, профессор, академик РАН, заведующий кафедрой хирургии, трансплантологии и прикладной онкологии ФГБОУ ДПО РМАНПО Минздрава России; директор ГБУЗ «ММНКЦ им. С.П. Боткина ДЗМ».
ORCID: https://orcid.org/0000-0002-4230-8033

Mikhail M. Tavobilov, Dr. of Sci. (Medicine), Professor, Department of Surgery, Transplantology and Applied Oncology, Russian Medical Academy of Continuing Professional Education; Senior Researcher, Head of the Department of Hepatopancreatobiliary Surgery, Botkin Hospital.
ORCID: https://orcid.org/0000-0003-0335-1204

Тавобилов Михаил Михайлович, д-р мед. наук, профессор кафедры хирургии, трансплантологии и прикладной онкологии ФГБОУ ДПО РМАНПО Минздрава России; старший научный сотрудник, заведующий отделением хирургии печени и поджелудочной железы ГБУЗ «ММНКЦ им. С.П. Боткина ДЗМ».
ORCID: https://orcid.org/0000-0003-0335-1204

Alexey A. Karpov, Dr. of Sci. (Medicine), Associate Professor, Department of Surgery, Transplantology and Applied Oncology, Russian Medical Academy of Continuing Professional Education; Senior Researcher, Deputy Chief Physician for Surgery, Botkin Hospital.
ORCID: https://orcid.org/0000-0002-5142-1302

Карпов Алексей Андреевич, д-р мед. наук, доцент кафедры хирургии, трансплантологии и прикладной онкологии ФГБОУ ДПО РМАНПО Минздрава России; старший научный сотрудник, заместитель главного врача по хирургии ГБУЗ «ММНКЦ им. С.П. Боткина ДЗМ».
ORCID: https://orcid.org/0000-0002-5142-1302

Mark N. Aladin✉, Junior Researcher, Surgeon, Department of Hepatopancreatobiliary Surgery, Botkin Hospital.
ORCID: https://orcid.org/0000-0001-9671-390X

Aysa V. Lantsynova, Cand. of Sci. (Medicine), Junior Researcher, Surgeon, Department of Hepatopancreatobiliary Surgery, Botkin Hospital.
ORCID: https://orcid.org/0000-0002-9461-6791

Kirill A. Abramov, Cand. of Sci. (Medicine), Junior Researcher, Surgeon, Department of Hepatopancreatobiliary Surgery, Botkin Hospital.
ORCID: https://orcid.org/0000-0001-9871-114X

Evgeny B. Kudryash, postgraduate student, Department of Surgery, Transplantology and Applied Oncology, Russian Medical Academy of Continuing Professional Education; Junior Researcher, Surgeon, Department of Hepatopancreatobiliary Surgery, Botkin Hospital.
ORCID: https://orcid.org/0000-0002-7870-808X

Аладин Марк Николаевич✉**,** младший научный сотрудник, врач-хирург отделения хирургии печени и поджелудочной железы ГБУЗ «ММНКЦ им. С.П. Боткина ДЗМ».
ORCID: https://orcid.org/0000-0001-9671-390X

Ланцынова Айса Владимировна, канд. мед. наук, младший научный сотрудник, врач-хирург отделения хирургии печени и поджелудочной железы ГБУЗ «ММНКЦ им. С.П. Боткина ДЗМ».
ORCID: https://orcid.org/0000-0002-9461-6791

Абрамов Кирилл Андреевич, канд. мед. наук, младший научный сотрудник, врач-хирург отделения хирургии печени и поджелудочной железы ГБУЗ «ММНКЦ им. С.П. Боткина ДЗМ».
ORCID: https://orcid.org/0000-0001-9871-114X

Кудряш Евгений Борисович, аспирант кафедры хирургии ФГБОУ ДПО РМАНПО Минздрава России; младший научный сотрудник, врач-хирург отделения хирургии печени и поджелудочной железы ГБУЗ «ММНКЦ им. С.П. Боткина ДЗМ».
ORCID: https://orcid.org/0000-0002-7870-808X

✉ Corresponding author / Автор, ответственный за переписку

Original article / Оригинальная статья
https://doi.org/10.47093/2218-7332.2025.16.4.20-30

Validation of a test setup for measuring compression load under elements of multilayer bandages: an *in vitro* study

Sergey K. Zazulin[1,✉], Svetlana M. Titkova[2], Mikhail V. Anurov[2], Gregory G. Gabuzov[2], Ekaterina Yu. Chizh[1,3], Alexey E. Brovkin[4]

[1] LLC "Innovative Technologies of Rehabilitation"
21, Mayskaya str., Pogorelki vill., Moscow Region, 141032, Russia
[2] N.I. Pirogov Russian National Research Medical University
1/6, Ostrovityanova str., Moscow, 117513, Russia
[3] Botkin Hospital
5, 2nd Botkinsky proezd, Moscow, 125284, Russia
[4] Central Clinical Military Hospital
20, Shchukinskaya str., Moscow, 123182, Russia

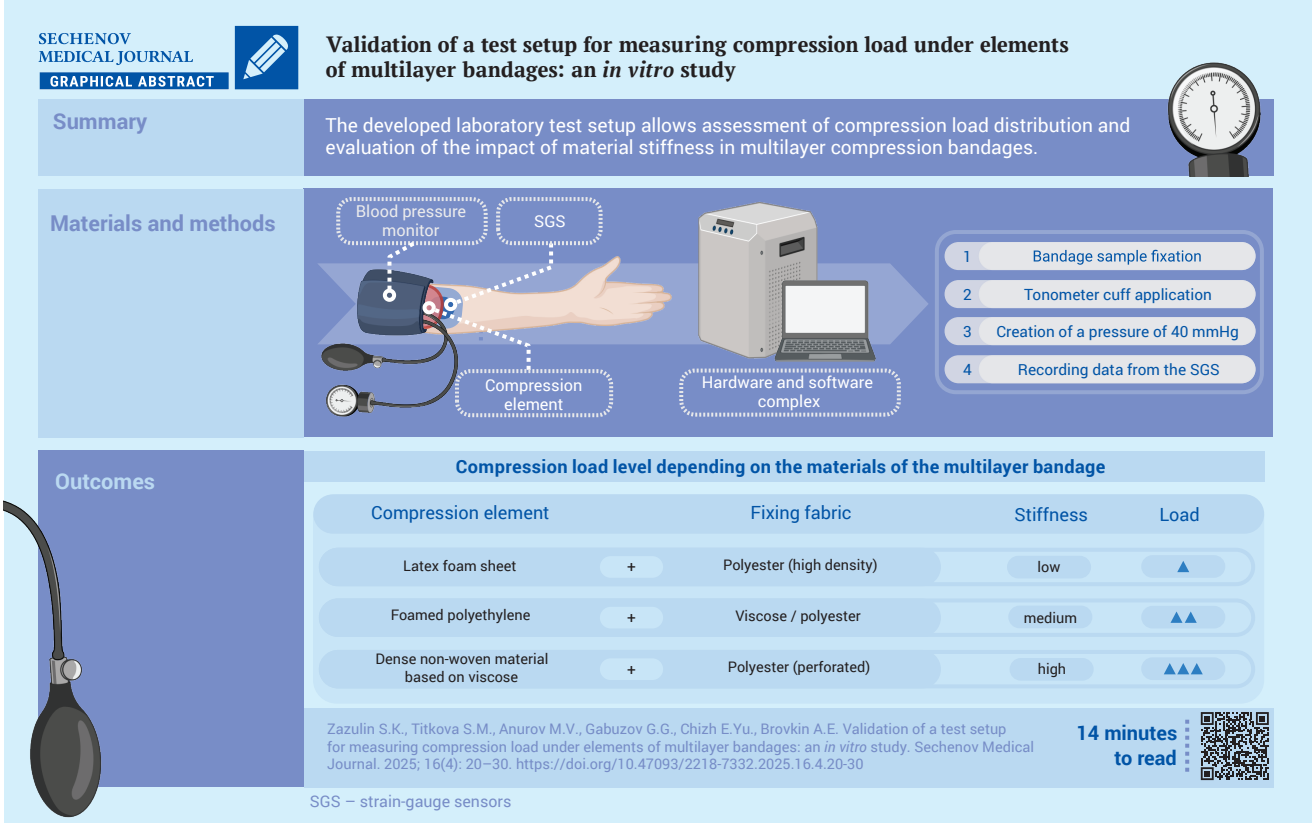

Abstract

Aim. To develop and validate a test setup for measuring the load under compression elements (CE) of multilayer bandages composed of materials with different stiffness.

Materials and methods. Prototypes of multilayer bandages were fabricated in the laboratory by combining three types of CEs (foam polymer and dense nonwoven viscose material) with three types of fixing fabrics (FF) based on polyester and viscose/polyester. The test setup consisted of an upper-limb model made of rigid plastic covered with artificial skin and a block with two strain-gauge sensors that recorded the load in gram-force (gf) under the CE area and in a control zone without a CE at an external pressure of 40 mmHg. For each CE–FF combination, 10 repeated

measurements were performed in two regions of the sample (60 values per sensor per group), and the data were analysed using nonparametric statistical tests.
Results. The load under the CE differed significantly between groups ($p < 0.001$) and depended on the type and stiffness of the material: the median load under type 3 CE with the highest stiffness was 259.4 (252.6; 263.3) gf, whereas under type 1 CE with the lowest stiffness it was 149.9 (145.1; 171.9) gf. Type 2 CE produced intermediate values of 241.7 (206.4; 259.3) gf. Testing of the FFs also showed statistically significant differences in pressure in the absence of a CE ($p < 0.001$): the highest load was recorded under type 2 FF (viscose/polyester) at 141.0 (140.2; 142.1) gf, and the lowest under type 1 FF made of polyester with higher surface density at 14.5 (14.3; 15.6) gf; type 3 FF provided an intermediate level of 65.7 (64.9; 69.3) gf.
Conclusion. The developed *in vitro* setup shows high sensitivity to differences in CE stiffness and FF properties and can be used as a screening tool for quantitative comparative assessment of multilayer bandage prototypes with locally differentiated compression areas prior to *in vivo* studies.

Keywords: peripheral edema; lymphedema; compression therapy; complex decongestant therapy, short-stretch bandage; differentiated compression
MeSH terms:
EDEMA – THERAPY
COMPRESSION BANDAGES
LYMPHEDEMA – THERAPY
For citation: Zazulin S.K., Titkova S.M., Anurov M.V., Gabuzov G.G., Chizh E.Yu., Brovkin A.E. Validation of a test setup for measuring compression load under elements of multilayer bandages: an *in vitro* study. Sechenov Medical Journal. 2025; 16(4): 20–30. https://doi.org/10.47093/2218-7332.2025.16.4.20-30

CONTACT INFORMATION:
Sergey K. Zazulin, Cand. of Sci. (Medicine), Scientific Director, LLC "Innovative Technologies of Rehabilitation".
Address: 21, Mayskaya str., Pogorelki vill., Moscow Region, 141032, Russia
E-mail: sk-z@mail.ru

Ethics statements. The study involved the development and in vitro testing of the experimental setup and did not include any experiments involving human participants or animals; therefore, approval by an ethics committee was not required.
Data availability. The data confirming the findings of this study are available from the authors upon reasonable request. Data and statistical methods used in the article were examined by a professional biostatistician on the Sechenov Medical Journal editorial staff.
Conflict of interest. The authors declare that there is no conflict of interest.
Financing. This study was supported by grant No. 89526 from the Foundation for Assistance to Small Innovative Enterprises (FASIE) dated December 11, 2023[1].

Received: 13.09.2025
Accepted: 25.11.2025
Date of publication: 30.12.2025

[1] https://online.fasie.ru/m/user-projects/registry (access date: 25.09.2025).

УДК 616-005.98-085.468.2

Валидация испытательного стенда для измерения компрессионной нагрузки под элементами многослойных повязок: исследование *in vitro*

С.К. Зазулин[1,✉], С.М. Титкова[2], М.В. Ануров[2], Г.Г. Габузов[2], Е.Ю. Чиж[1,3], А.Е. Бровкин[4]

[1] ООО «Инновационные технологии реабилитации»
ул. Майская, д. 21, д. Погорелки, Московская область, 141032, Россия
[2] ФГАОУ ВО «Российский национальный исследовательский медицинский университет имени Н.И. Пирогова» Министерства здравоохранения Российской Федерации
ул. Островитянова, д. 1, стр. 6, г. Москва, 117513, Россия
[3] ГБУЗ «Московский многопрофильный научно-клинический центр имени С.П. Боткина» Департамента здравоохранения города Москвы
пр-д 2-й Боткинский, д. 5, г. Москва, 125284, Россия
[4] ФГКУ «Центральный клинический военный госпиталь»
ул. Щукинская, д. 20, г. Москва, 123182, Россия

Аннотация

Цель. Разработать и валидировать испытательный стенд для измерения нагрузки под компрессионными элементами (КЭ) многослойных повязок, состоящих из различных по жесткости типов материала.

Материалы и методы. Лабораторно изготовлены прототипы многослойных повязок путем сочетания трех типов КЭ (из пенополимера и плотного нетканого материала из вискозы) и трех типов фиксирующих полотен (ФП) на основе полиэфира и вискозы/полиэфира. Испытательный стенд представлял собой макет верхней конечности из твердого пластика с искусственной кожей и блоком из двух тензорезистивных датчиков, регистрирующих нагрузку в граммах силы (гс) под участком с КЭ и контрольной зоной без КЭ при внешнем давлении 40 мм рт. ст. Для каждой комбинации КЭ–ФП выполняли по 10 повторных измерений в двух зонах образца (60 значений с датчика в группе); анализ проводили с использованием непараметрических критериев.

Результаты. Нагрузка под КЭ статистически значимо различалась между группами ($p < 0{,}001$) и зависела от типа и жесткости материала: медиана нагрузки под КЭ 3-го типа с максимальной жесткостью составила 259,4 (252,6; 263,3) гс, тогда как под КЭ 1-го типа с минимальной жесткостью – 149,9 (145,1; 171,9) гс. КЭ 2-го типа формировал промежуточные значения – 241,7 (206,4; 259,3) гс. Испытания ФП показали статистически значимые различия давления в отсутствие КЭ ($p < 0{,}001$): максимальная нагрузка зарегистрирована под ФП 2-го типа (вискоза/полиэфир) – 141,0 (140,2; 142,1) гс, минимальная – под ФП 1-го типа из полиэфира с большей поверхностной плотностью – 14,5 (14,3; 15,6) гс; ФП 3-го типа обеспечивало промежуточный уровень – 65,7 (64,9; 69,3) гс.

Заключение. Разработанный *in vitro* стенд демонстрирует высокую чувствительность к различиям жесткости КЭ и свойств ФП и может использоваться как скрининговый инструмент для количественной сравнительной оценки прототипов многослойных повязок с участками дифференцированной компрессии до проведения исследований *in vivo*.

Ключевые слова: периферические отеки; лимфедема; компрессионная терапия; комплексная деконгестивная терапия, бинт короткой растяжимости; дифференцированная компрессия

Рубрики MeSH:
ОТЕК – ТЕРАПИЯ
КОМПРЕССИОННЫЕ ПОВЯЗКИ
ЛИМФЕДЕМА – ТЕРАПИЯ

Для цитирования: Зазулин С.К., Титкова С.М., Ануров М.В., Габузов Г.Г., Чиж Е.Ю., Бровкин А.Е. Валидация испытательного стенда для измерения компрессионной нагрузки под элементами многослойных повязок: исследование *in vitro*. Сеченовский вестник. 2025; 16(4): 20–30. https://doi.org/10.47093/2218-7332.2025.16.4.20-30

КОНТАКТНАЯ ИНФОРМАЦИЯ:
Зазулин Сергей Константинович, канд. мед. наук, научный руководитель ООО «Инновационные технологии реабилитации».
Адрес: ул. Майская, д. 21, д. Погорелки, Московская область, 141032, Россия
E-mail: sk-z@mail.ru

Соответствие принципам этики. Исследование было посвящено разработке и *in vitro* испытаниям экспериментального стенда и не включало эксперименты с участием людей или животных, поэтому одобрение этического комитета не требовалось.
Доступ к данным исследования. Данные, подтверждающие выводы этого исследования, можно получить у авторов по обоснованному запросу. Данные и статистические методы, представленные в статье, прошли статистическое рецензирование редактором журнала – сертифицированным специалистом по биостатистике.
Конфликт интересов. Авторы заявляют об отсутствии конфликта интересов.
Финансирование. Исследование выполнено за счет гранта Фонда содействия инновациям № 89526 от 11.12.2023[2].

Поступила: 13.09.2025
Принята: 25.11.2025
Дата печати: 30.12.2025

Abbreviations:

CE – compression element
DC – differentiated compression
FF – fixing fabric
gf – gram-force
HSC – hardware and software complex
SGS – strain-gauge sensor

HIGHLIGHTS

Placement of two strain-gauge force sensors on the test bench enables simultaneous measurement of the applied load under standardized external pressure beneath distinct components of a multilayer bandage, including a compression element and a fixation nonwoven fabric.

The load distribution across bandage components is significantly influenced by both the stiffness of the compression elements and the type of the fixation nonwoven fabric. These factors should be taken into account in prototype design and material selection.

The proposed model represents a reproducible screening tool for the comparative assessment and optimization of multilayer bandage prototypes with differential compression zones during in vitro development.

Peripheral edema is a general clinical term used to describe chronic edema persisting for more than three months and characterized by complex, multivariate pathogenesis [1]. The prevalence of this condition reaches 20% among the working-age population, resulting in significant medical, social, and economic burden [2], including a significant reduction in patients' quality of life [3]. In clinical practice, peripheral edema often develops as a complication of anticancer treatment [4] and may be accompanied by the development of panniculitis [5] and progressive tissue fibrosis [6].

One of the leading clinically significant forms of peripheral edema is lymphedema, characterized by the accumulation of protein-rich interstitial fluid in the skin and subcutaneous tissue due to primary or secondary lymphatic drainage impairment [7]. According to literature data, over the past 10–15 years, the prevalence of lymphedema worldwide has been estimated at 140–250 million people [8–10]. In the Russian Federation, official statistics on lymphedema are not maintained. However, according to estimates by the Russian Association of Lymphologists, based on data from the World Health Organization, the number of patients with lymphedema in the country may could be as high as 10 million [11]. Over the past decade, there has been an increase in the incidence of lymphedema which is associated with an ageing population and the increase in the number of patients with cancer [4].

Due to its chronic nature, lymphedema requires long-term, step-by-step treatment based on the anatomical and functional characteristics of the lymphatic system [12]. Modern approaches to lymphedema therapy are based on the principles of Complex Decongestive Therapy, developed by M. Földi [13], which includes compression bandaging as a key component. Compression therapy determines the effectiveness of reducing the volume of limb edema [14].

To improve patient self-care and prevent recurrence of edema, multilayer compression bandaging techniques are widely used. In recent years, new materials and design solutions have been developed for the formation of

[2] Фонд содействия инновациям. https://online.fasie.ru/m/user-projects/registry (дата обращения: 25.09.2025).

multilayer compression bandages, including mobilizing systems with volumetric elements that perform a compressive function and generate locally differentiated pressure; hereinafter referred to as compression elements (CE). Examples of such systems that implement the principle of locally differentiated pressure through the use of foam polymer elements placed between layers of nonwoven materials are described in the literature. When exposed to external compression, areas of increased pressure are formed in the area of the volumetric elements, which facilitates the redistribution of edema fluid to surrounding areas with lower pressure and improves its reabsorption into venules and lymphatic capillaries [15, 16].

Currently, there are no registered mobilizing multilayer compression systems of this design on the Russian market, limiting the potential for comprehensive anti-edema therapy for lymphedema and edema of other etiologies. The development and commercialization of domestically produced alternatives is hampered, in part due to the lack of standardized testing methods and test setups for objectively evaluating the effectiveness of prototypes under development.

Aim. To develop and validate a test model for measuring the load beneath CE of multilayer bandages composed of materials with different stiffness.

MATERIALS AND METHODS

The study was conducted in two stages: the first stage (June 24, 2024–October 18, 2024) involved the production of multilayer compression bandage prototypes and the development of a test setup; the second stage (November 8, 2024–November 22, 2024) involved testing the developed model.

Stage 1
Manufacturing multilayer compression bandage prototypes

Nine multilayer bandage samples were laboratory-fabricated to replicate the differentiated compression (DC) achieved by similar compression bandages from foreign manufacturers. Each multilayer bandage consisted of a CE placed between two layers of fixing fabric (FF). Three types of CE and three types of FF were used in the study (Table).

Each multilayer bandage consisted of CE placed between two layers of FF. Nine types of multilayer bandages were studied: each of the three types of CE was married with each type of FF. The analysis used aggregated data separately by CE type or by FF type.

Development of a test setup

To simultaneously record pressure under various components of a multilayer bandages with DC areas, a test setup simulating a human limb was developed. The model is made of hard plastic covered with artificial skin. The setup has a rigid platform (mounting socket) for a block with two strain-gauge sensors (SGSs) and contact pads above them (Fig. 1). This block is placed inside the mounting socket. Herewith the SGSs are at the level of artificial leather and record in grams-force (gf) the applied load of the test object (compression bandages), placed under the cuff of a tonometer that generates external pressure.

To convert signals coming from the SGSs, a hardware and software complex (HSC) recorder was developed and manufactured. The HSC includes an ESP32 microcontroller (Espressif Systems, China), two analog-to-digital conversion modules based on the HX711 microcircuit (integrated circuit: Avia Semiconductor (Xiamen), China; module manufacturer: Shanghai Ruichi Industry Co., China), with a built-in programmable amplifier with a gain of up to 128 and 24-bit operation, as well as two MLC616C SGSs (Manyyear Technology Company Limited, China) with a permissible measurement range from 0 to 5 kg. The developed HSC is connected to a personal computer via a USB cable to receive power and transmit the recorded signals. A load recording system consisting of two SGSs and two contact pads above them, supports, and a unit with recording electronic devices was manufactured and mounted.

The developed microcontroller program code the initial initialization of the two SGSs and the amplifier

Table. **Characteristics of the components used in compression bandages**

Components compression bandages	Material	Density	Load at 40% sample deformation, kg/cm^2	Production
CE-1	Latex foam sheet	0.177 kg/cm^3	0.082	Experimental sample made by the authors
CE-2	Foamed polyethylene	0.225 kg/cm^3	0.123	Experimental sample made by the authors
CE-3	Dense non-woven material based on viscose	0.225 kg/cm^3	0.147	Experimental sample made by the authors
FF-1	Non-woven fabric – polyester 100%	45 g/m^2		Avangard LLC, Russia
FF-2	Non-woven fabric – viscose/ polyester 30/70%	40 g/m^2		Avangard LLC, Russia
FF-3	Non-woven perforated fabric – polyester 100%	40 g/m^2		Medline LLC, China

Note: CE – compression element of type 1, 2 or 3; FF – fixing fabric of type 1, 2 or 3.

FIG. 1. Test setup simulating a human limb.

Note: 1 and 2 – strain-gauge sensors, 3 – mounting socket.

chips with analog-to-digital converters. Then, readings are taken sequentially from the two SGSs, first from the first, then from the second, with a one-second interval between readings. The following data is transmitted to the PC via a USB cable and COM port every second: the measurement time elapsed since the HSC was turned on (in seconds), and the load values recorded on the first and second SGS (in gf). The accuracy of the SGSs readings is 0.01 gf. The data received from the HSC is written to a text file on the personal computer for subsequent processing and analysis.

Stage 2
Calibration of the developed model

The developed model was calibrated under experimental conditions before each series of tests. The load on the first SGS was recorded without a load and with a load equivalent to 5g. Before testing each of the three types of CE, five calibration tests were performed without the CE on the SGS I and with the CE secured on the SGS II without fixing bandage. For all tests, the CE size indicated the size of the sensor contact pad. The load was recorded during the first five seconds (Supplementary materials on the journal's website https://doi.org/10.47093/2218-7332.2025.16.4.20-30-annex).

Testing multilayer bandages prototypes

In three groups of samples, each grouped based on the type of CE material and the type of FF used, 10 repeated load measurements were taken in two randomly selected areas of each Prototype (a total of 60 readings from each sensor for each group). The Prototype size for the measurements was determined by assuming a clinically significant difference in load under the different CE types of 25% at a significance level of 0.05 and a power of 80% ($\beta = 0.20$).

During the study, the load values recorded on the first and second SGSs (in gs) were recorded every second for 10 minutes after applying the cuff of a mechanical tonometer and creating a pressure of 40 mmHg in it.

The strain gauge test protocol included the following steps:

1. Fixing the multilayer bandage sample to the test stand (Fig. 2A).
2. Mechanically removing the CE in the SGS I projection.
3. Fixing the sample to the test stand using a Peha-haft® cohesive self-adhesive bandage (Paul Hartmann AG, Germany).
4. Applying the mechanical tonometer cuff (Fig. 2B).
5. Inducing a predetermined pressure level in the cuff, simulating the pressure generated by a compression bandage on the specimen under a multilayer bandage.

This protocol allowed for simultaneous recording of the load under the area with CE and the control area without CE, allowing for a comparison of the contribution of the multilayer bandage construction and the applied FF to local pressure formation. This allowed for the evaluation of the effectiveness of different CE types under simulated imitation of local pression load. This allowed for the evaluation of the effectiveness of different CE types under simulated compression load.

Statistical analysis

Quantitative indicators were assessed for normal distribution using the Kolmogorov-Smirnov test. Descriptive statistics were presented as medians and interquartile ranges (25th and 75th percentiles) for

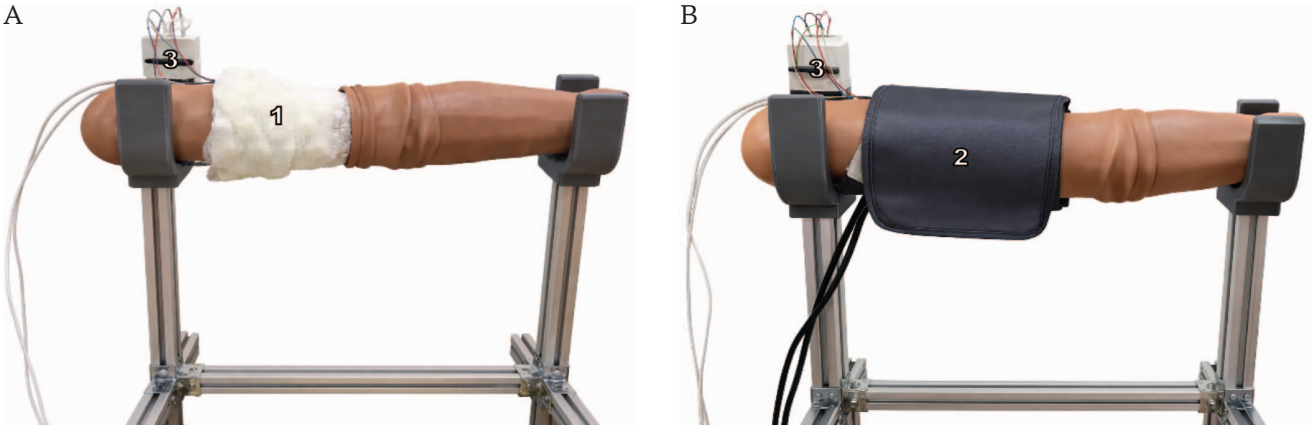

FIG. 2. Stages of strain gauge tests on the developed test setup.
A. Fixing the multilayer bandage sample to the simulator of a human upper limb.
B. Applying the cuff of a mechanical tonometer to the upper bandage to create an external pressure of 40 mm Hg.

Note: 1 – multilayer bandage; 2 – cuff of a mechanical tonometer; 3 – a hardware and software complex that records signals from strain-gauge sensors and transmits data to a personal computer.

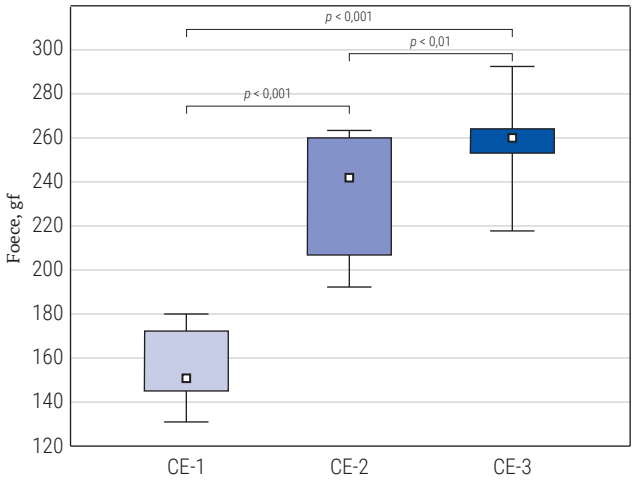

FIG. 3. Load recorded during the study of compression element sample.

Note: CE – compression element type 1, 2 or 3; gf – gram-force.

continuous variables with a non-normal distribution. Since the data were non-normally distributed, the Kruskal–Wallis test was used to compare results between groups. If statistically significant differences were detected between groups, paired comparisons were additionally performed using Dunn's *post-hoc* test. Differences in indicators were considered statistically significant at a significance level of $p < 0.05$. Statistical analysis was performed using Statistica 13.3 (StatSoft. Inc., USA).

RESULTS

The load recorded on the SGS II under the CE differed statistically significantly between groups and depended on the type and stiffness material of the CE ($p < 0.001$). The maximum load was recorded under the type 3 FF, characterized by the highest stiffness, and amounted to 259.4 (252.6; 263.3) gf. The minimum load was observed under the type 1 FF with the minimum stiffness – 149.9 (145.1; 171.9) gf (Fig. 3).

The type 2 FF occupied an intermediate position: the recorded load was 241.7 (206.4; 259.3) gf and statistically significantly differed from both the values obtained for the type 1 and type 3 FF. The data obtained showed that an increase in the CE stiffness was accompanied by an increase in the local load recorded beneath it, all other conditions being equal. The load recorded beneath the blended nonwoven viscose-polyester FF (FF-2) combined with CE 2 made of polyethylene foam was 1.6 times greater than the load recorded beneath the sample with FF-1 made of polyester nonwoven fabric combined with CE-1 made of latex foam.

The test setup also allowed us to record statistically significant differences in the load on the TSG I generated by different types of FF ($p < 0.001$). The highest load was recorded under FF type 2, made of a blended nonwoven material (viscose/polyester), and amounted to 141.0 (140.2; 142.1) gf.

The minimum load was recorded under FF type 1, made of polyester with the highest surface density – 14.5 (14.3; 15.6) gf. FF type 3, also made of polyester but with a lower density, generated an intermediate load level – 65.7 (64.9; 69.3) gf, which was statistically significantly different from the values for FF types 1 and 2 (Fig. 4).

DISCUSSION

One of the modern methods for treating peripheral edema, in whose pathogenesis lymphedema plays a significant role, is Complex Decongestive Therapy, and its effective component is compression bandaging

[15] using a multilayer bandage with areas of DC [16]. The development and production of such a product is associated with difficulties. It is necessary to select a material for each component (CE and FF), and also to study its compressive properties. While determining the mechanical properties of each component individually is not difficult, evaluating the effectiveness of a finished prototype of a multilayer bandage with areas of DC is currently practically impossible due to the lack of model setups and standard requirements for testing such products.

We developed a test setup consisting of simulating a human upper limb (a hard plastic covered with artificial skin) with a rigid platform for a block with two SGSs capable of simultaneously recording the load under various components of a multilayer bandage. The setup's design enables synchronous load recording in two zones: in the CE projection and in the zone under the FF in the absence of the CE. This measurement scheme is aimed at comparing the local CE impact with the "background" pressure of the multilayer structure, thereby enabling a more practical selection of prototypes.

In vitro pressure and stiffness measurement is a well-known method used to classify medical elastic compression devices. This relatively simple approach allows for easy reproducibility and recording of results [17–20]. There are models that measure pressure using a strain gauge and a pressure gauge. However, the sensors in these models record the overall pressure, not the selective pressure of the CE, while the external pressure gauge records the pressure on the surface of the limb [21, 22]. At the same time, it is the ratio of the pressure under the CE to the pressure under other zones of the multilayer bandage that can become a determining indicator for assessing the potential effectiveness of the product and selecting prototypes for further testing. Since it is assumed that multiple CEs, which are placed in a certain order in the bandages, create a significant pressure difference between the area in the projection of the CE and the area surrounding it, which improves lymph flow in the affected limb [23].

The developed test setup proved to be a sensitive instrument, allowing us to record statistically significant differences in the load under CEs with different stiffnesses, both when the stiffness difference reached 1.8 times (between CE types 1 and 3) and when the stiffness difference did not exceed 1.1 times (between FE types 2 and 3). Statistically significant differences were also recorded between the loads exerted by different types of FFs. The maximum load in the absence of FEs (141.0 gf) was demonstrated by a blended viscose/polyester nonwoven fabric.

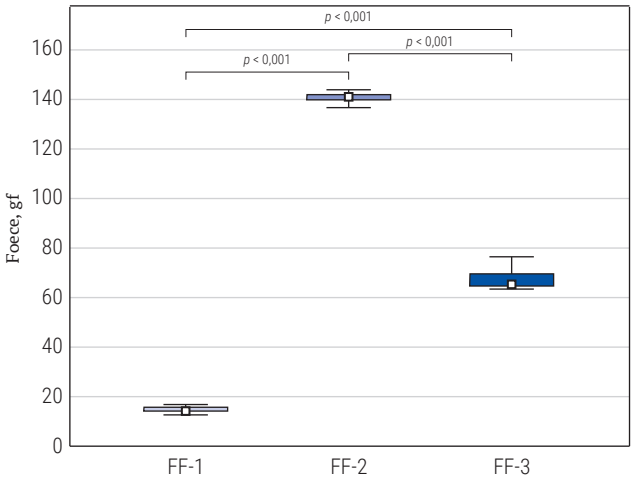

FIG. 4. Load recorded during the study of fixing fabric sample.

Note: FF – fixing fabric type 1, 2 or 3; gf – gram-force.

In the trials, a pressure of 40 mmHg was chosen to simulate the pressure generated by a multilayer compression bandage. The literature notes that lower pressure may be preferable for upper limb lymphedema, while the range of 40–60 mmHg appears to be more effective for lower limb lymphedema or when targeting specific areas of the upper limb (forearm, back of hand) [24, 25].

An original experimental model for recording pressure under the components of a multilayer bandage for *in vitro* studies has been developed. Comparison with existing international developments is difficult: despite the widespread use of SGS for assessing the functional characteristics of compression devises in preclinical and clinical studies [26, 27], no systems capable of recording selective pressure generated by individual layers of CE have been identified in the available literature.

An additional element of novelty is the choice of the limb model. Rigid limb mannequins are traditionally used to reproduce the conical shape of the limb [28]. However, even when using polyurethane foam pads, such systems do not consider natural skin turgor which can lead to significant discrepancies between the results and *in vivo* data. According to existing publications, similar approaches to experimental modeling have not been described; standardized data on protocols, device design, measurement methods, software, as well as the accuracy and permissible errors of pressure recording are also lacking [24].

Taken together, this allows us to consider the proposed model as an important intermediate link between the assessment of the properties of individual materials and subsequent studies of the functionality of multilayer compression bandages under conditions as close as possible to clinical ones.

Study limitations and directions for further research

The tests performed using the developed setup were conducted under experimental conditions and were static tests. This approach ensures standardization of external influences and comparability of results between samples but does not reflect the dynamic characteristics of compression textiles during limb movement and position changes.

This protocol did not evaluate changes in load with limb volume fluctuations, nor the possible evolution of the texture and mechanical properties of the materials over time. Furthermore, an *in vitro* model cannot fully reproduce the influence of physiological factors, including variability in soft tissue properties, skin turgor, and limb contour heterogeneity, which can alter load distribution under the bandage components.

A promising direction for further work could be to conduct a series of tests at different levels of external pressure to evaluate the load generated by individual components of a multilayer bandages with DC areas. It is also advisable to develop protocols that simulate dynamic conditions (movement, change in position and change in limb volume) and evaluate the stability of the load during long-term use of the bandage.

CONCLUSION

A test setup was developed and tested in vitro. It allows for the simultaneous recording of the load generated by different components of multilayer bandages with DC areas under a given external pressure (40 mmHg). The obtained data allow us to draw conclusions about the functional properties of the materials used (polymer foams and nonwoven fabrics) and use them as a basis for comparative evaluation when designing multilayer compression bandages.

Under experimental conditions, it was shown that the magnitude of the recorded load statistically significantly depends on both the stiffness of the CE material and the type of nonwoven FF. The highest load values were recorded under the CE with the highest stiffness. When developing prototypes, it is necessary to consider not only the density but also the composition of the material. For example, the maximum pressure on the simulation model was recorded under a blended nonwoven FF made of viscose and polyester combined with a CE in the form of foamed polyethylene. The obtained data justify the use of the developed setup as a screening tool for comparative evaluation and selection of samples of multilayer dressings with DC areas at the development stage.

AUTHORS CONTRIBUTION

Alexey E. Brovkin and Sergey K. Zazulin formulated the idea. Sergey K. Zazulin, Ekaterina Yu. Chizh, and Svetlana M. Titkova developed the study design. Gregory G. Gabuzov created and described the experimental setup. Ekaterina Yu. Chizh, Svetlana M. Titkova, and Gregory G. Gabuzov conducted the experiments and performed statistical processing of the results. Alexey E. Brovkin studied the literature and wrote the text of the article. Ekaterina Yu. Chizh and Svetlana M. Titkova designed the illustrations. Sergey K. Zazulin, Mikhail V. Anurov, and Svetlana M. Titkova performed scientific editing of the article. All authors of the article approved the final version of the article.

ВКЛАД АВТОРОВ

А.Е. Бровкин и С.К. Зазулин сформулировали идею. С.К. Зазулин, Е.Ю. Чиж и С.М. Титкова разработали дизайн исследования. Г.Г. Габузов создал и описал экспериментальный стенд. Е.Ю. Чиж, С.М. Титкова и Г.Г. Габузов провели эксперименты и выполнили статистическую обработку результатов. А.Е. Бровкин изучил литературные источники и написал текст статьи. Е.Ю. Чиж и С.М. Титкова оформили иллюстрации. С.К. Зазулин, М.В. Ануров и С.М. Титкова провели научную редактуру статьи. Все авторы статьи утвердили окончательную версию статьи

REFERENCES / ЛИТЕРАТУРА

1. *Besharat S., Grol-Prokopczyk H., Gao S., et al.* Peripheral edema: A common and persistent health problem for older Americans. PLoS One. 2021 Dec; 16(12): e0260742. https://doi.org/10.1371/journal.pone.0260742. PMID: 34914717
2. *Deutscher D., Kallen M.A., Hayes D., et al.* Lower quadrant edema patient-reported outcome measure is reliable, valid, and efficient for patients with lymphatic and venous disorders. Phys Ther. 2023 Oct; 103(10): pzad083. https://doi.org/10.1093/ptj/pzad083. PMID: 37682087
3. *Letellier M.E., Ibrahim M., Towers A., Chaput G.* Incidence of lymphedema related to various cancers. Med Oncol. 2024 Sep; 41(10): 245. https://doi.org/10.1007/s12032-024-02441-2. PMID: 39289260
4. *Burian EA, Karlsmark T, Nørregaard S, et al.* Wounds in chronic leg oedema. Int Wound J. 2022 Feb; 19(2): 411–425. https://doi.org/10.1111/iwj.13642. Epub 2021 Jul 13. PMID: 34258856
5. *Bowman C., Rockson S.G.* The role of inflammation in lymphedema: a narrative review of pathogenesis and opportunities for therapeutic intervention. Int J Mol Sci. 2024 Mar; 25(7): 3907. https://doi.org/10.3390/ijms25073907. PMID: 38612716
6. *Moffatt C., Keeley V., Quere I.* The concept of chronic edema-a neglected public health issue and an international response: The LIMPRINT study. Lymphat Res Biol. 2019 Apr; 17(2): 121–126. https://doi.org/10.1089/lrb.2018.0085. PMID: 30995179
7. *Executive Committee of the International Society of Lymphology.* The diagnosis and treatment of peripheral lymphedema: 2023 consensus document of the international society of lymphology. Lymphology. 2023; 56(4): 133–151. PMID: 39207406
8. *Mercier G., Pastor J., Moffatt C., et al.* LIMPRINT: health-related quality of life in adult patients with chronic edema. Lymphat Res Biol. 2019 Apr; 17(2): 163–167. https://doi.org/10.1089/lrb.2018.0084. PMID: 30995189
9. *Kim D.J., Kim D.S., Yu Y., et al.* Cross-sectional analysis for lymphedema epidemiology in South Korea by HIRA data: An observational study. Medicine (Baltimore). 2024 Jul; 103(27): e38779. https://doi.org/10.1097/MD.0000000000038779. PMID: 38968506

10. *Moffatt C.J., Gaskin R., Sykorova M., et al.* Prevalence and risk factors for chronic edema in u.k. Community nursing services. Lymphat Res Biol. 2019 Apr; 17(2): 147–154. https://doi.org/10.1089/lrb.2018.0086. PMID: 30995181
11. *McNeely M.L., Al Onazi M.M., Bond M., et al.* Essential components of the maintenance phase of complex decongestive therapy. Med Oncol. 2024; 41: 289. https://doi.org/10.1007/s12032-024-02442-1
12. *Foeldi E.* Complex physical decongestive therapy for lymphedema (CDT). In: Liu N., editor. Peripheral Lymphedema. Singapore: Springer; 2021. P. 189–194. https://doi.org/10.1007/978-981-16-3484-0_24
13. *Moffatt C.J., Burian E., Karlsmark T., et al.* Factors predicting limb volume reduction using compression bandaging within decongestive lymphatic therapy in lymphedema: a multicountry prospective study. Lymphat Res Biol. 2021 Oct; 19(5): 412–422. https://doi.org/10.1089/lrb.2021.0060. PMID: 34672790
14. *Dhar A., Srivastava A., Pandey R.M., et al.* Safety and efficacy of a mobiderm compression bandage during intensive phase of decongestive therapy in patients with breast cancer-related lymphedema: a randomized controlled trial. Lymphat Res Biol. 2023 Feb; 21(1): 52–59. https://doi.org/10.1089/lrb.2021.0104. Epub 2022 Jun 8. PMID: 35675677
15. *Bergmann A., Baiocchi J.M.T., de Andrade M.F.C.* Conservative treatment of lymphedema: the state of the art. J Vasc Bras. 2021 Oct; 20: e20200091. https://doi.org/10.1590/1677-5449.200091. PMID: 34777487
16. *Nair H.K.R., Lew X., Liew K.Y., et al.* Efficacy of Mobiderm® bandage in compression therapy for venous ulcers: a prospective case series. Int J Low Extrem Wounds. 2023 Dec; 22(4): 759–766. https://doi.org/10.1177/15347346211058273. Epub 2021 Nov 22. PMID: 34806457
17. *Маринкина М.А., Зимина М.В., Чагина Л.Л. и др.* Разработка метода и устройства для определения давления компрессионных трикотажных изделий на тело человека. Известия высших учебных заведений. Технология текстильной промышленности. 2021; 3(393): 60–67. https://doi.org/10.47367/0021-3497_2021_3_60. EDN: PCXQDU / *Marinkina M.A., Zimina M.V., Chagina L.L., et al.* Development of a method and device for determining the pressure of compression knitwear on the human body. Proceedings of the Higher Educational Institutions. Textile Industry Technology. 2021; 3(393): 60–67 (In Russian). https://doi.org/10.47367/0021-3497_2021_3_60. EDN: PCXQDU
18. *Gefen A., Alves P., Beeckman D., et al.* How should clinical wound care and management translate to effective engineering standard testing requirements from foam dressings? Mapping the existing gaps and needs. Adv Wound Care (New Rochelle). 2024 Jan; 13(1): 34–52. https://doi.org/10.1089/wound.2021.0173. Epub 2022 Apr 5. PMID: 35216532
19. *DelPreto J., Brunelle C.L., Taghian A.G., Rus D.* Sensorizing a compression sleeve for continuous pressure monitoring and lymphedema treatment using pneumatic or resistive sensors. In: Proceedings of the 2023 IEEE International Conference on Soft Robotics (RoboSoft). Singapore, Singapore; 2023. P. 1–8. https://doi.org/10.1109/RoboSoft55895.2023.10122068
20. *Richards C.J., Steele J.R., Spinks G.M.* Experimental evaluation and analytical model of the pressure generated by elastic compression garments on a deformable human limb analogue. Med Eng Phys. 2020 Sep; 83: 93–99. https://doi.org/10.1016/j.medengphy.2020.05.015. Epub 2020 May 17. PMID: 32507675
21. *Daneshgaran G., Lo A.Y., Paik C.B., et al.* A pre-clinical animal model of secondary head and neck lymphedema. Sci Rep. 2019; 9(1): 18264. https://doi.org/10.1038/s41598-019-54201-2. Epub 20191204. PMID: 31797883
22. *Gebruers N., Hendriks J.M.H., Tjalma W., et al.* Pressure curves, static and dynamic stiffness of different two-component compression systems for the treatment of chronic edema of the lower limbs. Lymphat Res Biol. 2022; 20(3): 335–341. https://doi.org/10.1089/lrb.2021.0016. Epub 2021 Aug 31. PMID: 34463159
23. *Cho S.C., Kwak S.G., Cho H.K.* Effectiveness of Mobiderm® bandages in the treatment of cancer-related secondary lymphedema: A pilot study. Medicine (Baltimore). 2022 Sep; 101(35): e30198. https://doi.org/10.1097/MD.0000000000030198. PMID: 36107527
24. *Mosti G., Cavezzi A.* Compression therapy in lymphedema: Between past and recent scientific data. Phlebology. 2019 Sep; 34(8): 515–522. https://doi.org/10.1177/0268355518824524.
25. *Duygu-Yildiz E., Bakar Y., Hizal M.* The effect of complex decongestive physiotherapy applied with different compression pressures on skin and subcutaneous tissue thickness in individuals with breast cancer-related lymphedema: a double-blinded randomized comparison trial. Support Care Cancer. 2023 Jun; 31(7): 383. https://doi.org/10.1007/s00520-023-07843-y. PMID: 37285046
26. *Ning J., Ma W., Fish J., et al.* Interface pressure changes under compression bandages during period of wearing. J Vasc Surg Venous Lymphat Disord. 2021 Jul; 9(4): 971–976. https://doi.org/10.1016/j.jvsv.2020.11.007. Epub 2020 Nov 11. PMID: 33188960
27. *Chi Y.W., Lin R., Tseng K.H., Durbin-Johnson B.* Effect of subsurface pressure on the interface pressure measurement in an in vitro experiment. Phlebology. 2020 Mar; 35(2): 134–138. https://doi.org/10.1177/0268355519857627. Epub 2019 Jun 24. PMID: 31234751
28. *Brorson H., Hansson E., Jense E., Freccero C.* Development of a pressure-measuring device to optimize compression treatment of lymphedema and evaluation of change in garment pressure with simulated wear and tear. Lymphat Res Biol. 2012 Jun; 10(2): 74–80. https://doi.org/10.1089/lrb.2012.0003. PMID: 22720662

INFORMATION ABOUT THE AUTHORS / ИНФОРМАЦИЯ ОБ АВТОРАХ

Sergey K. Zazulin✉, Cand. of Sci. (Medicine), Scientific Director, LLC "Innovative Technologies of Rehabilitation".
ORCID: https://orcid.org/0009-0000-2460-6881

Svetlana M. Titkova, Senior Researcher, Department of Experimental Surgery, Institute of Surgery, Pirogov Russian National Research Medical University.
ORCID: https://orcid.org/0000-0001-5477-0084

Зазулин Сергей Константинович✉, канд. мед. наук, научный руководитель ООО «Инновационные технологии реабилитации».
ORCID: https://orcid.org/0009-0000-2460-6881

Титкова Светлана Михайловна, старший научный сотрудник отдела экспериментальной хирургии Института хирургии ФГАОУ ВО «РНИМУ им. Н.И. Пирогова» Минздрава России (Пироговский Университет).
ORCID: https://orcid.org/0000-0001-5477-0084

Mikhail V. Anurov, Dr. of Sci. (Medicine), Head of Department of Experimental Surgery, Institute of Surgery, Pirogov Russian National Research Medical University.
ORCID: https://orcid.org/0000-0001-7512-2641

Grigory G. Gabuzov, Engineer, Department of Neurocomputer Interfaces, Department of Experimental Surgery, Institute of Surgery, Pirogov Russian National Research Medical University.
ORCID: https://orcid.org/0000-0003-1511-3692

Ekaterina Yu. Chizh, Medical Director, LLC "Innovative Technologies of Rehabilitation".
ORCID: https://orcid.org/0000-0002-2846-3854

Alexey E. Brovkin, Chief Surgeon, Central Clinical Military Hospital.
ORCID: https://orcid.org/0009-0007-8872-2401

Ануров Михаил Владимирович, д-р мед. наук, заведующий отделом экспериментальной хирургии Института хирургии ФГАОУ ВО «РНИМУ им. Н.И. Пирогова» Минздрава России (Пироговский Университет).
ORCID: https://orcid.org/0000-0001-7512-2641

Габузов Григорий Георгиевич, инженер отдела нейрокомпьютерных интерфейсов, отдела экспериментальной хирургии Института хирургии ФГАОУ ВО «РНИМУ им. Н.И. Пирогова» Минздрава России (Пироговский Университет).
ORCID: https://orcid.org/0000-0003-1511-3692

Чиж Екатерина Юрьевна, медицинский директор ООО «Инновационные технологии реабилитации».
ORCID: https://orcid.org/0000-0002-2846-3854

Бровкин Алексей Евгеньевич, главный хирург Центрального клинического военного госпиталя.
ORCID: https://orcid.org/0009-0007-8872-2401

✉ Corresponding author / Автор, ответственный за переписку

Original article / Оригинальная статья
https://doi.org/10.47093/2218-7332.2025.16.4.31-40

Development and validation of an environmental protocol to enhance sleep and pain outcomes in intensive care unit patients

Barkah Waladani✉, **Endah Setianingsih, Muhammad N.W. Hidayah**
Universitas Muhammadiyah Gombong (UNIMUGO)
461, Yos Sudarso str., Gombong, Kebumen, 54412, Indonesia

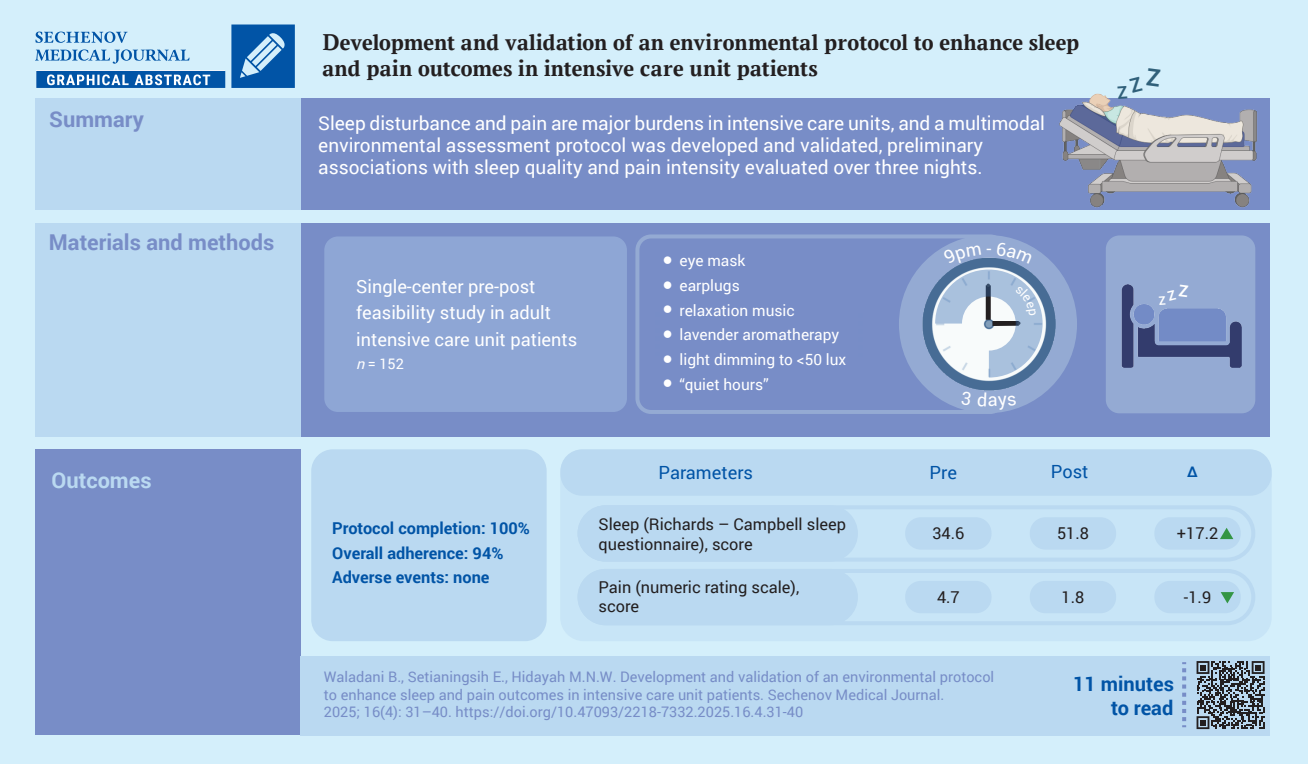

Abstract

Aim. To develop a multimodal environmental modification protocol for the intensive care unit (ICU) and evaluate its feasibility and preliminary associations with sleep quality and pain intensity in patients.

Materials and methods. A quasi-experimental, single-arm study involving 152 adult patients was conducted from June to August 2025 in the ICU of a Type B hospital in Central Java, Indonesia. Environmental modifications included six interventions: earplugs, eye masks, music therapy, lavender aromatherapy, lighting adjustments, and noise reduction measures, which were applied daily for three consecutive nights (content validity = 0.94). Sleep quality was measured using the Richards-Campbell Sleep Questionnaire (RCSQ), and pain intensity was measured using the numeric rating scale (NRS). Paired t-tests, 95% confidence intervals (CI), and Cohen's d were used to describe intervention effectiveness. Normality of distribution was tested using the Shapiro–Wilk test.

Results. All 152 ICU participants completed the three-day protocol, with overall adherence being 94%. Mean RCSQ scores improved from 34.6 with 11.3 to 51.8 with 10.6 (95% CI: 15.46–18.94; paired *t*-test, $p < 0.001$; Cohen's $d = 1.57$). Mean NRS scores decreased from 4.7 with 1.8 to 2.8 with 1.3 (95% CI: −2.15 to −1.65; paired *t*-test, $p < 0.001$; Cohen's $d = 1.21$). No adverse events were noted. Objective environmental monitoring (subsample $n = 40$) showed a mean reduction in noise and lighting levels at the patient's bedside during the intervention.

Conclusion. The protocol for creating a positive environment in the ICU was feasible, acceptable, and resulted in subjective improvements in sleep quality and pain intensity in patients.

Keywords: intensive care unit; environmental modification; sleep quality; pain management; feasibility study
MeSH terms:
DYSSOMNIAS – DIAGNOSIS
DYSSOMNIAS – THERAPY
DYSSOMNIAS – ETIOLOGY
ENVIRONMENTAL EXPOSURE – ANALYSIS
ENVIRONMENTAL EXPOSURE – PREVENTION & CONTROL
INTENSIVE CARE UNITS
SLEEP QUALITY
For citation: Waladani B., Setianingsih E., Hidayah M.N.W. Development and validation of an environmental protocol to enhance sleep and pain outcomes in intensive care unit patients. Sechenov Medical Journal. 2025; 16(4): 31–40. https://doi.org/10.47093/2218-7332.2025.16.4.31-40

CONTACT INFORMATION:
Barkah Waladani, Assistant Professor, Department of Critical Care Nursing, Faculty of Health and Science, Universitas Muhammadiyah Gombong (UNIMUGO).
Address: 461, Yos Sudarso str. Gombong, Kebumen, 54412, Indonesia
E-mail: barkah.waladani@gmail.com

Ethics statements. The study was conducted in accordance with the ethical principles outlined in the World Medical Association Declaration of Helsinki for biomedical research involving human subjects. The protocol was reviewed and approved by the Health Research Ethics Committee of Universitas Muhammadiyah Gombong, Approval No. 110.6/II.3.AU/F/KEPK/V/2025. Written informed consent was obtained from all patients included in the study or their legally authorized representatives.
Data availability. The data that support the findings of this study are available from the corresponding authors on reasonable request. Data and statistical methods used in the article were examined by a professional biostatistician on the Sechenov Medical Journal editorial staff.
Conflict of interest. The authors declare that there is no conflict of interests.
Financing. The study was supported by a research grant from the Ministry of Education, Culture, Research, and Technology of the Republic of Indonesia (Kemendiktisaintek), Grant No. 0070/C3/AL.04/2025[1].

Received: 03.10.2025
Accepted: 09.12.2025
Date of publication: 30.12.2025

УДК 616.8-009.836.14-084

Разработка и валидация протокола модификации окружающей среды, влияющей на качество сна и интенсивность боли у пациентов отделения интенсивной терапии

Б. Валадани✉, Э. Сетианингсих, М.Н.В. Хидая
Университет Мухаммадия в Гомбонге (UNIMUGO)
ул. Йос Сударсо, д. 461, г. Гомбонг, Кебумен, 54412, Индонезия

Аннотация

Цель. Разработать мультимодальный протокол модификации окружающей среды для отделения реанимации и интенсивной терапии (ОРИТ), провести оценку его осуществимости и предварительных связей с качеством сна и интенсивностью боли у пациентов.

Материалы и методы. Квазиэкспериментальное одногрупповое исследование с участием 152 взрослых пациентов проводилось с июня по август 2025 года в ОРИТ больницы типа B в провинции Центральная Ява, Индонезия. Модификация окружающей среды включала 6 инструментов: беруши, маски для глаз, музыкотерапия, ароматерапия с лавандой, регулировка освещения и меры по снижению шума, которые применялись

[1] List of Research Program Funding Recipients 2025, Indonesia. Number: 0070/C3/AL.04/2025. Grant No. 127/C3/DT.04.00/PL/2025 (access date: 12.12.2025).

ежедневно в течение трех последовательных ночей (содержательная валидность = 0,94). Качество сна измерялось с помощью опросника сна Ричардса – Кэмпбелла (RCSQ, Richards – Campbell Sleep Questionnaire), а интенсивность боли – с помощью числовой рейтинговой шкалы (NRS, numeric rating scale). Для описания эффективности вмешательства использовались парные *t*-критерии, 95% доверительные интервалы (ДИ) и стандартное отклонение *d* Коэна. Нормальность распределения проверялась с помощью критерия Шапиро – Уилка.

Результаты. Все 152 участника ОРИТ завершили трехдневный протокол, общая приверженность составила 94%. Средние баллы по шкале RCSQ улучшились с 34,6 ± 11,3 до 51,8 ± 10,6 (95% ДИ: 15,46–18,94; парный *t*-критерий, p <0,001; коэффициент Коэна d = 1,57). Средние баллы по шкале NRS снизились с 4,7 ± 1,8 до 2,8 ± 1,3 (95% ДИ: от −2,15 до −1,65; парный *t*-критерий, p < 0,001; коэффициент Коэна d = 1,21). Нежелательных явлений не отмечено. Объективный мониторинг окружающей среды (подвыборка n = 40) показал среднее снижение уровня шума и освещения у постели больного в часы проведения вмешательства.

Заключение. Протокол по созданию благоприятной среды в ОРИТ оказался осуществимым, приемлемым и обеспечил субъективное улучшение качества сна и снижение интенсивности боли у пациентов.

Ключевые слова: отделение интенсивной терапии; модификация окружающей среды; качество сна; обезболивание; анализ осуществимости

Рубрики MeSH:

ДИССОМНИЯ – ДИАГНОСТИКА
ДИССОМНИЯ – ТЕРАПИЯ
ДИССОМНИЯ – ЭТИОЛОГИЯ
ОКРУЖАЮЩЕЙ СРЕДЫ ФАКТОРЫ ВОЗДЕЙСТВИЯ – АНАЛИЗ
ОКРУЖАЮЩЕЙ СРЕДЫ ФАКТОРЫ ВОЗДЕЙСТВИЯ – ПРОФИЛАКТИКА И КОНТРОЛЬ
ИНТЕНСИВНОЙ ТЕРАПИИ ОТДЕЛЕНИЕ
СНА КАЧЕСТВО

Для цитирования: Валадани Б., Сетианингсих Э., Хидая М.Н.В. Разработка и валидация протокола модификации окружающей среды, влияющей на качество сна и интенсивность боли у пациентов отделения интенсивной терапии. Сеченовский вестник. 2025; 16(4): 31–40. https://doi.org/10.47093/2218-7332.2025.16.4.31-40

КОНТАКТНАЯ ИНФОРМАЦИЯ:
Валадани Барках, ассистент кафедры сестринского дела в анестезиологии и реаниматологии факультета здравоохранения и естественных наук Университета Мухаммадия в Гомбонге (UNIMUGO).
Адрес: ул. Йос Сударсо, д. 461, г. Гомбонг, Кебумен, 54412, Индонезия
E-mail: monchai@g.swu.ac.th

Соответствие принципам этики. Исследование проводилось в соответствии с Хельсинкской декларацией (версия 2024 года) Всемирной медицинской ассоциации об этических принципах проведения биомедицинских исследований**.** Протокол № 110.6/II.3.AU/F/KEPK/V/2025 одобрен Комитетом по этике медицинских исследований Университета Мухаммадия в Гомбонге. Получено письменное информированное согласие от всех пациентов, включенных в исследование, или их законных представителей.
Доступ к данным исследования. Данные, подтверждающие результаты этого исследования, доступны у соответствующих авторов по обоснованному запросу. Данные и статистические методы, использованные в статье, были проверены профессиональным биостатистиком из редакционного отдела журнала «Сеченовский вестник».
Конфликт интересов. Авторы заявляют об отсутствии конфликта интересов.
Финансирование. Исследование было поддержано грантом Министерства образования, культуры, исследований и технологий Республики Индонезия (Kemendiktisaintek), грант № 0070/C3/AL.04/2025[2].

Поступила: 03.10.2025
Принята: 09.12.2025
Дата печати: 30.12.2025

[2] Список получателей финансирования исследовательских программ 2025, Индонезия. Номер: 0070/C3/AL.04/2025. Grant No. 127/C3/DT.04.00/PL/2025 (дата обращения: 12.12.2025).

Abbreviations:
AE – adverse events
ICU – intensive care unit
NRS – numeric rating scale
RCSQ – Richards-Campbell sleep questionnaire
SD – standard deviation

HIGHLIGHTS	КЛЮЧЕВЫЕ ПОЛОЖЕНИЯ
Despite advances in critical care technologies, nurses continue to face constant stress, heavy workloads, and limited capacity to address patients' non-pharmacological needs.	Несмотря на достижения в области технологий интенсивной терапии, медицинские сестры по-прежнему сталкиваются с постоянными стрессовыми факторами, высокой рабочей нагрузкой и ограниченными возможностями для удовлетворения немедикаментозных потребностей пациентов.
Routine clinical priorities often focus on physiological stabilization of patients, while environmental factors such as sleep disturbances and pain sensitivity receive less systematic attention.	Приоритеты рутинной клинической работы часто сосредоточены на физиологической стабилизации пациентов, в то время как нарушения их сна и восприимчивость боли, связанные с окружающими факторами, получают меньше систематического внимания.
In resource-limited intensive care settings, the absence of standardized, nurse-led environmental protocols further limits the integration of holistic care into daily practice.	В условиях ограниченных ресурсов в отделениях интенсивной терапии отсутствие стандартизированных протоколов по улучшению окружающей среды, разработанных медсестрами, еще больше ограничивает интеграцию целостного подхода к уходу в повседневную практику.
Addressing these gaps requires feasible, structured, and context-appropriate interventions that can be consistently implemented by bedside nurses.	Для устранения этих пробелов необходимы осуществимые, структурированные и соответствующие контексту вмешательства, которые могут последовательно внедряться медсестрами у постели больного.

Sleep disturbance and pain management remain major issues in intensive care unit (ICU) worldwide [1, 2]. A systematic review and meta-analysis A. Ashghab et al. [3] reported that approximately 66% of critically ill adult patients experienced sleep disturbance during their ICU stay, with these disturbances persisting for months after discharge. Another large observational study L. Alegria et al. [4] involving non-sedated ICU patients suggested that not only pain, but also environmental lighting, noise, and frequent nighttime care interventions were strongly correlated with poor sleep quality; similar findings have been reported previously [5, 6]. Sleep disturbances have been linked to impaired respiratory performance, an increased risk of delirium, longer duration of mechanical ventilation, and higher ICU mortality [7–10].

Despite growing awareness, most interventions assessed in recent years focused on single-component strategies such as earplugs, eye masks, noise suppression, or music therapy [11, 12]. In many studies, these interventions produced modest improvements, but standardization of combined environmental modification was lacking. Reviews called for multicomponent protocols, validated tools, and feasibility data to implementation guide [13]. Studies assessing the content validity of such interventions, adherence, and acceptability among ICU patients under real-world constraints were often lacking in healthcare settings in low- and middle-income countries [14–17].

The novelty of this study remained in designing integrated, validated environmental protocols and evaluating them for feasibility before large-scale trials. The development of intervention was informed by environmental theory in nursing, particularly the work of Florence Nightingale, which emphasizes the role of external factors such as light, noise, and ventilation in supporting patient recovery [18, 19]. Concepts from behavioral sleep medicine, including stimulus control and relaxation theory, also guided the selection of intervention components [20–22]. By integrating these theoretical foundations, the protocol combined environmental modifications and sensory stimulation to create conditions conducive to improved sleep and reduced pain, thereby addressing the multifactorial challenges faced by ICU patients.

Aim of the study: to develop and clinically test a comprehensive environmental modification protocol in ICU and to evaluate its feasibility, acceptability, and preliminary associations with subjective sleep quality and pain intensity in adult patients. Secondary aims were to estimate effect sizes and to document adherence, safety, and operational issues relevant to the design of future randomized trials.

MATERIALS AND METHODS

This study used a quasi-experimental, single-arm design with pre- and post-intervention feasibility assessment conducted between June and September 2025 in the ICU of a Type B accredited hospital in Central Java, Indonesia. Eligible patients were identified daily and consecutively recruited during the study period.

Patient Enrollmen

A total of 180 patients were screened between June and August 2025, of whom 152 met the inclusion criteria and were consecutively enrolled in the study (Fig.). 28 patients were excluded (did not meet criteria or declined).

Inclusion criteria were:

- age ⩾18 years;
- being conscious and able to communicate verbally;
- expected ICU stay of ⩾3 consecutive nights with hemodynamically stability during data collection, defined as mean arterial pressure ⩾65 mmHg with no escalating vasopressor requirement in the previous 12 hours (low-dose vasopressor use of ⩽0.05 μg/kg/min was permitted).

Exclusion criteria were:

- deep sedation (Richmond Agitation–Sedation Scale ⩽ −3);
- continuous mechanical ventilation;
- severe cognitive impairment or delirium at screening.

Lavender/essential oil allergy screening involved a baseline question regarding known allergies to fragrances or essential oils – patients with known allergy were excluded from the study. For patients without a known allergy a 5-minute bedside inhalation tolerance test was performed prior to the first night; if any adverse reactions occurred, aromatherapy was withheld.

Protocol for environmental modification in ICU

The intervention protocol consisted of multiple non-pharmacological tools applied simultaneously: 1) Eye masks: soft cotton fabric eye masks (Lanaform, Belgium) with elastic bands, designed to block ambient light; 2) Earplugs: disposable polyurethane foam earplugs (3M™ 1100, USA) providing noise reduction rating of 29 dB; 3) Music therapy: instrumental relaxation music (tempo 60–80 beats per minute, volume 40–50 dB), delivered via bedside loudspeakers (Sony SRS-XB12, Japan). Music tracks were selected from a standardized relaxation playlist validated in prior ICU studies, consisting of slow-tempo instrumental music designed to promote relaxation and reduce environmental stress [23]; 4) Lavender aromatherapy: pure lavender essential oil (*Lavandula angustifolia*, Now Foods®, USA) diluted to 2% concentration in distilled water, was administered using an ultrasonic diffuser (InnoGear®, China) placed 1.5 m from the patient's bed; 5) Lighting adjustment: overhead ICU fluorescent lamps were dimmed to <50 lux at patient bedside using adjustable dimmer

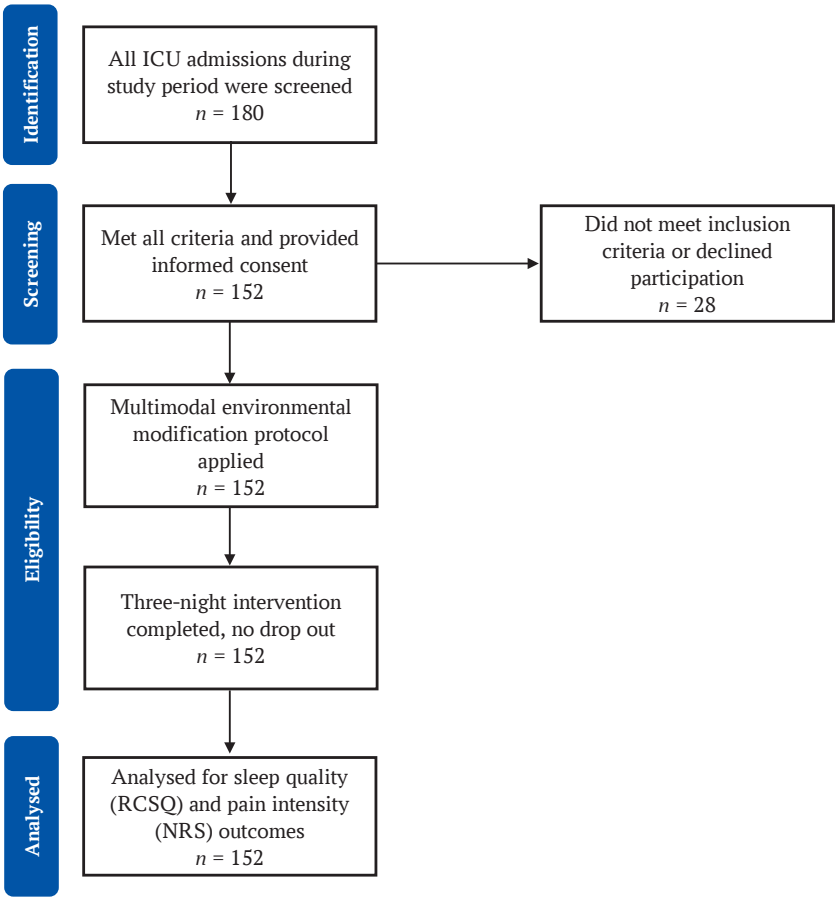

FIG. TREND flowchart.

Note: ICU – intensive care unit; NRS – numeric rating scale; RCSQ – Richards-Campbell sleep questionnaire.

switches installed in each cubicle; 6) Noise reduction: non-essential alarms and conversations near the patient were minimized. Staff were instructed to maintain voice levels <50 dB during nighttime hours. Noise reduction was implemented through staff education and the creation of an appropriate environment. ICU nurses received brief instructions to silence non-essential alarms when clinically appropriate, promptly responding to active alarms, and limiting non-urgent conversations at the patient's bedside during nighttime hours. Visual reminders were posted at the patient's bedside, and compliance with these rules was monitored by the nurse on duty during each shift.

The protocol was implemented over three consecutive nights from 21:00 to 06:00. Each night at 21:00, patients were assisted with the application of eye masks and earplugs, lavender aromatherapy diffuser was activated, lights were dimmed, and background music was played for 30 minutes prior to the sleep period. Earplugs and eye masks were maintained throughout the night unless removed by the patient. ICU staff adhered to a "quiet hours" policy to reduce avoidable disturbances. Intervention fidelity was monitored by bedside nurses and recorded in feasibility logs. The intervention was delivered individually at the bedside for each patient. All procedures were implemented by trained ICU nurses, under the supervision of the research team. To enhance protocol compliance, nurses assisted patients in applying earplugs and eye masks, monitored patient comfort throughout the night, and documented compliance using structured checklists. The individual ICU patient served as the unit of analysis, consistent with the unit of assignment.

Critical alarms remained active at all times. The protocol required that only non-critical alarms could be minimized (e.g., lowering non-urgent monitor volumes or relocating equipment alarms) while continuous physiological monitoring and rapid alarm escalation procedures were maintained. Nurses were instructed to immediately return devices to full volume if any clinical deterioration was observed. Adverse events (AE) were recorded using a structured AE log; trial staff reviewed logs daily. For aromatherapy intervention, patients underwent the pre-exposure tolerance check (5 minutes) under observation; any signs of respiratory distress, rash, or intolerance led to immediate discontinuation and reporting. No intervention-related AE occurred in this cohort.

The protocol, assessed by five experts, demonstrated high content validity across four criteria: relevance (1.00), clarity (0.92), simplicity (0.88), and applicability (0.96) with an overall average scale-level content validity index (S-CVI/Ave) of 0.94.

Validated tools for feasibility assessment

Data were collected using validated instruments to assess the feasibility of the intervention and its preliminary associations with sleep quality and pain intensity. Sleep quality was measured using the Richards-Campbell sleep questionnaire (RCSQ) [24], a widely used five-item visual analog scale ranging from 0 (very poor) to 100 (excellent): sleep depth, sleep latency, number of awakenings, efficiency of returning to sleep, and overall sleep quality. Pain intensity was evaluated daily using the numeric rating scale (NRS) [25], a simple and reliable tool in which patients rated their pain from 0 (no pain) to 10 (worst possible pain).

Primary feasibility outcomes were: recruitment rate, protocol completion (defined as participant completion of all 3 nights), per-component adherence (checklist), acceptability, and AE. Secondary exploratory outcomes: subjective sleep quality (RCSQ) and pain intensity (NRS). Objective environmental measures (bedside LAeq noise and bedside light level) were recorded in a subsample (n = 40) using calibrated instruments. The sample size was pragmatic for a feasibility study and included all eligible patients during the 3-month period (n = 152). No formal power calculation for hypothesis testing was performed; effect size estimates from this cohort will inform sample size calculations for future randomized controlled trials.

Blinding was not implemented in this study due to the nature of the intervention, which required ICU patients and nurses to be aware of the environmental modifications. Participants were informed of the interventions they received, and ICU nurses were responsible for administering and monitoring the protocol. Outcome assessment relied on validated self-report instruments (RCSQ and NRS), which minimized observer bias, but neither patients nor assessors were blinded to study condition.

Statistical Analysis

Pre-post differences were assessed with paired t-tests (unless otherwise stated). Normality of difference scores was checked using Shapiro–Wilk tests; approximate normality supported use of parametric tests. We report means with standard deviations (SD), mean differences with 95% confidence intervals, paired t-statistics and p-values, and conservative Cohen's d effect sizes calculated using the pooled SD: d = (Mean_post − Mean_pre) / SD_pooled, where SD_pooled = $\sqrt{[(SD\_pre^2 + SD\_post^2)/2]}$. For categorical pre-post changes (e.g., RCSQ category shifts), McNemar tests were used to formally assess whether observed category transitions were statistically significant beyond descriptive visualization. Missing data: none (all 152 completed). A significance level of $\alpha = 0.05$ (two-tailed) was used. Data were analyzed using IBM SPSS Statistics 31.

RESULTS

A total of 152 adult patients were consecutively enrolled during the study period. Baseline characteristics

are shown in Table 1. All 152 participants completed the full 3-night protocol (100% completion). Adherence was calculated as the proportion of scheduled components correctly delivered per patient across 3 nights (component checklist). Overall adherence was 94%. Component adherence (n = 152) included: eye mask 98%, earplug 96%, music therapy 92%, aromatherapy 94%, lighting adjustment 95%, staff quiet hours 88%. No intervention-related AE were recorded. Objective environmental monitoring in a subsample (n = 40) indicated reductions in bedside noise and light levels during intervention hours; however, quantitative logs were incomplete, so the results are presented descriptively.

Sleep quality, measured by the RCSQ, increased markedly after the intervention, while pain intensity, assessed with the NRS, decreased substantially (Table 2). Both outcomes demonstrated large effect size estimates, indicating potential benefit within this feasibility context. Confidence intervals for mean changes indicated the precision of these estimates. No null or negative results were observed, and no mediation or causal inference analyses were performed, as the study was designed to assess feasibility and preliminary effects only.

The clinical significance of these improvements is further illustrated in Table 3, which shows categorical shifts in outcome distributions. The proportion of patients reporting high sleep quality more than tripled, while the number experiencing mild pain nearly doubled. At the same time, the incidence of severe pain decreased significantly, demonstrating its clinical relevance within this feasibility context.

DISCUSSION

This single-center feasibility study demonstrates that a standardized multimodal environmental protocol can be implemented with high completion and adherence rates in an ICU setting and is associated with preliminary, clinically meaningful improvements in patient-reported sleep quality and reductions in pain intensity. Given the single-arm design, these results should be interpreted as preliminary associations rather than as evidence of effectiveness. These results are consistent with our initial expectation that the protocol would be feasible, acceptable, and associated with preliminary improvements in patient outcomes. The absence of AE and the 100% completion rate suggest that the intervention was well tolerated, indicating that the protocol may be suitable for integration into routine ICU care pending further evidence [23–25]. Importantly, the large effect sizes observed highlight the potential value of environmental interventions when structured into a combined protocol.

The novelty of this study lies in the systematic development and validation of a protocol that integrated earplugs, eye masks, music therapy, aromatherapy, noise reduction, and lighting adjustment into a single intervention. Previous research has generally examined individual non-pharmacological components in isolation, such as earplugs, eye masks, music, or noise reduction strategies, often reporting modest or inconsistent effects on sleep and pain-related outcomes [26–28]. While fragmented interventions address only single aspects of the ICU environment, this multimodal approach

***Table 1*. Demographic and clinical characteristics of intensive care unit patients**

Variable	Value	%
Age, years, mean ± SD	56.2 ± 14.7	
Sex		
male, *n* (%)	89	58.6
female, *n* (%)	63	41.4
Diagnosis at admission[a]		
stroke	41	27.0
sepsis	33	21.7
cardiac disease	28	18.4
respiratory failure	25	16.4
others	25	16.4
Intensive care unit length of stay, days, mean ± SD	6.8 ± 2.5	

Notes: [a] presented as mutually exclusive primary diagnoses assigned at intensive care unit admission. Percentages do not represent a single diagnostic category because the study population consisted of patients with diverse clinical conditions admitted to the intensive care unit. SD – standard deviation.

***Table 2*. Changes in sleep quality and pain intensity before and after intervention**

Outcome	Pre-intervention (Mean ± SD)	Post-intervention (Mean ± SD)	Mean difference	95% CI	*p*-value	Cohen's *d*
RCSQ (sleep quality)	34.6 ± 11.3	51.8 ± 10.6	+17.2	15.46–18.94	<0.001	1.57
NRS (pain intensity)	4.7 ± 1.8	2.8 ± 1.3	−1.9	−2.15…−1.65	<0.001	1.21

Note: CI – confidence intervals; NRS – numeric rating scale; RCSQ – Richards-Campbell sleep questionnaire; SD – standard deviation.

Table 3. **Categorical changes in sleep quality and pain intensity pre- and post-intervention**

Outcome (category)	Pre-intervention, *n* (%)	Post-intervention, *n* (%)	*p*-value
RCSQ (Sleep quality)			
low (0–25)	46 (30.3)	17 (11.2)	
moderate (26–50)	81 (53.3)	56 (36.8)	<0.001
high (>50)	25 (16.4)	79 (52.0)	
NRS (Pain intensity)			
severe (7–10)	29 (19.1)	6 (3.9)	
moderate (4–6)	86 (56.6)	45 (29.6)	<0.001
mild (1–3)	37 (24.3)	101 (66.5)	

Notes: *p*-values derived from McNemar tests assessing within-subject pre-post category changes.
NRS – numeric rating scale; RCSQ – Richards-Campbell sleep questionnaire.

integrates multiple strategies. In this feasibility study, the combined protocol was associated with larger pre- and post-intervention changes, although synergistic effects cannot be confirmed within the context of a single-arm feasibility design [29–31].

The observed improvements could be related to reductions in environmental stressors such as noise and light, as well as sensory and relaxation effects of aromatherapy and music therapy. However, alternative explanations cannot be ruled out, including reassurance and increased staff engagement [26, 27]. These mechanisms align with previous international studies reporting improved sleep quality with earplugs and eye masks [11, 12] and reduced anxiety and pain with music therapy and lavender inhalation [27, 28, 32]. However, increased patient calming and staff attention may also have contributed.

Implementation fidelity was high: adherence exceeded 94% and no safety concerns reported. Minor barriers included occasional discomfort from earplugs or masks, which required reassurance from nurses. Overall, these results underscore the feasibility of integrating environmental modifications into ICU workflows as a non-invasive, low-cost adjunct to pharmacological management. Clinically, such interventions have the potential to influence broader patient outcomes, as suggested by previous literature [33, 34], although these aspects were not assessed in this feasibility study.

The intervention protocol demonstrated high feasibility and acceptability in this setting, suggesting its potential applicability to broader ICU environments pending further evaluation. Because the protocol consisted of simple, low-cost, and non-invasive environmental modifications, it could be readily adopted in a variety of healthcare settings, including hospitals in low- and middle-income countries where pharmacological options may be limited or carry greater risks. The high completion rate achieved without financial incentives underscores the relevance of these findings to real-world practice. Although the study was conducted in Type B hospital with a short follow-up period, the intervention components are universally applicable and can be easily integrated into ICU care packages worldwide. Future multicenter studies will be valuable to confirm these results and to guide global policy development in this area.

Limitations of the study

Key limitations include the single-center, single-arm pre-post study design, short follow-up period (three nights), subjective outcome measures, and potential expectancy/observer bias as the intervention was administered by staff and patients were informed about it. Objective measures were included for a subsample but full objective sleep assessment (actigraphy/polysomnography) and multicenter randomized controlled trials are recommended.

Directions for further research

Future studies should employ randomized controlled designs with appropriate control groups to strengthen causal inference regarding the intervention's potential effectiveness. To complement self-reported outcomes, objective measurements, such as actigraphy, polysomnography, or physiological biomarkers should be included. Multicenter trials are recommended to enhance generalizability of results across diverse ICU environments and patient populations. In addition, longer-term follow-up periods are needed to evaluate the sustained impact of environmental modifications on clinical recovery, delirium incidence, ICU length of stay, and post-discharge quality of life. Exploring cost-effectiveness and integration into standard ICU protocols may also provide valuable insights for broader implementation.

CONCLUSIONS

The validated multimodal environmental modification protocol demonstrated both feasibility and acceptability in this ICU study and was associated with significant improvements in patient-reported sleep quality (by 17.2% in 3 nights) and reductions in pain intensity (by 1.9% in 3 nights). These preliminary results support progression to larger randomized controlled trials with objective sleep measures and longer follow-up periods to evaluate potential effectiveness and generalizability.

AUTHOR CONTRIBUTIONS

Barkah Waladani was responsible for the study concept and design, conducted the experiment, and drafted the manuscript. Endah Setianingsih contributed to data acquisition, supported the implementation of the intervention, and participated in the critical revision of the manuscript. Muhammad N.W. Hidayah performed the statistical analysis, assisted in the analysis and interpretation of data, and contributed to the revision of the final manuscript. All authors approved the final version of the article.

ВКЛАД АВТОРОВ

Б. Валадани отвечала за концепцию и дизайн исследования, провела эксперимент и подготовила рукопись. Э. Сетианингсих внесла вклад в сбор данных, сопровождала эксперимент и участвовала в критическом пересмотре рукописи. М.Н.В. Хидая выполнил статистический анализ, оказал помощь в анализе и интерпретации данных и внес вклад в редактирование окончательной версии рукописи. Все авторы одобрили окончательную версию статьи.

REFERENCES / ЛИТЕРАТУРА

1. *Bolin M.C., Sweetman M.M.* Sleep in the intensive care unit (ICU): an overlooked opportunity for occupational therapists to fill a gap in health care service. Open J Occup Ther. 2022; 10(1): 1–5. https://doi.org/10.15453/2168-6408.1846
2. *Hillman D.R.* Sleep loss in the hospitalized patient and its influence on recovery from illness and operation. Anesth Analg. 2021 May; 132(5): 1314–1320. https://doi.org/10.1213/ANE.0000000000005323. PMID: 33857973
3. *Ashghab A., Vahedian-Azimi A., Vafadar Z., et al.* Nursing interventions to improve the sleep quality of hospitalized patients: a systematic review and meta-analysis. Intensive Care Res. 2024; 4: 55–71. https://doi.org/10.1007/s44231-024-00056-9
4. *Alegria L., Brockmann P., Repetto P., et al.* Improve sleep in critically ill patients: study protocol for a randomized controlled trial for a multi-component intervention of environment control in the ICU. PLoS One. 2023 May; 18(5): e0286180. https://doi.org/10.1371/journal.pone.0286180. PMID: 37228142
5. *Honarmand K., Bosma K.J.* Risk factors for disrupted sleep in the ICU. In: Weinhouse G.L., Devlin J.W., editors. Sleep in Critical Illness. Cham: Springer; 2022. P. 91–108. https://doi.org/10.1007/978-3-031-06447-0_6
6. *Vaishnav P.P., Suresh A., Kooragayalu S., Kooragayalu S.* Sleep disturbances in hospitalized and intensive care unit patients. In: BaHammam A.S., Hunasikatti M., editors. Sleep Apnea Frontiers. Progress in Sleep Research. Singapore: Springer; 2023. P. 231–253. https://doi.org/10.1007/978-981-99-7901-1_15
7. *Li H.C., Yeh T.Y., Wei Y.C., et al.* Association of incident delirium with short-term mortality in adults with critical illness receiving mechanical ventilation. JAMA Netw Open. 2022 Oct; 5(10): e2235339. https://doi.org/10.1001/jamanetworkopen.2022.35339. PMID: 36205994
8. *Stollings J.L., Kotfis K., Chanques G., et al.* Delirium in critical illness: clinical manifestations, outcomes, and management. Intensive Care Med. 2021 Oct; 47(10): 1089–1103. https://doi.org/10.1007/s00134-021-06503-1. Epub 2021 Aug 16. PMID: 34401939
9. *Mart M.F., Williams Roberson S., Salas B., et al.* Prevention and management of delirium in the intensive care unit. Semin Respir Crit Care Med. 2021 Feb; 42(1): 112–126. https://doi.org/10.1055/s-0040-1710572. Epub 2020 Aug 3. PMID: 32746469
10. *Wu N., Zhang B., Wang Y., et al.* Incidence, prevalence and risk factors of delirium in ICU patients: A systematic review and meta-analysis. Nurs Crit Care. 2023; 28: 653–669. https://doi.org/10.1111/nicc.12857
11. *Waladani B., Utami W., Ernawati, Suwaryo P.A.W.* Improving sleep quality among ICCU patients – evaluating the effectiveness of ear plug and eye mask interventions. Eur J Clin Exp Med. 2024; 22(4): 748–755. https://doi.org/10.15584/ejcem.2024.4.9
12. *Bahcecioglu Turan G., Gürcan F., Özer Z.* The effects of eye masks and earplugs on sleep quality, anxiety, fear, and vital signs in patients in an intensive care unit: a randomised controlled study. J Sleep Res. 2024 Apr; 33(2): e14044. https://doi.org/10.1111/jsr.14044. Epub 2023 Sep 18. PMID: 37723617
13. *Holm A., Nikolajsen L., Dreyer P.* A multicomponent intervention to optimise nurse–patient communication in the intensive care unit: a mixed-methods acceptability and feasibility study. Aust Crit Care. 2022 Nov; 35(6): 616–622. https://doi.org/10.1016/j.aucc.2021.09.008. Epub 2021 Nov 18. PMID: 34802842
14. *Ijaz N., Nader M., Ponticiello M., et al.* Contextual factors influencing bubble continuous positive airway pressure implementation for paediatric respiratory distress in low-income and middle-income countries: a realist review. Lancet Glob Health. 2025 Feb; 13(2): e232–e245. https://doi.org/10.1016/S2214-109X(24)00453-4. Epub 2024 Dec 12. PMID: 39675373
15. *Rendon A., Luhning S., Bardin P., et al.* Recommendations for improving discharge-related care following a COPD exacerbation: an expert panel consensus with emphasis on low- and middle-income countries. Int J Chron Obstruct Pulmon Dis. 2025 Apr; 20: 1111–1129. https://doi.org/10.2147/COPD.S502971. PMID: 40260081
16. *Bartlett E.S., Lim A., Kivlehan S., et al.* Critical care delivery across health care systems in low-income and low-middle-income country settings: a systematic review. J Glob Health. 2023 Dec; 13: 04141. https://doi.org/10.7189/jogh.13.04141. PMID: 38033248
17. *Macey A., O'Reilly G., Williams G., Cameron P.* Critical care nursing role in low and lower middle-income settings: a scoping review. BMJ Open 2022 Jan; 12(1): e055585. https://doi.org/10.1136/bmjopen-2021-055585. PMID: 34983772
18. *Cardoso S.B., Oliveira I.C.S., Souza T.V., Carmo S.A.* Pediatric intensive care unit: reflection in the light of Florence Nightingale's environmental theory. Rev Bras Enferm. 2021; 74(5): e20201267. https://doi.org/10.1590/0034-7167-2020-1267. PMID: 34320154
19. *Riegel F., Crossetti M.G.O., Martini J.G., Nes A.A.G.* Florence Nightingale's theory and her contributions to holistic critical thinking in nursing. Rev Bras Enferm. 2021; 74(2): e20200139. https://doi.org/10.1590/0034-7167-2020-0139. PMID: 33950115
20. *Shkodina A.D., Boiko D.I.* A conception of integrated phased model combining sleep hygiene and stimulus control as an adult sleep education approach. Front Neurol. 2024 Dec; 15: 1513509. https://doi.org/10.3389/fneur.2024.1513509. PMID: 39744111
21. *Edinger J.D., Arnedt J.T., Bertisch S.M., et al.* Behavioral and psychological treatments for chronic insomnia disorder in adults: an American Academy of Sleep Medicine clinical practice guideline. J Clin Sleep Med. 2021 Feb; 17(2): 255–262. https://doi.org/10.5664/jcsm.8986. PMID: 33164742
22. *Blampied N.M., van Deurs J.* A conceptual framework for understanding and designing behavioral interventions for sleep problems in children on the autism spectrum. In: McLay L.K., France K.G., Blampied, N.M., editors. Clinical Handbook of Behavioral Sleep Treatment in Children on the Autism Spectrum.

Cham: Springer; 2022. P. 59–74. https://doi.org/10.1007/978-3-030-99134-0_5
23. *Kakar E., Ottens T., Stads S., et al.* Effect of a music intervention on anxiety in adult critically ill patients: a multicenter randomized clinical trial. J Intensive Care. 2023 Aug; 11(1): 36. https://doi.org/10.1186/s40560-023-00684-1. PMID: 37592358
24. *Richards K.C., O'Sullivan P.S., Phillips R.L.* Measurement of sleep in critically ill patients. J Nurs Meas. 2000 Fall-Winter; 8(2): 131–144. PMID: 11227580
25. *Breivik H., Borchgrevink P.C., Allen S.M., et al.* Assessment of pain. Br J Anaesth. 2008 Jul; 101(1): 17–24. https://doi.org/10.1093/bja/aen103. Epub 2008 May 16. PMID: 18487245
26. *Wu T., Qi H., Hui K., et al.* Effect of noise isolation with noise-cancelling earmuffs during laparoscopic surgery on acute postoperative pain: a clinical randomised controlled trial. BMC Anesthesiol. 2025 Oct; 25(1): 498. https://doi.org/10.1186/s12871-025-03369-4. PMID: 41087929
27. *Hu L., Wang E.J.* Sleep as a therapeutic target for pain management. Curr Pain Headache Rep. 2023 Jun; 27(6): 131–141. https://doi.org/10.1007/s11916-023-01115-4. Epub 2023 May 10. PMID: 37162641
28. *Rampes S., Ma K., Divecha Y.A., et al.* Postoperative sleep disorders and their potential impacts on surgical outcomes. J Biomed Res. 2019 Aug; 34(4): 271–280. https://doi.org/10.7555/JBR.33.20190054. PMID: 32519977
29. *Bienefeld N., Keller E., Grote G.* AI interventions to alleviate healthcare shortages and enhance work conditions in critical care: qualitative analysis. J Med Internet Res. 2025 Jan; 27: e50852. https://doi.org/10.2196/50852. PMID: 39805110
30. *McNelly A., Langan A., Bear D.E., et al.* A pilot study of alternative substrates in the critically Ill subject using a ketogenic feed. Nat Commun. 2023 Dec; 14(1): 8345. https://doi.org/10.1038/s41467-023-42659-8. PMID: 38102152
31. *Zhang X.L., Zhang X., Hua W., et al.* Expert consensus on the diagnosis, treatment, and prevention of respiratory syncytial virus infections in children. World J Pediatr. 2024 Jan; 20(1): 11–25. https://doi.org/10.1007/s12519-023-00777-9. Epub 2023 Dec 8. Erratum in: World J Pediatr. 2024 Feb 25. https://doi.org/10.1007/s12519-023-00792-w. PMID: 38064012
32. *Whale K., Dennis J., Wylde V., et al.* The effectiveness of non-pharmacological sleep interventions for people with chronic pain: a systematic review and meta-analysis. BMC Musculoskelet Disord. 2022 May; 23(1): 440. https://doi.org/10.1186/s12891-022-05318-5. PMID: 35546397
33. *Chlan L.L., Weinert C.R., Heiderscheit A., et al.* Effects of Patient-Directed Music Intervention on Anxiety and Sedative Exposure in Critically Ill Patients Receiving Mechanical Ventilatory Support: A Randomized Clinical Trial. JAMA. 2013 Jun; 309(22): 2335–2344. https://doi.org/10.1001/jama.2013.5670. PMID: 23689789
34. *Devlin J.W., Skrobik Y., Gélinas C., et al.* Clinical Practice Guidelines for the Prevention and Management of Pain, Agitation/Sedation, Delirium, Immobility, and Sleep Disruption in Adult Patients in the ICU. Crit Care Med. 2018 Sep; 46(9): e825–e873. https://doi.org/10.1097/CCM.0000000000003299. PMID: 30113379

INFORMATION ABOUT THE AUTHORS / ИНФОРМАЦИЯ ОБ АВТОРАХ

Barkah Waladani✉, Assistant Professor, Department of Critical Care Nursing, Faculty of Health and Science, Universitas Muhammadiyah Gombong (UNIMUGO).
ORCID: https://orcid.org/0000-0002-6813-270X

Endah Setianingsih, Senior Lecturer, Department of Critical Care Nursing, Faculty of Health and Science, Universitas Muhammadiyah Gombong (UNIMUGO).
ORCID: https://orcid.org/0009-0005-3265-5364

Muhammad N.W. Hidayah, Senior Lecturer, Department of Industrial Engineering, Faculty of Science and Humanities, Universitas Muhammadiyah Gombong (UNIMUGO).
ORCID: https://orcid.org/0000-0001-7258-287X

Валадани Барках✉**,** ассистент кафедры сестринского дела в анестезиологии и реаниматологии факультета здравоохранения и естественных наук Университета Мухаммадия в Гомбонге (UNIMUGO).
ORCID: https://orcid.org/0000-0002-6813-270X

Сетианингсих Энда, старший преподаватель кафедры сестринского дела в анестезиологии и реаниматологии факультета здравоохранения и естественных наук Университета Мухаммадия в Гомбонге (UNIMUGO).
ORCID: https://orcid.org/0009-0005-3265-5364

Хидая Мухаммад Нур Вахью, старший преподаватель кафедры промышленной инженерии факультета естественных и гуманитарных наук Университета Мухаммадия в Гомбонге (UNIMUGO).
ORCID: https://orcid.org/0000-0001-7258-287X

✉ Corresponding author / Автор, ответственный за переписку

Clinical case / Клинический случай
https://doi.org/10.47093/2218-7332.2025.16.4.41-48

Management of a massive retrosternal goiter after prior thyroid surgery: a clinical case

Didiek D.T. Setyo, Iwan Sidharta✉
Airlangga University, Dr. Soetomo Regional General Hospital
47, Jl. Mayjen Prof. Dr. Moestopo, Surabaya, 60131, Indonesia

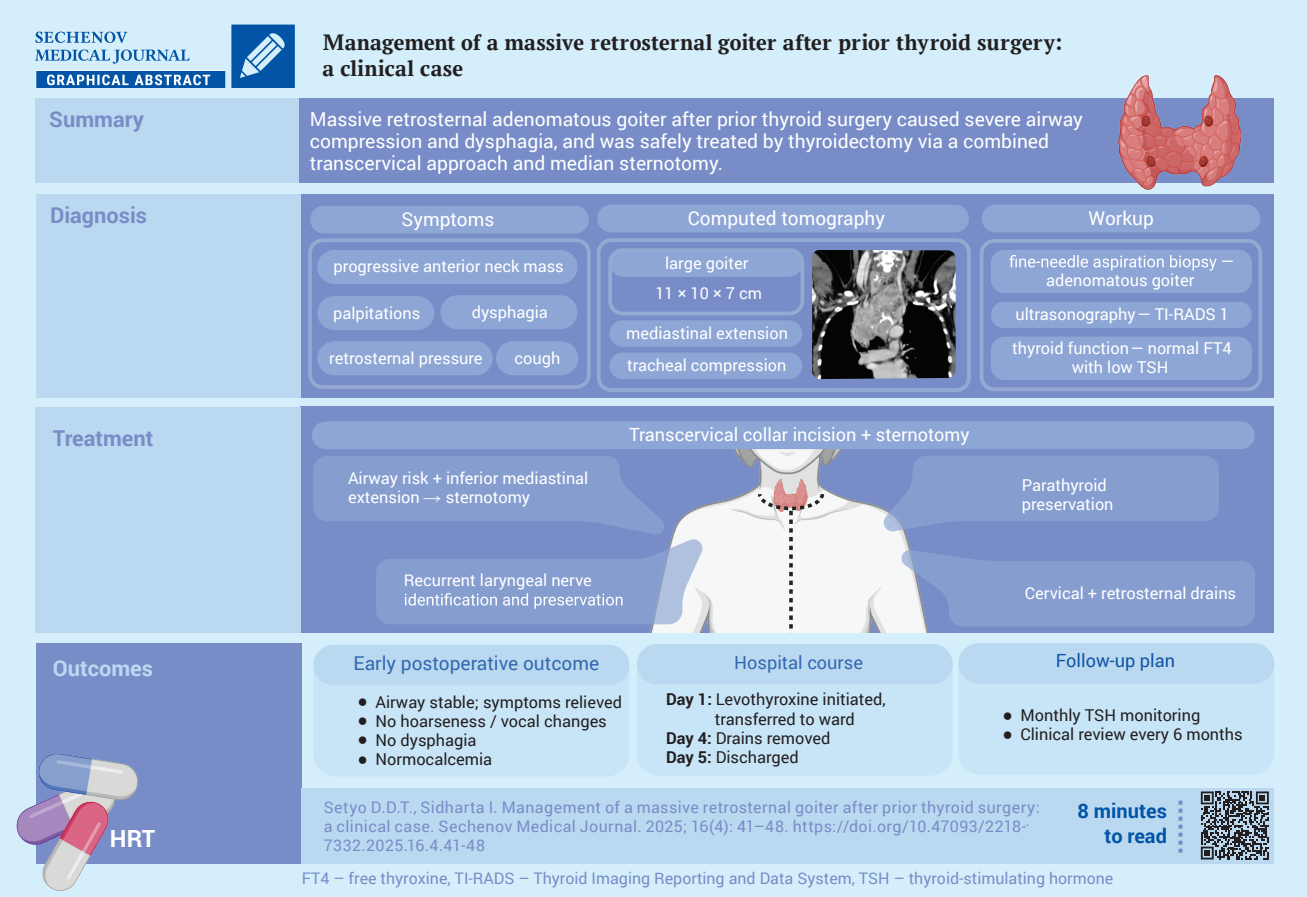

Abstract

Adenomatous goiter is a common benign thyroid condition that can become surgically challenging when it extends into the mediastinum, including in patients with a history of partial thyroid surgery. Retrosternal goiter is often diagnosed at a late stage, and its management is frequently complex due to distorted mediastinal anatomy.

Case report. A 58-year-old woman with a history of left isthmolobectomy performed in 2006 presented with a rapidly enlarging right-sided neck mass accompanied by dysphagia. Although the cervical findings initially suggested right thyroid lobe involvement, contrast-enhanced computed tomography revealed a massive retrosternal goiter originating from residual left thyroid tissue. The lesion extended retrosternally into the anterior mediastinum, resulting in significant tracheal narrowing, displacement of the esophagus, and close anatomical relationships with major mediastinal vessels. Management was undertaken by a multidisciplinary team, and the patient underwent complete thyroidectomy using a combined transcervical approach and median sternotomy, achieving complete resection of the retrosternal component.

Discussion. This case highlights delayed retrosternal progression of adenomatous goiter after partial thyroid surgery. Cross-sectional imaging guided surgical planning, and median sternotomy enabled safe complete resection, underscoring the importance of long-term follow-up and multidisciplinary management.

Keywords: adenomatous goiter; thyroidectomy; sternotomy; recurrent case
MeSH terms:
CASE REPORTS
GOITER, SUBSTERNAL – DIAGNOSIS
GOITER, SUBSTERNAL – DIAGNOSTIC IMAGING
GOITER, SUBSTERNAL – SURGERY
RECURRENCE
THYROIDECTOMY – METHODS
For citation: Setyo D.D.T., Sidharta I. Management of a massive retrosternal goiter after prior thyroid surgery: a clinical case. Sechenov Medical Journal. 2025; 16(4): 41–48. https://doi.org/10.47093/2218-7332.2025.16.4.41-48

CONTACT INFORMATION:
Iwan Sidharta, Associate Professor, Department of Head and Neck Surgery, Faculty of Medicine, Airlangga University, Dr. Soetomo Regional General Hospital.
Address: 47, Jl. Mayjen Prof. Dr. Moestopo, Surabaya, 60131, Indonesia
E-mail: iwansidh@yahoo.com

Compliance with ethical standards. Consent statement. The patient consented to the publication of the article "Management of a massive retrosternal goiter after prior thyroid surgery: a clinical case" in the "Sechenov Medical Journal".
Conflict of interest. The authors declare that there is no conflict of interests.
Financing. The study was not sponsored (own resources).

Received: 02.10.2025
Accepted: 28.11.2025
Date of publication: 30.12.2025

УДК 616.441-006.6-089.87

Стратегия лечения массивного ретростернального зоба после ранее перенесенной операции на щитовидной железе: клинический случай

Д.Д.Т. Сетьо, И. Сидхарта✉
Университет Айрлангга, Региональная больница общего профиля имени доктора Сутомо
ул. Мейджен проф. д-ра Мустопо, д. 47, г. Сурабая, 60131, Индонезия

Аннотация

Аденоматозный зоб является распространенным доброкачественным заболеванием щитовидной железы, которое может представлять значительные хирургические трудности при распространении в средостение, в том числе у пациентов с анамнезом частичной тиреоидэктомии. Ретростернальный зоб часто выявляется на поздних стадиях, а его лечение нередко осложняется измененной анатомией шеи и средостения.
Клинический случай. Пациентка 58 лет с анамнезом удаления левой доли щитовидной железы и перешейка, выполненной в 2006 году, обратилась по поводу быстро увеличивающегося правостороннего образования шеи, сопровождающегося дисфагией. Клинические данные указывали на вовлечение правой доли щитовидной железы, вместе с тем по данным компьютерной томографии с контрастированием выявлен массивный ретростернальный зоб, исходящий из остаточной ткани левой доли. Образование распространялось ретростернально в переднее средостение, вызывая выраженное сужение трахеи, смещение пищевода, и находилось вблизи магистральных сосудов средостения. Мультидисциплинарной командой пациентке была выполнена тотальная тиреоидэктомия с использованием комбинированного шейного доступа и медианной стернотомии, что позволило добиться полного удаления ретростернального компонента.

Обсуждение. Представленный клинический случай демонстрирует отсроченное ретростернальное распространение аденоматозного зоба после частичной тиреоидэктомии. Методы лучевой диагностики сыграли ключевую роль в планировании хирургического вмешательства, а медианная стернотомия обеспечила безопасное и радикальное удаление образования, что подчеркивает необходимость длительного наблюдения и мультидисциплинарного подхода к ведению таких пациентов.

Ключевые слова: аденоматозный зоб; тиреоидэктомия; стернотомия; рецидивирующий случай
MeSH terms:
ОПИСАНИЕ СЛУЧАЕВ
ЗОБ ЗАГРУДИННЫЙ – ДИАГНОСТИКА
ЗОБ ЗАГРУДИННЫЙ – ДИАГНОСТИЧЕСКОЕ ИЗОБРАЖЕНИЕ
ЗОБ ЗАГРУДИННЫЙ – ХИРУРГИЯ
РЕЦИДИВ
ТИРЕОИДЭКТОМИЯ – МЕТОДЫ
Для цитирования: Сетью Д.Д.Т., Сидхарта И. Стратегия лечения массивного ретростернального зоба после ранее перенесенной операции на щитовидной железе: клинический случай. Сеченовский вестник. 2025; 16(4): 41–48. https://doi.org/10.47093/2218-7332.2025.16.4.41-48

КОНТАКТНАЯ ИНФОРМАЦИЯ:
Сидхарта Иван, доцент кафедры хирургии головы и шеи медицинского факультета университета Айрлангга региональной больницы общего профиля им. доктора Сутомо
Адресс: ул. Мейджен проф. д-ра Мустопо, д. 47, г. Сурабая, 60131, Индонезия
E-mail: iwansidh@yahoo.com

Соблюдение этических норм. Заявление о согласии. Пациент дал согласие на публикацию представленной статьи «Стратегия лечения массивного ретростернального зоба после ранее перенесенной операции на щитовидной железе: клинический случай» в журнале «Сеченовский вестник».
Конфликт интересов. Авторы заявляют об отсутствии конфликта интересов.
Финансирование. Исследование не имело спонсорской поддержки (собственные ресурсы).

Получена: 02.10.2025
Принята: 28.11.2025
Дата печати: 30.12.2025

Abbreviations:
CT – computed tomography
RSG – retrosternal goiter
TSH – thyroid-stimulating hormone

HIGHLIGHTS	КЛЮЧЕВЫЕ ПОЛОЖЕНИЯ
A retrosternal goiter can remain asymptomatic until the late stages, when the mediastinal extension becomes life-threatening by compressing the airway, compromising the vascular system and causing dysphagia.	Ретростернальный зоб может длительное время оставаться бессимптомным; на поздних стадиях его медиастинальное распространение становится жизнеугрожающим вследствие компрессии дыхательных путей, сосудистых структур и пищевода.
Contrast-enhanced computed tomography is essential for assessing mediastinal extent and preoperative planning in substernal goiter.	Компьютерная томография с контрастированием – ключевой метод для оценки медиастинального распространения и предоперационного планирования при ретростернальном зобе.
Safe management of retrosternal goiter depends on meticulous surgical technique, preservation of vital structures, and coordinated multidisciplinary planning.	Безопасное хирургическое лечение ретростернального зоба основано на тщательной хирургической технике, сохранении жизненно важных анатомических структур и скоординированной междисциплинарной работе.
Use of standardized classification systems, such as the Mukhtar et al. metric, improves decision-making regarding the need for sternotomy in retrosternal goiter.	Использование стандартизированных классификационных систем, таких как метрическая классификация Mukhtar и соавт., способствует более обоснованному принятию решений о необходимости стернотомии при ретростернальном зобе.

Retrosternal goiter (RSG), also referred to as substernal or intrathoracic goiter, remains a rare but clinically significant condition, often emerging many years after prior thyroid surgery. Its extension into the mediastinum can lead to airway compression, dysphagia, and cardiovascular compromise, creating both diagnostic and operative challenges [1]. Residual thyroid tissue after hemithyroidectomy or incomplete resection can progressively enlarge, representing a major cause of goiter recurrence [2]. Such recurrence typically manifests many years after the initial surgery, often presenting with progressive compressive symptoms and mediastinal extension, as in the present case.

Advances in cross-sectional imaging have improved the ability to determine the extent of retrosternal involvement and predict surgical risks. Computed tomography (CT) is particularly valuable in delineating mediastinal spread and airway narrowing, allowing surgeons to plan operative strategy with greater accuracy [3, 4]. Such imaging data are critical because RSGs have been shown to be associated with perioperative morbidity compared with purely cervical counterparts, reinforcing the importance of meticulous preparation and multidisciplinary planning [3, 5].

Thyroidectomy is the treatment of choice for RSG [6]. In parallel with these technical developments, operative excellence has become central in modern endocrine surgery. Classification systems provide structured guidance in complex cases, and the recently proposed metric classification by Mukhtar H. et al. [7] offers standardized criteria for determining the necessity for sternotomy. This framework not only enhances surgical safety but also supports reproducibility and staff training in high-risk thyroid surgery. This report describes a case of bilateral recurrent adenomatous RSG, presenting nearly two decades after isthmolobectomy, successfully managed with combined thyroidectomy and sternotomy.

CASE REPORT

The patient, a 53-year-old woman, presented with a right-sided neck mass and dysphagia. She first noted bilateral thyroid nodules in 2000 and underwent a left isthmolobectomy in 2006 because of enlargement of the left lobe, while the right-sided nodules were small and asymptomatic; histopathological data from the initial surgery were unavailable. The right-sided nodules remained stable and asymptomatic for many years and therefore did not initially require surgical treatment.

Following the initial surgery, the patient was placed on levothyroxine replacement therapy at a dose of 100 µg/day, with a target thyroid-stimulating hormone (TSH) level of 1–2 mIU/L. She remained asymptomatic until 2009, when gradual enlargement of the right thyroid lobe was noted. However, no clinical or imaging follow-up was performed between 2009 and early 2025, as the patient remained asymptomatic and did not seek further evaluation until the right-sided neck mass began to enlarge.

By February 2025, the neck mass had shown progressive enlargement, and dysphagia had developed and worsened, requiring liquid intake to facilitate swallowing; this was accompanied by retrosternal discomfort described as a sensation of chest pressure, intermittent pain, and palpitations, while excessive sweating and voice changes were denied.

On examination, the patient was in good general condition and hemodynamically stable, with normal body mass index, no respiratory distress, no significant cardiovascular, pulmonary or metabolic comorbidities, and no overt hyperthyroidism, so she was considered suitable for major surgery including possible sternotomy. Physical examination revealed a large right-sided cervical mass that moved with deglutition. The overlying skin was unremarkable. On palpation, the mass measured approximately 6×3×3 cm, firm-elastic in consistency, with a smooth surface, well-defined margins, and mobile over the underlying structures. The lower pole was not palpable. The lesion was non-tender, and no cervical lymphadenopathy was detected.

Laboratory examination revealed suppressed TSH levels (0.215 mIU/L; reference range 0.4–4.0 mIU/L) with normal free thyroxine (FT4) concentrations (1.23 ng/dL; reference range 0.8–1.8 ng/dL), consistent with subclinical hyperthyroidism.

Neck ultrasonography on February 18, 2025 demonstrated bilateral purely anechoic cystic nodules – benign, cystic type, with smooth margins, absent internal vascularity, and no suspicious cervical lymphadenopathy. The findings were consistent with benign cystic lesions and classified as American College of Radiology Thyroid Imaging Reporting and Data System (ACR TI-RADS) category 1[1] (Figs. 1A, B) [8].

Fine-needle aspiration biopsy of the cervical mass confirmed adenomatous goiter. A bone survey revealed no lytic or blastic lesions, thereby excluding metastatic bone disease. Thyroid scintigraphy was not performed. Contrast-enhanced CT scan of the cervicothoracic region performed on July 25, 2025 demonstrated a large retrosternal thyroid mass measuring approximately 11×10×7 cm, predominantly solid with areas of necrosis and coarse calcification.

The lesion originated from the left thyroid lobe and extended retrosternally into the anterior mediastinum, causing severe tracheal narrowing and posterior and lateral displacement of the esophagus. It was in close relation to major mediastinal vessels, including the aortic arch, common carotid, subclavian artery, and

[1] American College of Radiology. Thyroid Imaging Reporting and Data System. https://www.acr.org/Clinical-Resources/Clinical-Tools-and-Reference/Reporting-and-Data-Systems/TI-RADS (access date: 25.09.2025).

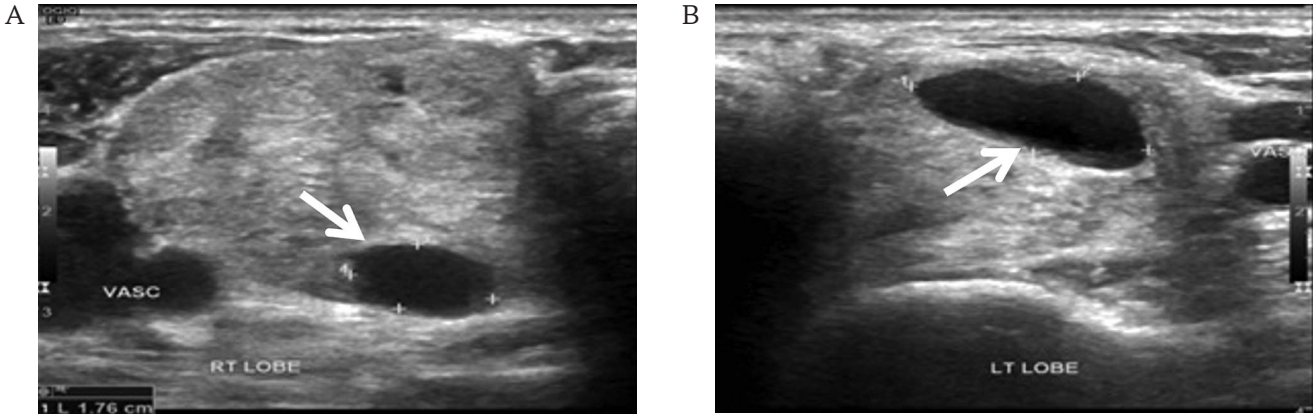

FIG. 1. Neck ultrasonography of a 58-year-old female patient with massive retrosternal goiter.
A. Transverse ultrasound image of the right thyroid lobe showing a purely anechoic cystic nodule (arrow) with smooth margins and absent internal vascularity
B. Longitudinal ultrasound image of the left thyroid lobe demonstrating a similar benign-appearing cystic nodule (arrow) with smooth margins and no evidence of cervical lymphadenopathy

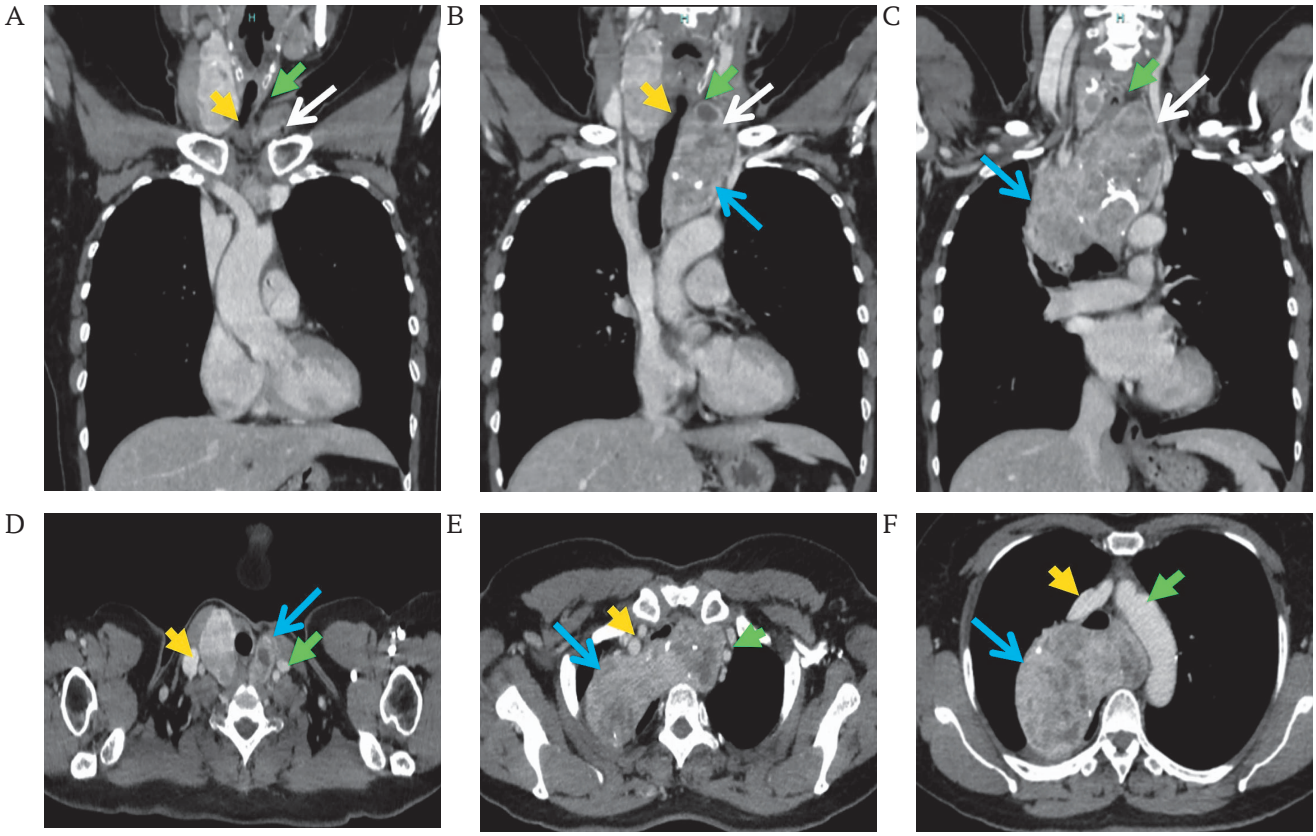

FIG. 2. Contrast-enhanced computed tomography of the cervicothoracic region in a 58-year-old female patient with massive retrosternal goiter.
A–C. Coronal sections: enlarged left thyroid lobe (white arrow) and large retrosternal thyroid mass (blue arrow) compressing the trachea (yellow arrowhead) and displacing the esophagus (green arrowhead).
D–F. Axial sections: inferior extension of the mass (blue arrow) into the anterior mediastinum with close anatomical relationship to the aorta arch and the branchs (yellow arrowhead) (green arrowhead).

brachiocephalic trunk, while the margins with these structures remained preserved. Additional findings included minimal right pleural effusion, multiple hepatic cysts, and left-sided nephrolithiasis (Figs. 2A–F).

Preoperative planning was conducted through a multidisciplinary team discussion involving head and neck surgery, anesthesiology, radiology, and pathology. The team reviewed contrast-enhanced CT

findings demonstrating severe tracheal narrowing and mediastinal extension, ultrasound results confirming bilateral benign cystic nodules, and fine-needle aspiration biopsy indicating adenomatous goiter. Based on these evaluations, the team agreed that a combined transcervical approach with median sternotomy was necessary to achieve complete resection and ensure airway safety.

The clinical diagnosis was recurrent bilateral retrosternal adenomatous goiter with concomitant subclinical hyperthyroidism in a patient with a history of left isthmolobectomy.

On July 31, 2025, a complete thyroidectomy with sternotomy was performed under general anesthesia with endotracheal intubation. The operative sequence included a cervical collar incision followed by right lobectomy with preservation of the recurrent laryngeal nerve and parathyroid glands; the isthmus was absent. Dissection then proceeded to the deeply located left lobe, during which the left recurrent laryngeal nerve was identified and protected, although the left parathyroid glands were not visualized. The inferior retrosternal extension of goiter necessitated median sternotomy to expose the lower trachea, esophagus, and aortic arch, enabling downward traction and blunt dissection, while the contralateral mediastinal extension was released using finger dissection.

Intraoperatively, the left thyroid gland remnant was found extending into the anterior mediastinum, compressing the trachea and displacing the esophagus. Careful dissection allowed for complete removal of the goiter mass, and after excision of the retrosternal component the final surgical field demonstrated the exposed trachea and preserved mediastinal structures (Figs. 3A–D).

The goiter mass was successfully removed, despite the dense adhesions to the posterior thoracic wall

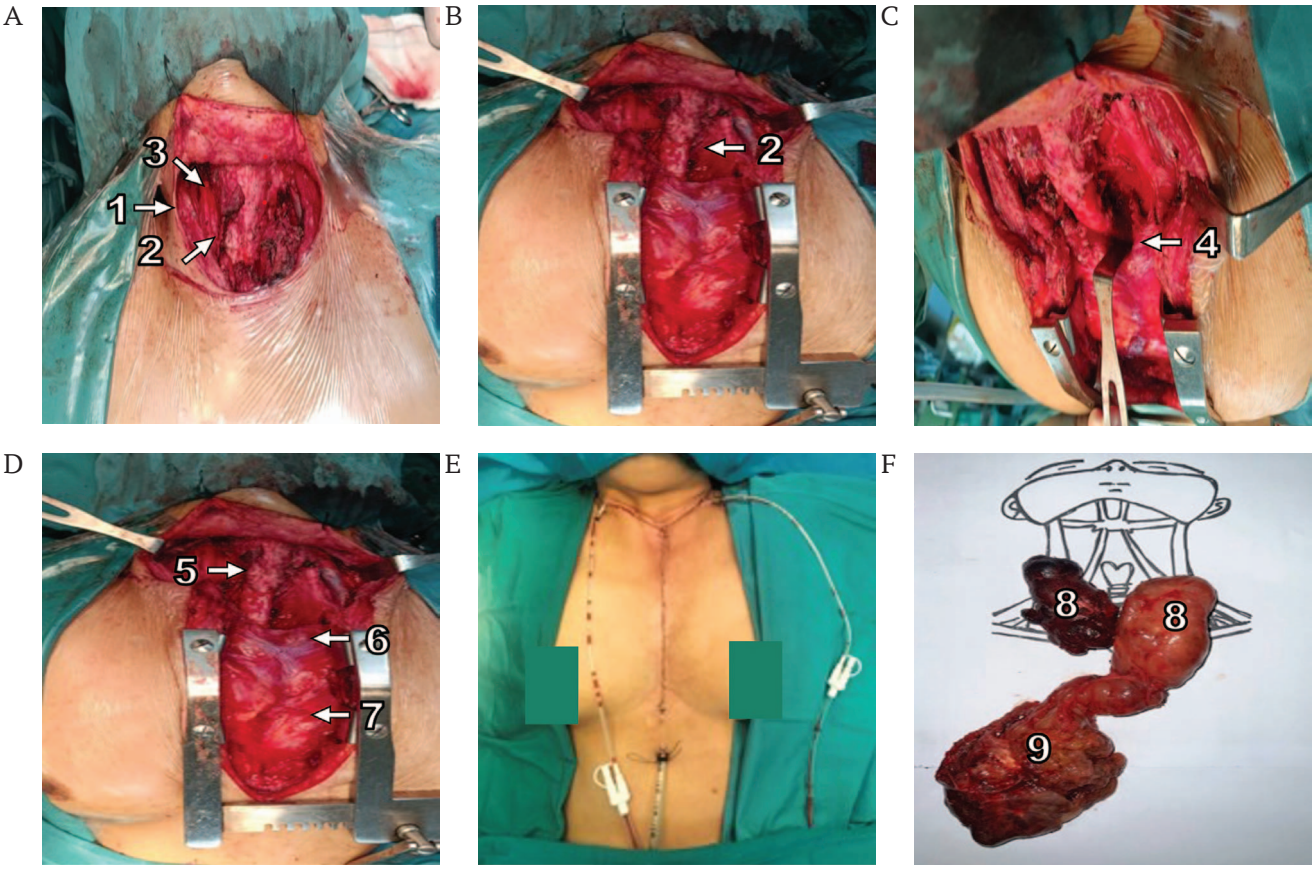

FIG. 3. Complete thyroidectomy with sternotomy in a 58-year-old female patient with massive retrosternal goiter
A. Right thyroid lobectomy (1) with preservation of the recurrent laryngeal nerve (2) and parathyroid glands (3); the isthmus was absent.
B. Dissection of the deeply located left thyroid lobe; the left recurrent laryngeal nerve was identified and protected (2), while the parathyroid glands were not visualized.
C. Retrosternal component (4) mobilized with downward traction and blunt dissection, including contralateral release using finger dissection.
D. Tumor bed following complete resection of the retrosternal thyroid component, showing the exposed trachea (5) and preserved mediastinal structures such as aortic arch (6), and Heart (7) after median sternotomy.
E. Final wound closure with placement of cervical and retrosternal drains
F. Gross specimen showing the resected bilateral thyroid gland (8) with massive retrosternal extension (9).

which added technical difficulty. The excised specimen confirmed bilateral retrosternal adenomatous goiter (Fig. 3E). Recurrent laryngeal nerve preservation was performed anatomically, as intraoperative neuromonitoring was unavailable. Parathyroid glands were carefully identified and preserved *in situ* with their vascular supply whenever possible. Auto-transplantation into the sternocleidomastoid muscle was performed only in cases of devascularization. Fiberoptic laryngoscopy was used at the end of surgery to confirm vocal fold mobility. Hemostasis was secured, drains were placed in the cervical and substernal regions, and the sternum was closed with wire (Fig. 3F).

Postoperative care included routine monitoring for bleeding, pain, airway stability, recurrent or superior laryngeal nerve injury symptoms, and early signs of hypocalcemia. Levothyroxine replacement therapy was initiated on the first postoperative day at a dose of 100 mcg/day, with a target TSH level of 1–2 mIU/L. During hospitalization, the patient remained stable, with stepwise transfer from the intensive care to the general ward, and drains were removed on the fourth day. Patient was discharged on the fifth postoperative day without dysphagia, hoarseness, or hypocalcemia. After discharge, the planned follow-up consisted of monthly TSH monitoring and clinical evaluations every six months.

DISCUSSION

RSG presents unique diagnostic and operative challenges due to mediastinal extension, tracheal compression, and close relation to great vessels, resulting in higher perioperative morbidity compared with purely cervical goiter [2, 3]. Although this case of adenomatous goiter in a patient with a history of left isthmolobectomy was initially described as a recurrence, the absence of imaging or operative records from the patient's first surgery in 2006 makes it impossible to exclude a pre-existing retrosternal component. Therefore, the present clinical case may more accurately represent a progression of longstanding multinodular goiter with retrosternal extension rather than a true recurrence. This distinction has been clarified in order to align terminology with the underlying clinical uncertainty. A recent international multicenter evaluation confirmed higher rates of transient hypoparathyroidism and surgical complications in RSG patients, underscoring the need for meticulous preparation and high-level surgical expertise [3].

Compared with the transcervical approach, sternotomy carries higher risks of bleeding, wound complications, and transient hypocalcemia [3, 9, 10]. In the present case, these risks were mitigated through multidisciplinary planning, optimized anesthetic and airway preparedness, careful anatomical preservation of the recurrent laryngeal nerves, protection and selective auto-transplantation of the parathyroid glands, and meticulous hemostasis. All of this also ensured an uncomplicated postoperative course. This multidisciplinary planning involved coordinated assessment by head and neck surgery, anesthesiology, radiology, and pathology, ensuring consensus on airway preparedness, the need for sternotomy, and the safest operative trajectory. Cross-sectional imaging is indispensable in modern RSG management. Contrast-enhanced CT provides an accurate assessment of cranio-caudal extent, tracheal narrowing, and anatomical relationships with mediastinal structures, which are essential for airway and surgical planning [4]. Recent series report tracheal deviation in ~60% and compression in ~40% of large RSG, with postoperative hypocalcemia and airway-related events not infrequent, highlighting the tight coupling between imaging severity and perioperative risk [10]. In this case, CT demonstrated significant airway narrowing and mediastinal spread, making sternotomy the most reliable and safe approach for complete resection.

Newer classification frameworks, such as the metric system proposed by Mukhtar H. et al. [7], provide standardized criteria for determining the need for sternotomy. The metric classification showed that Grade I (<3 cm) rarely required sternotomy, whereas most Grade III (>6 cm) did. Applied to this case, the extent and airway compromise met criteria favoring sternotomy, improving team alignment and reproducibility of decisions.

Not all RSG demand sternotomy; many are resectable transcervically, and complication profiles vary with gland size, previous thyroid surgery, and tracheal deviation. A 2019–2023 cohort study found transient hypocalcemia as the most common complication; however, malignancy and larger glands were independently associated with surgical outcomes, reinforcing the role of individualized risk stratification beyond access planning [9]. Comparative series similarly show that RSG patients represent a different risk phenotype than cervical goiter patients [3].

Surgical excellence, including meticulous dissection, preservation of the recurrent laryngeal nerves and parathyroid glands, effective hemostasis, and coordinated multidisciplinary airway planning, remains essential for optimizing outcomes in patients with RSG, particularly in cases with severe tracheal compression [3, 9, 10]. Although most RSG are benign multinodular or adenomatous lesions, several reports suggest that their oncologic risk profile differs from that of cervical multinodular goiters [6, 11]. Therefore, total thyroidectomy remains the treatment of choice for symptomatic or compressive RSG, ensuring both oncologic safety and long-term airway relief. Hybrid approaches, such as transcervical combined with video-assisted thoracoscopic surgery (VATS), may reduce chest wall morbidity in selected patients; however, sternotomy remains indispensable for massive mediastinal disease or when adhesions to vascular structures are extensive [12].

CONCLUSION

The atypical recurrence of a RSG almost two decades after partial thyroidectomy highlights the unpredictability of the long-term course of thyroid disease. Contrast-enhanced CT and metric-based classifications are essential to determine mediastinal extension and the need for sternotomy with total thyroidectomy in cases of compressive goiter. The importance of long-term follow-up of RSG patients, structured preoperative planning and multidisciplinary teamwork in cases of goiter extension beyond the sternum, remains undeniable.

AUTHOR CONTRIBUTIONS

Iwan Sidharta was the attending physician responsible for the patient and served as the primary surgeon. Didiek D.T. Setyo acted as the first assistant during the procedure, and also collected research data, analyzed the literature, and contributed to the development of the scientific concept. All authors approved the final version of the publication.

ВКЛАД АВТОРОВ

И. Сидхарта был лечащим врачом пациента и выполнял функции основного оперирующего хирурга. Д.Д.Т. Сетьо выступал первым ассистентом во время операции, а также осуществлял сбор исследовательских данных, анализ литературы и внес вклад в разработку научной концепции. Все авторы одобрили окончательную версию публикации.

REFERENCES / ЛИТЕРАТУРА

1. *Yankov G., Alexieva M., Mekov E.V.* Residual retrosternal goiter and thymolipoma after cervical thyroid resection. Cureus. 2024 Oct; 16(10): e71627. https://doi.org/10.7759/cureus.71627. PMID: 39553011
2. *Gurrado A., Prete F.P., Di Meo G., et al.* Retrosternal, forgotten, and recurrent goiter. In: Testini M., Gurrado A., editors. Thyroid Surgery. Updates in Surgery. Cham: Springer; 2024. P. 39–46. https://doi.org/10.1007/978-3-031-31146-8_5
3. *Cappellacci F., Canu G.L., Rossi L., et al.* Differences in surgical outcomes between cervical goiter and retrosternal goiter: an international, multicentric evaluation. Front Surg. 2024 Feb; 11: 1341683. https://doi.org/10.3389/fsurg.2024.1341683. PMID: 38379818
4. *Akinci O., Aygan S., Inci E., et al.* Computed tomography findings affecting the decision of sternotomy in substernal goiter. Sisli Etfal Hastan Tip Bul. 2023 Sep; 57(3): 305–311. https://doi.org/10.14744/SEMB.2023.25307. PMID: 37900343
5. *Sahbaz A., Aksakal N., Ozcinar B., et al.* The "forgotten" goiter after total thyroidectomy. Int J Surg Case Rep. 2013; 4(3): 269–271. https://doi.org/10.1016/j.ijscr.2012.11.014. Epub 2012 Dec 7. PMID: 23336990
6. *Prete F.P., De Luca G.M., Sgaramella L.I., et al.* Prevalence and clinical risk factors of thyroid cancer in retrosternal goiter: a retrospective comparative study with cervical multinodular goiter. J Clin Med. 2025 Jan; 14(2): 489. https://doi.org/10.3390/jcm14020489. PMID: 39860494
7. *Mukhtar H., Zahid H., Khan I.M., et al.* A new metric classification system for surgical management of retrosternal goitres. J Coll Physicians Surg Pak. 2025 Jun; 35(6): 708–711. https://doi.org/10.29271/jcpsp.2025.06.708. PMID: 40491102
8. *Tessler F.N., Middleton W.D., Grant E.G., et al.* ACR Thyroid Imaging, Reporting and Data System (TI-RADS): White Paper of the ACR TI-RADS Committee. J Am Coll Radiol. 2017 May; 14(5): 587–595. https://doi.org/10.1016/j.jacr.2017.01.046. Epub 2017 Apr 2. PMID: 28372962
9. *Obadiel Y.A., Al-Shehari M., Algmaly Y., et al.* Surgical Management and Predictors of Postoperative Complications of Retrosternal Goiters: A Retrospective Study. Cureus. 2024 Mar; 16(3): e56573. https://doi.org/10.7759/cureus.56573. PMID: 38646310
10. *Sridar K., Mohiyuddin S.A., A S., et al.* Outcomes of total thyroidectomy in large goiters with retrosternal extension and tracheal compression: a multivariate analysis. Cureus. 2024 Nov; 16(11): e73921. https://doi.org/10.7759/cureus.73921. PMID: 39697941
11. *Chen Q., Su A., Zou X., et al.* Clinicopathologic characteristics and outcomes of massive multinodular goiter: a retrospective cohort study. Front Endocrinol. 2022 May; 13: 850235. https://doi.org/10.3389/fendo.2022.850235. PMID: 35685217
12. *Al Jadeedi S., Usama M., Al Harthi H., et al.* A hybrid surgical approach for retrosternal goiter: surgical experience at a tertiary thoracic and endocrine surgery center. J Endocr Surg. 2025 Sep; 25(3): 89-100. https://doi.org/10.16956/jes.2025.25.3.89

INFORMATION ABOUT THE AUTHORS / ИНФОРМАЦИЯ ОБ АВТОРАХ

Didiek D.T. Setyo, surgical intern, Department of Head and Neck Surgery, Faculty of Medicine, Airlangga University, Dr. Soetomo Regional General Hospital.
ORCID: https://orcid.org/0009-0001-7821-4012

Iwan Sidharta✉, Associate Professor, Department of Head and Neck Surgery, Faculty of Medicine, Airlangga University, Dr. Soetomo Regional General Hospital.
ORCID: https://orcid.org/0009-0009-7108-6052

Сетьо Дидик Дармади Три, врач-интерн хирургического профиля кафедры хирургии головы и шеи медицинского факультета Университета Айрлангга Региональной больницы общего профиля им. доктора Сутомо.
ORCID: https://orcid.org/0009-0001-7821-4012

Сидхарта Иван✉**,** доцент кафедры хирургии головы и шеи медицинского факультета Университета Айрлангга Региональной больницы общего профиля им. доктора Сутомо.
ORCID: https://orcid.org/0009-0009-7108-6052

✉ Corresponding author / Автор, ответственный за переписку

Clinical case / Клинический случай
https://doi.org/10.47093/2218-7332.2025.16.4.1344

Familial co-occurrence of diffuse leiomyomatosis and Alport syndrome: a clinical case report

Muqaddas Boltaboeva[1,✉], Abdulhamid Haydarov[1], Marifat Ganieva[1], Davron Kholmatov[1], Oksana Efimenko[1], Lola Rakhmanova[2]
[1]Andijan State Medical Institute
1, S.Yu. Otabekova str., Andijan, 170100, Republic of Uzbekistan
[2]Tashkent State Medical University
2, S.A. Farobiy str., Tashkent, 100109, Republic of Uzbekistan

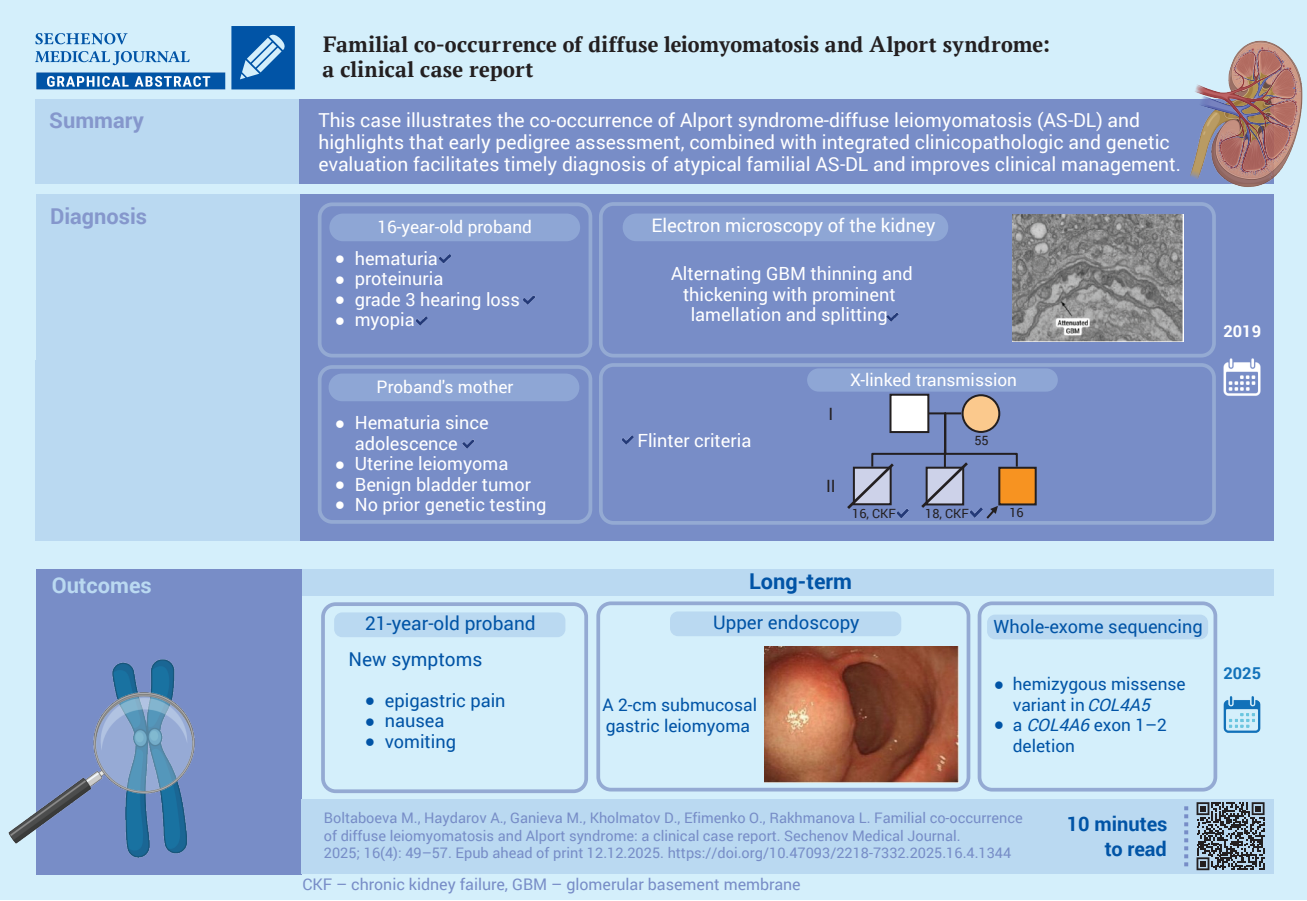

Abstract

Alport syndrome (AS) is a hereditary nephropathy caused by mutations in the *COL4A3*, *COL4A4*, and *COL4A5* genes. Rare contiguous *COL4A5–COL4A6* alterations cause AS with diffuse leiomyomatosis (AS-DL).

Case report. A 16-year-old male had mild proteinuria, hematuria, hearing loss and myopia since childhood. Estimated glomerular filtration rate was 82.8 mL/min/1.73 m^2. Kidney biopsy showed segmental mesangial sclerosis; immunofluorescence was negative. Electron microscopy demonstrated diffuse glomerular basement membrane thinning and podocyte foot-process effacement. Two deceased brothers had end stage kidney disease; the mother had hematuria, uterine myoma, and a benign bladder tumor. A diagnosis of X-linked AS was established according to the Flinter criteria and nephroprotective treatment was initiated. Since 2024, the patient had complained of epigastric symptoms. An endoscopy revealed a 2-cm gastric submucosal lesion. A whole-exome sequencing identified a hemizygous missense variant in *COL4A5* and a *COL4A6* exon 1–2 deletion, confirming AS-DL.

Discussion. This case demonstrates the co-occurrence of AS-DL and shows that early pedigree assessment, combined with integrated clinicopathologic-genetic evaluation in a multidisciplinary framework, enables a timely diagnosis of atypical familial AS-DL and improves clinical management.

Keywords: leiomyoma; nephritic syndrome; uterine neoplasms; X-linked genetic diseases; smooth muscle tumors
MeSH terms:
CASE REPORTS
LEIOMYOMATOSIS – GENETICS
LEIOMYOMATOSIS – DIAGNOSIS
LEIOMYOMATOSIS – PATHOLOGY
NEPHRITIS, HEREDITARY – GENETIC
NEPHRITIS, HEREDITARY – DIAGNOSIS
NEPHRITIS, HEREDITARY – PATHOLOGY
GENETIC TECHNIQUES
EARLY DIAGNOSIS
HISTOLOGICAL TECHNIQUES
UTERINE NEOPLASMS – GENETICS
UTERINE NEOPLASMS – DIAGNOSIS
UTERINE NEOPLASMS – PATHOLOGY
For citation: Boltaboeva M., Haydarov A., Ganieva M., Kholmatov D., Efimenko O., Rakhmanova L. Familial co-occurrence of diffuse leiomyomatosis and Alport syndrome: a clinical case report. Sechenov Medical Journal. 2025; 16(4): 49–57. Epub ahead of print 12.12.2025. https://doi.org/10.47093/2218-7332.2025.16.4.1344

CONTACT INFORMATION:
Muqaddas Boltaboeva, PhD, Assistant Professor, Department of Hospital Pediatrics, Andijan State Medical Institute.
Address: 1, S.Yu. Otabekova str., Andijan, 170100, Republic of Uzbekistan
E-mail: Doctormeeeee1999@gmail.com

Compliance with ethical standards. Consent statement. The patient's parents consented to the publication of the article "Familial co-occurrence of diffuse leiomyomatosis and Alport syndrome: a clinical case report" in the "Sechenov Medical Journal". Ethical approval for conducting the study was granted by the Ethics Committee of Andijan State Medical Institute (Approval No: 4/80, dated: 12.05.2025).
Conflict of interests. The authors declare that there is no conflict of interest.
Financing. The study had no sponsorship (own resources).

Received: 06.09.2025
Accepted: 13.11.2025
Date of publication online: 12.12.2025
Date of publication: 30.12.2025

УДК [618.14-006.363::616.61]-053.1-07

Семейное сочетание диффузного лейомиоматоза и синдрома Альпорта: клинический случай

М. Болтабоева[1,✉], А. Хайдаров[1], М. Ганиева[1], Д. Холматов[1], О. Ефименко[1], Л. Рахманова[2]

[1]Андижанский государственный медицинский институт
ул. С.Ю. Отабекова, д. 1, г. Андижан, 170100, Республика Узбекистан
[2]Ташкентский государственный медицинский университет
ул. С.А. Фаробий, д. 2, г. Ташкент, 100109, Республика Узбекистан

Аннотация

Синдром Альпорта (СА) – наследственная нефропатия, обусловленная мутациями в генах *COL4A3*, *COL4A4* и *COL4A5*. Редкие смежные варианты *COL4A5–COL4A6* вызывают СА с диффузным лейомиоматозом (СА-ДЛ).

Описание случая. У 16-летнего пациента с детства отмечались умеренная протеинурия, гематурия, снижение слуха и миопия. Расчетная СКФ – 82,8 мл/мин/1,73 м^2. Биопсия почки: сегментарный мезангиальный склероз; иммунная флюоресценция отрицательна. Электронная микроскопия: диффузное истончение гломерулярной базальной мембраны и слияние ножек подоцитов. Двое братьев с терминальной почечной недостаточностью умерли в подростковом возрасте; у матери – гематурия, миома матки и доброкачественная опухоль мочевого пузыря. Диагноз Х-сцепленного СА установлен по критериям Флинтера; начата нефропротективная терапия. С 2024 года появились эпигастральные жалобы; эндоскопия выявила подслизистое образование желудка размером 2 см. Полногеномное секвенирование обнаружило гемизиготный миссенс-вариант в *COL4A5* и делецию экзонов 1–2 *COL4A6*, что подтвердило СА-ДЛ.
Обсуждение. Представленный случай демонстрирует сочетание СА с ДЛ и показывает, что ранний семейный скрининг в сочетании с мультидисциплинарным клиническим, гистопатологическим и генетическим обследованием обеспечивает своевременную диагностику атипичных семейных форм СА-ДЛ и улучшает тактику ведения пациентов.

Ключевые слова: лейомиома; нефритический синдром; опухоли матки; Х-сцепленные генетические заболевания; опухоли гладкой мускулатуры
Рубрики MeSH:
ОПИСАНИЕ СЛУЧАЕВ
ЛЕЙОМИОМАТОЗ – ГЕНЕТИКА
ЛЕЙОМИОМАТОЗ – ДИАГНОСТИКА
ЛЕЙОМИОМАТОЗ – ПАТОЛОГИЯ
НЕФРИТ НАСЛЕДСТВЕННЫЙ – ГЕНЕТИКА
НЕФРИТ НАСЛЕДСТВЕННЫЙ – ДИАГНОСТИКА
НЕФРИТ НАСЛЕДСТВЕННЫЙ – ПАТОЛОГИЯ
ГЕНЕТИЧЕСКИЕ МЕТОДЫ
ДИАГНОСТИКА РАННЯЯ
ГИСТОЛОГИЧЕСКИЕ МЕТОДЫ
МАТКИ НОВООБРАЗОВАНИЯ – ГЕНЕТИКА
МАТКИ НОВООБРАЗОВАНИЯ – ДИАГНОСТИКА
МАТКИ НОВООБРАЗОВАНИЯ – ПАТОЛОГИЯ
Для цитирования: Болтабоева М., Хайдаров А., Ганиева М., Холматов Д., Ефименко О., Рахманова Л. Семейное сочетание диффузного лейомиоматоза и синдрома Альпорта: клинический случай. Сеченовский вестник. 2025; 16(4): 49–57. Epub ahead of print 12.12.2025. https://doi.org/10.47093/2218-7332.2025.16.4.1344

КОНТАКТНАЯ ИНФОРМАЦИЯ:
Болтабоева Мукаддас, PhD, ассистент кафедры госпитальной педиатрии Андижанского государственного медицинского института.
Адрес: ул. С.Ю. Отабекова, д. 1, г. Андижан, 170100, Республика Узбекистан
E-mail: Doctormeeeee1999@gmail.com

Соблюдение этических норм. Заявление о согласии. Родители пациента дали согласие на публикацию представленной статьи «Семейное сочетание диффузного лейомиоматоза и синдрома Альпорта: клинический случай» в журнале «Сеченовский вестник». Этическое одобрение проведения исследования выдано Этическим комитетом Андижанского государственного медицинского института (№ 4/80 от 12.05.2025).
Конфликт интересов. Авторы заявляют об отсутствии конфликта интересов.
Финансирование. Исследование не имело спонсорской поддержки (собственные ресурсы).

Поступила: 06.09.2025
Принята: 13.11.2025
Дата публикации онлайн: 12.12.2025
Дата печати: 30.12.2025

Abbreviations:
AS – Alport syndrome
DL – diffuse leiomyomatosis

HIGHLIGHTS	КЛЮЧЕВЫЕ ПОЛОЖЕНИЯ
In settings with limited molecular access, X-linked Alport syndrome can be diagnosed according to the Flinter criteria by integrating clinical phenotype, renal histopathology, and a compatible family history.	При недоступности молекулярно-генетического тестирования синдром Альпорта, сцепленный с Х-хромосомой, можно диагностировать на основании критериев Флинтера при наличии у пациента характерного клинического фенотипа, гистопатологических изменений почек и соответствующего семейного анамнеза.
Familial X-linked Alport syndrome may coexist with diffuse leiomyomatosis in 2–5% of cases, typically due to combined mutations in *COL4A* genes.	Семейная Х-сцепленная форма синдрома Альпорта в 2–5% случаев может сочетаться с диффузным лейомиоматозом вследствие смежных мутаций в генах *COL4A*.
Early pedigree analysis combined with coordinated multidisciplinary care such as genetic counseling, and organ-specific surveillance by nephrology, audiology, ophthalmology, and gastroenterology, accelerates diagnosis, enables risk stratification, and improves outcomes.	Ранний анализ родословной и скоординированный многопрофильный подход, сочетающий генетическое консультирование, наблюдение нефролога, оториноларинголога, офтальмолога и гастроэнтеролога, ускоряет диагностику, улучшает клинические исходы и эффективность ведения пациентов.

Alport syndrome (AS) is a hereditary disease defined by progressive kidney failure, sensorineural hearing loss, and ocular abnormalities. AS results from pathogenic variants in *COL4A3*, *COL4A4*, or *COL4A5* genes, which encode type IV collagen, a structural component essential to the integrity of the glomerular basement membrane [1–4]. The most frequent form is X-linked AS caused by *COL4A5* variants; *COL4A3* and *COL4A4* variants typically underlie autosomal-recessive disease. The prevalence of AS is estimated at approximately 1 per 5000–10,000 individuals; but the true burden is probably higher because of late recognition and atypical presentations, particularly among females with lyonization-mediated variability [5, 6].

A subset of individuals with X-linked AS develop diffuse leiomyomatosis (DL) due to contiguous deletions involving *COL4A5* and *COL4A6*, with reported rates of roughly 2–5% [7]. By 2021, only around 30 families with genetically confirmed AS-DL had been described worldwide [8]. DL is more frequently observed in women and most often involves the esophagus, trachea, and genital tract, requiring multidisciplinary care [9, 10].

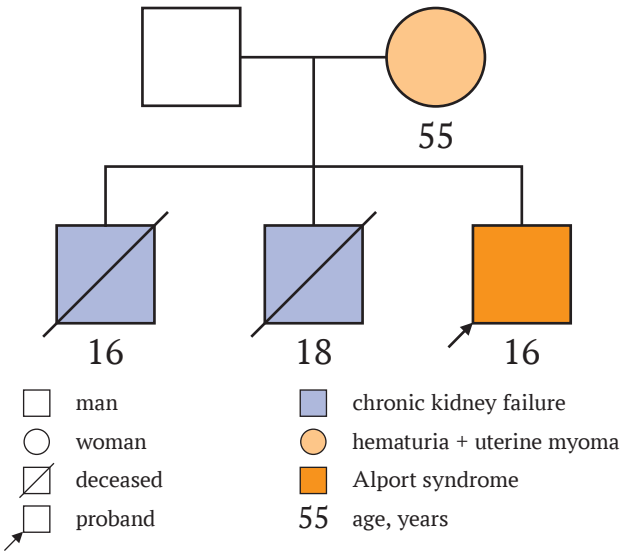

FIG. 1. Pedigree chart of family Alport syndrome with diffuse leiomyomatosis

Heterozygous *COL4A3* or *COL4A4* variants may manifest with isolated proteinuria and focal segmental glomerulosclerosis, without the classic ocular and auditory symptoms, which can often lead to misdiagnosis [11–14]. Recent studies also implicate digenic inheritance, mosaic variants, and deep intronic changes as contributors to disease pathogenesis and to the breadth of phenotypes observed. These findings support the incorporation of expanded genetic testing into routine evaluation, especially when the clinical picture is atypical [9, 15, 16]. In a recent paper, a child with X-linked AS was diagnosed with esophageal DL, emphasizing the usefulness of integrating clinical evaluation, histology, and family studies for early detection of non-renal manifestations [17].

The aim of this case report is to describe a rare familial co-occurrence of AS and DL, and to emphasize the diagnostic value of combining genealogical assessment with clinical examination, renal histology, and genetic testing.

CASE REPORT

A 16-year-old patient had been followed for eleven years at the Nephrology Department of the Andijan Regional Multidisciplinary Children's Medical Center for suspected AS. He reported long-standing microscopic hematuria, mild proteinuria, progressive decline in hearing, and myopia. Maternal pregnancy was complicated by first-trimester toxicosis; the patient was delivered at term with a birth weight of 4200 g and was breastfed until three years of age. Past medical history included pneumonia, recurrent tonsillitis, and repeated upper-respiratory infections (6–8 episodes per year).

The pedigree suggested X-linked transmission (Fig. 1). Two elder brothers died in adolescence from end-stage kidney disease attributed to glomerulonephritis. The patient's mother had adolescent-onset hematuria, underwent surgery for symptomatic uterine myoma at

age 36 after unsuccessful medical therapy, and three years before the proband's evaluation was found to have a benign bladder tumor (histologic subtype not available). Chemotherapy was recommended at that time and was followed by increased hematuria. She had not undergone genetic testing for AS, and no additional genealogic information from maternal grandparents or siblings was available.

In 2019 proband underwent a kidney biopsy. Three renal cores (total length 37 mm) were obtained, with a 1.5-mm cortical fragment reserved for electron microscopy. Light microscopy demonstrated a mesangial and sclerosing pattern with segmental mesangial sclerosis (Fig. 2A). Interstitial fibrosis involved approximately 10% of the cortical area. Immunofluorescence showed no specific glomerular deposition (Fig. 2B). Congo red staining for amyloid was not performed. Electron microscopy revealed diffuse thinning of glomerular basement membrane with podocyte foot-process effacement, consistent with AS (Fig. 2C).

Electrocardiography revealed sinus rhythm with a normal electrical axis. Renal ultrasonography demonstrated diffuse parenchymal changes without hydronephrosis. An ophthalmologic assessment showed grade II myopia; anterior lenticonus and dot-and-fleck retinopathy were not documented. Audiometry demonstrated bilateral grade III mixed hearing loss (Fig. 3).

Integrating the clinical phenotype (hematuria, proteinuria, mixed hearing loss, myopia), the histopathologic features, and the family history of adolescent renal failure in male relatives, a diagnosis of X-linked AS was established according to Flinter criteria [18]. At that time, molecular testing was not available. Nephroprotective treatment with angiotensin converting enzyme inhibitors was initiated.

Since 2024, the patient complained of fatigue, epigastric pain, nausea, and vomiting. A cardiopulmonary examination did not show up anything.

Laboratory testing indicated moderate anemia – hemoglobin 89 g/L, red blood cells 3.6×10^{12}/L (RBC)

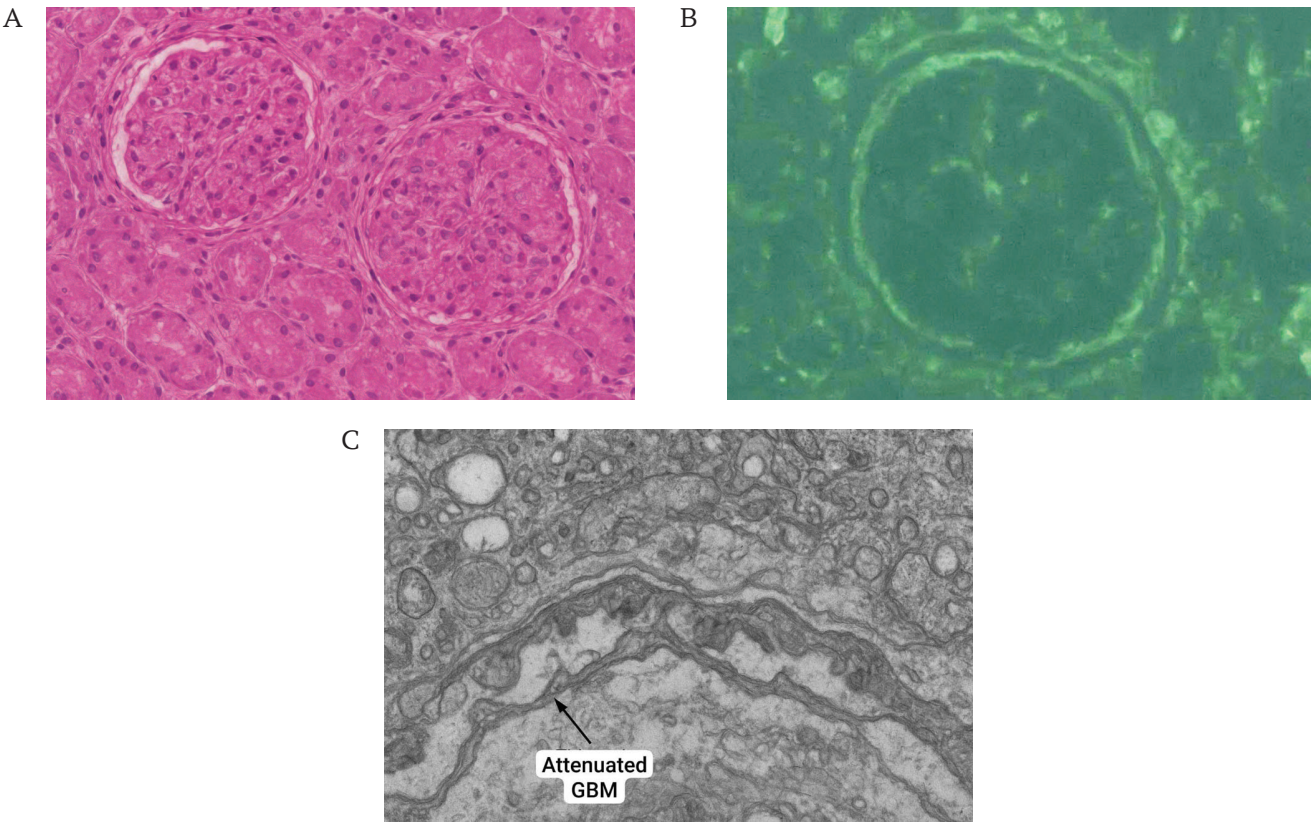

FIG. 2. Kidney biopsy of proband with Alport syndrome and diffuse leiomyomatosis
A. Light microscopy (hematoxylin and eosin, magnification ×400). A total of 30 glomeruli were identified, of which 4 were globally sclerosed. Some glomeruli showed segmental sclerosis with adhesions to Bowman's capsule. Mesangial hypercellularity: mild. Mesangial matrix expansion: mild. Glomerular hypertrophy: moderate. Tubular epithelial cells contained reabsorption droplets. Tubular atrophy involved approximately 10% of the cortical area. Interstitial inflammation involved about 3% of the cortex. The interstitium showed fibrosis and mononuclear cellular infiltrates with numerous foam cells. Arteries and arterioles appeared unremarkable.
B. Immunofluorescence study (paraffin-embedded kidney blocks, magnification ×200). No specific fluorescence for IgA, IgG, IgM, C3, or C1q.
C. Electron microscopy (one glomerulus, magnification ×10,000). Diffuse effacement of podocyte foot processes. Glomerular basement membranes exhibited areas of thinning and thickening with marked lamellation and splitting.

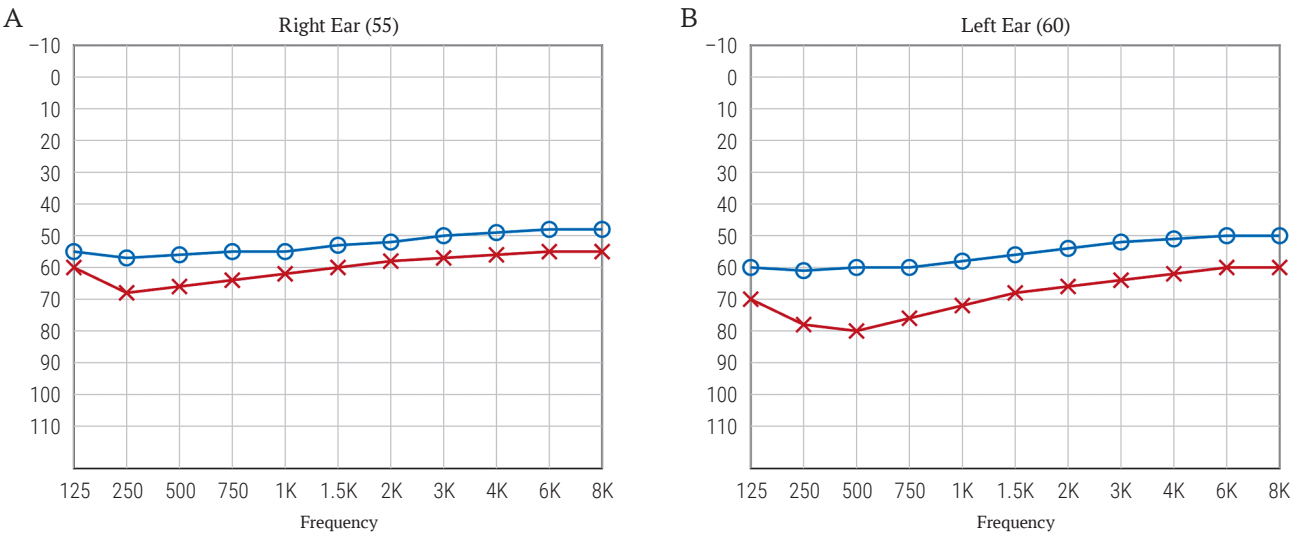

FIG. 3. Audiogram of proband with Alport syndrome and diffuse leiomyomatosis

Note: air conduction (red), bone conduction (blue).

and mild leukopenia (leukocytes 3.9×10^9/L). Serum biochemistry showed total protein 54 g/L, creatinine 116 μmol/L, urea 9.2 mmol/L, with an estimated glomerular filtration rate of 82.8 mL/min/1.73 m^2. Urinalysis revealed protein 0.33 g/L, white blood cells 6–8 per high-power field, dysmorphic RBCs 10–12, isomorphic RBCs 4–6, and hyaline casts 2–5.

In July 2025, an upper endoscopy was performed and identified a 2-cm submucosal lesion in the body of the stomach (Fig. 4). The endoscopic appearance was consistent with a smooth-muscle neoplasm, and surgical resection was recommended. The patient remained clinically stable under a joint follow-up by gastroenterology and pediatric surgery while preoperative work-up was arranged.

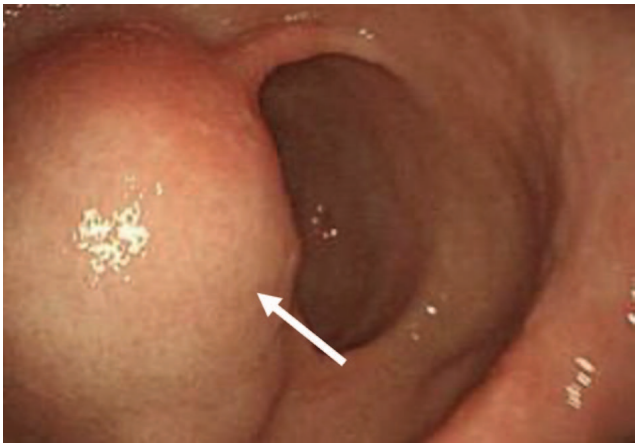

FIG. 4. Upper endoscopy of proband with Alport syndrome and diffuse leiomyomatosis

Note: submucosal gastric lesion located in the body of the stomach measuring 2 cm (arrow).

In light of the clinical features suggestive of AS and the additional identification of a gastric smooth muscle neoplasm consistent with DL, molecular genetic testing was warranted to confirm the diagnosis and guide appropriate clinical management. Whole-exome sequencing identified two pathogenic alterations: a hemizygous missense variant in *COL4A5* (NM_000495.5:c.2879G>A, p.Gly960Asp), consistent with X-linked AS and affecting the α5(IV) collagen chain, and a deletion encompassing exons 1–2 of *COL4A6* (NM_000096.4), indicative of a contiguous *COL4A5–COL4A6* rearrangement on the X chromosome that underlies DL associated with AS. Both variants were classified as pathogenic based on current annotations in the OMIM (Online Mendelian Inheritance in Man) database[1] and interpreted according to the American College of Medical Genetics and Genomics guidelines[2]. The classification may be subject to revision as additional evidence accumulates.

DISCUSSION

AS is a progressive congenital nephropathy caused by type IV collagen defects and classically involves kidneys, hearing, and eyes. The X-linked dominant form is more common [8]. Our patient showed the renal-auditory phenotype early on and, at 16 years, developed epigastric symptoms. An endoscopy revealed a 2-cm submucosal lesion in the gastric body, compatible with smooth-muscle proliferations seen in AS with DL.

Family history strengthens the inference of X-linked inheritance: two elder brothers died in adolescence from end-stage kidney disease, and the patient's mother had adolescent-onset hematuria, underwent surgery for

[1] An Online Catalog of Human Genes and Genetic Disorders. https://www.omim.org/ (access date: 12.06.2025).
[2] American College of Medical Genetics and Genomics guidelines. 2018. https://www.acmg.net (access date: 12.06.2025).

uterine myoma at 36 years, and later a benign bladder tumor. These clinical features may suggest a rare form of AS potentially caused by microdeletions in the *COL4A5* and *COL4A6* genes [7, 19]. However, a direct association between uterine fibroids and AS has not been clearly demonstrated at either the clinical or genetic level. Moreover, uterine fibroids are common, and a direct causal relationship with AS cannot be assumed without genetic confirmation. This case may also be a possible example of AS being milder disease expression in females compared to males.

The mother's nonspecific symptoms and the occurrence of end-stage kidney failure in two brothers reflect severe outcomes of delayed genetic assessment. The pedigree supports X-linked inheritance and illustrates variable multi-organ involvement. Concurrent involvement of kidneys, ears, eyes, stomach, and uterus is syndromic and underscores need for multidisciplinary consultation. These observations reinforce the value of multidisciplinary management in AS-DL, with regular follow-up by nephrologists, audiologists, ophthalmologists, and gastroenterologists to facilitate early detection and timely intervention.

Clinicopathologic correlation was consistent. A kidney biopsy showed segmental mesangial sclerosis with 10% interstitial fibrosis and classic ultrastructural abnormalities of the glomerular basement membrane. Immunofluorescence revealed no immunoglobulin or complement deposition, supporting a structural basement-membrane disorder rather than immune-complex disease. An audiometry confirmed bilateral grade III mixed hearing loss, and ophthalmologic assessment documented myopia, aligning with the recognised extra-renal spectrum of AS. Recurrent upper-respiratory infections may indicate underlying immunological dysfunction, possibly associated with AS [15, 20].

In this patient, kidney function was relatively preserved (estimated glomerular filtration rate 82.8 mL/min/1.73 m^2). This finding may suggest a slowly progressive clinical phenotype of the AS rather than a rapid decline often seen in adolescent males with X-linked disease. Nonetheless, AS is typically progressive, and vigilant surveillance is warranted. Priorities include renin-angiotensin-aldosterone system blockade as tolerated, periodic assessment of proteinuria and glomerular filtration rate, and longitudinal audiologic and ophthalmologic follow-up [21].

This case also illustrates diagnostic pathways when access to molecular testing is limited. A structured approach that integrates pedigree analysis, multi-organ evaluation, and kidney pathology can establish a presumptive diagnosis and triage patients for genetic confirmation when feasible [22–24]. The genetic counselling for at-risk relatives can serve as a practical and cost-effective alternative to molecular analysis and diagnosis could be established according to Flinter criteria [18].

CONCLUSION

This case demonstrates X-linked AS with DL, highlighting multisystem expression and familial burden. The deaths of two brothers with chronic kidney failure and the mother's long-standing hematuria with leiomyomatous disease emphasizes the importance of timely genealogical analysis and a multidisciplinary approach for early diagnosis. Genealogic assessment and targeted genetic testing enable clinicians to achieve better outcomes for patients and their relatives in the cases of atypical hereditary diseases.

AUTHORS CONTRIBUTIONS

Muqaddas Boltaboeva contributed to the conceptualization, and preparation of the original draft. Muqaddas Boltaboeva and Marifat Ganieva participated in compiling the data curation and the research. Marifat Ganieva, Oksana Efimenko and Davron Kholmatov contributed to the review and editing of the text. Abdulhamid Haydarov performed the formal analysis. Lola Rakhmanova contributed to the methodology and provided supervision throughout the study. All authors approved the final version of the article.

ВКЛАД АВТОРОВ

М. Болтабоева разработала концепцию и подготовила черновик рукописи. М. Болтабоева и М. Ганиева участвовали в сборе данных и обследовании пациента. М. Ганиева, О. Ефименко и Д. Холматов внесли вклад в рецензирование и редактирование текста. А. Хайдаров выполнил формальный анализ. Л. Рахманова отвечала за методологию и осуществляла научное руководство на протяжении всего исследования. Все авторы одобрили окончательную версию статьи.

REFERENCES / ЛИТЕРАТУРА

1. *Gregorio V., Caparali E.B., Shojaei A., et al.* Alport syndrome: Clinical spectrum and therapeutic advances. Kidney Med. 2023 Mar; 5(5): 100631. https://doi.org/10.1016/j.xkme.2023.100631. PMID: 37122389
2. *Huang H.X., Tsai I.J., Greenbaum L.A.* Alport syndrome: Expanding diagnosis and treatment. Pediatr Neonatol. 2025 Feb; 66(Suppl1): S13–S17. https://doi.org/10.1016/j.pedneo.2024.10.005. Epub 2024 Oct 30. PMID: 39521677
3. *Puapatanakul P., Miner J.H.* Alport syndrome and Alport kidney diseases – elucidating the disease spectrum. Curr Opin Nephrol Hypertens. 2024 May; 33(3): 283–290. https://doi.org/10.1097/MNH.0000000000000983. Epub 2024 Mar 13. PMID: 38477333
4. *Savige J.* Heterozygous pathogenic *COL4A3* and *COL4A4* variants (autosomal dominant Alport syndrome) are common, and not typically associated with end-stage kidney failure, hearing loss, or ocular abnormalities. Kidney Int Rep. 2022 Jun; 7(9): 1933–1938. https://doi.org/10.1016/j.ekir.2022.06.001. PMID: 36090501
5. *Gibson J., Fieldhouse R., Chan M.M.Y., et al.* Prevalence estimates of predicted pathogenic *COL4A3-COL4A5* variants in a population sequencing database and their implications for Alport syndrome. J Am Soc Nephrol. 2021 Sep; 32(9): 2273–2290.

https://doi.org/10.1681/ASN.2020071065. Epub 2021 Jun 18. PMID: 34400539
6. *Torra R., Lipska-Zietkiewicz B., Acke F., et al.* Diagnosis, management and treatment of the Alport syndrome – 2024 guideline on behalf of ERKNet, ERA and ESPN. Nephrol Dial Transplant. 2025 May; 40(6): 1091-1106. https://doi.org/10.1093/ndt/gfae265. PMID: 39673454
7. *Zhou X., Wang J., Mao J., Ye Q.* Clinical manifestations of Alport syndrome-diffuse leiomyomatosis patients with contiguous gene deletions in *COL4A6* and *COL4A5*. Front Med (Lausanne). 2021 Oct; 8: 766224. https://doi.org/10.3389/fmed.2021.766224. PMID: 34778325
8. *Takeda F.R., De Meira J.D. Junior, Sallum R.A.A.* A case report of esophageal leiomyoma in Alport's syndrome treated with robotic-assisted distal myotomy: A surgical technique to avoid esophagectomy. International Journal of Surgery Case Reports. 2023 Jun; 108: 108433. https://doi.org/10.1016/j.ijscr.2023.108433. PMID: 37352772
9. *Kashtan C.E.* Alport syndrome: Achieving early diagnosis and treatment. Am J Kidney Dis. 2021 Feb; 77(2): 272–279. https://doi.org/10.1053/j.ajkd.2020.03.026. Epub 2020 Jul 22. PMID: 32712016
10. Алексеева Т.А., Аксенова М.Е., Заикова Н.М. Особенности течения и диагностики Х-сцепленного синдрома Альпорта с диффузным лейомиоматозом желудочно-кишечного тракта: клинический случай. Нефрология и диализ. 2025; 27(2): 228–229. https://doi.org/10.28996/2618-9801-2025-2-228-229. EDN: ABCXTZ / Alekseeva T.A., Aksenova M.E., Zaikova N.M. Characteristics of the course and diagnostics of X-linked Alport syndrome with diffuse leiomyomatosis of the gastrointestinal tract: a clinical case. Nephrology and Dialysis. 2025; 27(2): 228–229 (In Russ.). https://doi.org/10.28996/2618-9801-2025-2-228-229. EDN: ABCXTZ\
11. *Gatseva A., Sin Y.Y., Brezzo G., Van Agtmael T.* Basement membrane collagens and disease mechanisms. Essays Biochem. 2019 Sep; 63(3): 297–312. https://doi.org/10.1042/EBC20180071. PMID: 31387942
12. *Lee J.M., Nozu K., Choi D.E., et al.* Features of autosomal recessive Alport syndrome: A systematic review. J Clin Med. 2019 Feb; 8(2): 178. https://doi.org/10.3390/jcm8020178. PMID: 30717457
13. *Zhang Y., Böckhaus J., Wang F., et al.* Genotype-phenotype correlations and nephroprotective effects of RAAS inhibition in patients with autosomal recessive Alport syndrome. Pediatr Nephrol. 2021 Sep; 36(9): 2719–2730. https://doi.org/10.1007/s00467-021-05040-9. Epub 2021 Mar 27. PMID: 33772369
14. *Shulman C., Liang E., Kamura M., et al.* Type IV collagen variants in CKD: Performance of computational predictions for identifying pathogenic variants. Kidney Med. 2021 Feb; 3(2): 257–266. https://doi.org/10.1016/j.xkme.2020.12.007. PMID: 33851121
15. *Savige J., Lipska-Zietkiewicz B.S., Watson E., et al.* Guidelines for genetic testing and management of Alport syndrome. Clin J Am Soc Nephrol. 2022 Jan; 17(1): 143–154. https://doi.org/10.2215/CJN.04230321. Epub 2021 Dec 20. Erratum in: Clin J Am Soc Nephrol. 2023 Apr 1; 18(4): 510. https://doi.org/10.2215/CJN.0000000000000095. PMID: 34930753
16. *Groopman E.E., Marasa M., Cameron-Christie S., et al.* Diagnostic utility of exome sequencing for kidney disease. N Engl J Med. 2019 Jan; 380(2): 142–151. https://doi.org/10.1056/NEJMoa1806891. Epub 2018 Dec 26. PMID: 30586318
17. *Thanachatchairattana P., Losty P.* Paediatric diffuse oesophageal leiomyomatosis with Alport syndrome. BMJ Case Rep. 2024 Aug; 17(8): e260442. https://doi.org/10.1136/bcr-2024-260442. PMID: 39179268
18. *Flinter F.A., Cameron J.S., Chantler C., et al.* Genetics of classic Alport's syndrome. Lancet. 1988 Oct; 2(8618): 1005–1007. https://doi.org/10.1016/s0140-6736(88)90753-2. PMID: 2902439
19. *Chen F., Ahimaz P., Nguyen Q.M., et al.* Phenotype driven molecular genetic test recommendation for diagnosing pediatric rare disorders. NPJ Digit Med. 2024 Nov; 7(1): 333. https://doi.org/10.1038/s41746-024-01331-1. PMID: 39572625
20. Аксенова М.Е. Синдром Альпорта: современные представления. Нефрология. 2021; 25(3): 75–83. https://doi.org/10.36485/1561-6274-2021-25-3-75-83. EDN: LYSGFH / Aksenova M.E. Alport syndrome: our knowledge update. Nephrology (Saint-Petersburg). 2021; 25(3): 75–83 (In Russ.). https://doi.org/10.36485/1561-6274-2021-25-3-75-83. EDN: LYSGFH
21. Kidney Disease: Improving Global Outcomes (KDIGO) CKD Work Group. KDIGO 2024 Clinical Practice Guideline for the Evaluation and Management of Chronic Kidney Disease. Kidney Int. 2024 Apr; 105(4S): S117–S314. https://doi.org/10.1016/j.kint.2023.10.018. PMID: 38490803
22. *Gibson J.T., de Gooyer M., Huang M., Savige J.* A systematic review of pathogenic *COL4A5* variants and proteinuria in women and girls with X-linked Alport syndrome. Kidney Int Rep. 2022 Aug; 7(11): 2454–2461. https://doi.org/10.1016/j.ekir.2022.08.021. PMID: 36531881
23. *Kim J.H., Lim S.H., Song J.Y., et al.* Genotype-phenotype correlation of X-linked Alport syndrome observed in both genders: a multicenter study in South Korea. Sci Rep. 2023 Apr; 13(1): 6827. https://doi.org/10.1038/s41598-023-34053-7. PMID: 37100867
24. *Matthaiou A., Poulli T., Deltas C.* Prevalence of clinical, pathological and molecular features of glomerular basement membrane nephropathy caused by *COL4A3* or *COL4A4* mutations: a systematic review. Clin Kidney J. 2020 Feb; 13(6): 1025–1036. https://doi.org/10.1093/ckj/sfz176. PMID: 33391746

INFORMATION ABOUT THE AUTHORS / ИНФОРМАЦИЯ ОБ АВТОРАХ

Muqaddas Boltaboeva✉, PhD, Assistant Professor, Department of Hospital Pediatrics, Andijan State Medical Institute.
ORCID: https://orcid.org/0009-0000-8421-9592

Abdulhamid Haydarov, Student, Andijan State Medical Institute.
ORCID: https://orcid.org/0009-0007-7195-2542

Marifat Ganieva, Cand. of Sci. (Medicine), Associate Professor, Department of Hospital Pediatrics, Andijan State Medical Institute.
ORCID: https://orcid.org/0009-0000-2637-1932

Болтабоева Мукаддас✉, PhD, ассистент кафедры госпитальной педиатрии Андижанского государственного медицинского института.
ORCID: https://orcid.org/0009-0000-8421-9592

Хайдаров Абдулхамид, студент Андижанского государственного медицинского института.
ORCID: https://orcid.org/0009-0007-7195-2542

Ганиева Марифат, канд. мед. наук, доцент кафедры госпитальной педиатрии Андижанского государственного медицинского института.
ORCID: https://orcid.org/0009-0000-2637-1932

Davron Kholmatov, Cand. of Sci. (Medicine), Associate Professor, Department of Hospital Pediatrics, Andijan State Medical Institute.
ORCID: https://orcid.org/0009-0001-1014-5428

Oksana Efimenko, Cand. of Sci. (Medicine)**,** Associate Professor, Department of Hospital Pediatrics, Andijan State Medical Institute.
ORCID: https://orcid.org/0009-0004-6817-0935

Lola Rakhmanova, Dr. of Sci. (Medicine), Associate Professor, Department of Internal Diseases in family medicine No 2, Tashkent State Medical University.
ORCID: https://orcid.org/0000-0001-7361-9953

Холматов Даврон, канд. мед. наук, доцент кафедры госпитальной педиатрии Андижанского государственного медицинского института.
https://orcid.org/0009-0001-1014-5428

Ефименко Оксана, канд. мед. наук, доцент кафедры госпитальной педиатрии Андижанского государственного медицинского института.
ORCID: https://orcid.org/0009-0004-6817-0935

Рахманова Лола, д-р мед. наук, доцент кафедры внутренних болезней в семейной медицине № 2 Ташкентского государственного медицинского университета.
ORCID: https://orcid.org/0000-0001-7361-9953

✉ Corresponding author / Автор, ответственный за переписку

Acknowledgements for peer review and assistance in preparing manuscripts for publication

The editors of the Sechenov Medical Journal would like to express their gratitude to our highly regarded reviewers. Their invaluable assistance in selecting manuscripts for publication in 2025 is greatly appreciated:

- Vasily V. Alexandrov (Volgograd, Russia)
- Vladimir A. Aliyev (Moscow, Russia)
- Guram G. Ahladze (Moscow, Russia)
- Sergey N. Avdeev (Moscow, Russia)
- Stanislav Kh. Ali (Moscow, Russia)
- Nikolai N. Bagmet (Moscow, Russia)
- Igor I. Bobintsev (Kursk, Russia)
- Mikhail I. Bokarev (Moscow, Russia)
- Artem S. Chaban (Munich, Germany)
- Natalia V. Chebotareva (Moscow, Russia)
- Valentina N. Diomidova (Cheboksary, Russia)
- Alexey V. Egorov (Moscow, Russia)
- Andrey V. Gavryushin (Moscow, Russia)
- Sherly Deborah George (Manipal, Malaysia)
- Alexander V. Gusev (Moscow, Russia)
- Yulia V. Ilyina (Moscow, Russia)
- Hidehito Kimura (Kobe, Japan)
- Yuri V. Kivelev (Moscow, Russia)
- Alexander V. Kochatkov (Moscow, Russia)
- Evgeny A. Kolchanov (St. Petersburg, Russia)
- Alexander A. Kozhevnikov (Moscow, Russia)
- Alexey V. Kovalev (Moscow, Russia)
- Dmitry V. Litvinenko (Krasnodar, Russia)
- Magomed R. Mamatkhanov (St. Petersburg, Russia)
- Natalia V. Mazurina (Moscow, Russia)
- Andrey O. Morozov (Moscow, Russia)
- Olga L. Morozova (Moscow, Russia)
- Jorge Mura (Santiago, Chile)
- Chavdar S. Pavlov (Moscow, Russia)
- Sergey V. Pirozhkov (Moscow, Russia)
- Rodion V. Ponomarev (Moscow, Russia)
- Tatyana E. Potemina (Nizhny Novgorod, Russia)
- Veronika A. Prikhodko (St. Petersburg, Russia)
- Iwan Purnawan (Purwokerto, Indonesia)
- Rakhmonjon R. Rustamov (Tyumen, Russia)
- Nadezhda V. Rusyaeva (Moscow, Russia)
- Sergey V. Sapelkin (Moscow, Russia)
- Natalia N. Silina (St. Petersburg, Russia)
- Andrey P. Stolbov (Moscow, Russia)
- Albert A. Sufianov (Tyumen, Russia)
- Yulia P. Sych (Moscow, Russia)
- Evgeny A. Tarabrin (Moscow, Russia)
- Mark S. Taratkin (Moscow, Russia)
- Alexander S. Shershever (Yekaterinburg, Russia)
- Yefim M. Shifman (Moscow, Russia)
- Yulia O. Shulpekova (Moscow, Russia)
- Sergey P. Vetshev (Moscow, Russia)
- Yuri A. Yakimov (Tyumen, Russia)
- Ekaterina I. Yakovleva (Moscow, Russia)
- Maria A. Zatolokina (Kursk, Russia)
- Angelina V. Zorkina (Saransk, Russia)

The editors of the Sechenov Medical Journal would like to thank the following Sechenov University students for their help: Denis P. Volkov, Diana A. Daduns, and Evelina M. Trashkun for technical editing and reference list checking; Egor A. Kuzmin for creating illustrations.

The editors would like to express their gratitude to the students of Sechenov University for their assistance with the post-publication promotion of the articles on the journal's social networks (https://t.me/sechmedj, https://vk.com/sechmedj): Diana V. Serednyakova (design development), and Natalia G. Bezusenko, Oksana V. Kravchenko, Anastasia P. Myshkova, Dmitrii D. Podgalo, Ulyana D. Andreeva (creating posts).

СЕЧЕНОВСКИЙ УНИВЕРСИТЕТ
НАУК О ЖИЗНИ

ФГАОУ ВО «Первый МГМУ им. И.М. Сеченова» Минздрава России
(Сеченовский Университет)